

Formulation and Mechanical Properties of Polypropylene Nanocomposites

Shenggong Lei

A Thesis

in

the Department

of

Mechanical and Industrial Engineering

Presented in Partial Fulfilment of the Requirements

For the Degree of Master of Applied Science at

Concordia University

Montreal, Quebec, Canada

December 2003

© Shenggong Lei, 2003



National Library
of Canada

Bibliothèque nationale
du Canada

Acquisitions and
Bibliographic Services

Acquisitions et
services bibliographiques

395 Wellington Street
Ottawa ON K1A 0N4
Canada

395, rue Wellington
Ottawa ON K1A 0N4
Canada

Your file *Votre référence*
ISBN: 0-612-91062-8
Our file *Notre référence*
ISBN: 0-612-91062-8

The author has granted a non-exclusive licence allowing the National Library of Canada to reproduce, loan, distribute or sell copies of this thesis in microform, paper or electronic formats.

L'auteur a accordé une licence non exclusive permettant à la Bibliothèque nationale du Canada de reproduire, prêter, distribuer ou vendre des copies de cette thèse sous la forme de microfiche/film, de reproduction sur papier ou sur format électronique.

The author retains ownership of the copyright in this thesis. Neither the thesis nor substantial extracts from it may be printed or otherwise reproduced without the author's permission.

L'auteur conserve la propriété du droit d'auteur qui protège cette thèse. Ni la thèse ni des extraits substantiels de celle-ci ne doivent être imprimés ou autrement reproduits sans son autorisation.

In compliance with the Canadian Privacy Act some supporting forms may have been removed from this dissertation.

Conformément à la loi canadienne sur la protection de la vie privée, quelques formulaires secondaires ont été enlevés de ce manuscrit.

While these forms may be included in the document page count, their removal does not represent any loss of content from the dissertation.

Bien que ces formulaires aient inclus dans la pagination, il n'y aura aucun contenu manquant.

Canada

ABSTRACT

Formulation and Mechanical Properties of Polypropylene Nanocomposites

Shenggong Lei

Polymer nanocomposites (PNC) are a new type of material, in which the reinforcement must have at least one dimension in a nanoscale. Polymer/clay nanocomposites provide great advantages in terms of different properties in comparison with conventional mineral-filled polymers. In this work, the preparation of polypropylene (PP)/clay nanocomposites by melt process (Brabender mixer) from five different chemistries of organo-nanoclays and five different coupling agents with different functional groups, such as maleic anhydride (MA), amine (NH_2), onium ion (NH_3^+), has been carried out. It should be noted here that the NH_3^+ modified PP were first studied in this work. The effect of impurities in conventional coupling agents has also been investigated for the first time. Different processing temperatures, residence times and shear rates have been examined. The effects of parameters, such as type of coupling agent and clay, processing conditions, dispersion and interface interaction, were evaluated using different means, such as XRD, DSC, SEM, DMA, and mechanical properties. The rheological behavior of nanocomposites was also studied. The results obtained from this study provide a certain understanding on the

relationship between the formulation, processing condition and performance. Significant improvement in stiffness and storage modulus was observed in nanocomposites formulated with coupling agent. However, the extent of the improvement of the nanocomposites' performance depends on the type of the clay and the coupling agent. In addition, the processing condition had great effects on the properties of PP nanocomposites.

Acknowledgement

I would like to express my sincere gratitude to my supervisors **Dr. S. V. Hoa** and **Dr. M. T. Ton-That** for their guidance, support and encouragement throughout all of the stages of this research.

I acknowledge the cooperation and help provided by all technicians who were involved in this study from Industrial Materials Institute-National Research Council of Canada, Concordia Center for Composites and McGill University. I also thank Dr. Lixin Wu, Mr. Weiping Liu and Mr. Shilian Hu for their help and suggestions.

Finally, I wish to express my appreciation to my family for their support and encouragement.

Shenggong Lei

Table of Contents

List of Figures

List of Tables

List of nomenclatures

Chapters

1	Introduction.....	1
	<u>1.1 Polymer composites and polymer nanocomposites (PNC).....</u>	1
	<u>1.2 Polypropylene and its nanocomposites.....</u>	3
2	Literature survey	
	<u>2.1Development of PNC.....</u>	7
	<u>2.2 Montmorillonite clay.....</u>	9
	<u>2.3 PNC structures.....</u>	15
	<u>2.4 PNC fabrication.....</u>	19
	2.4.1 In-situ polymerization process.....	19
	2.4.2 Solution process.....	21
	2.4.3 Melt intercalation (compounding) process.....	21
	<u>2.5 PP nanocomposites.....</u>	23
	2.5.1 Challenges in formulation of PP nanocomposites.....	23

2.5.2 Miscibility strategies	24
2.5.2.1 Modifying clay surface	24
2.5.2.2 Modifying matrix.....	25
2.5.2.3 Modifying matrix and clay surface	26
2.5.3 Research in polypropylene nanocomposites.....	26
<u>2.6 Summary</u>	32
<u>2.7 Objectives of the thesis</u>	34
3 Materials and Experiments	36
<u>3.1 Selection of materials and experiments design</u>	36
3.1.1 Clay.....	36
3.1.2 Coupling agents.....	37
3.1.3 Processing parameters.....	38
3.1.4 Equipment.....	39
3.1.5 Composition.....	39
3.1.6 Study parameters.....	40
3.1.7 Experimental procedure.....	41
<u>3.2 Materials</u>	42
3.2.1 Polypropylene	42
3.2.2 Coupling agents.....	43
3.2.3 Nanoclays	46
3.2.4 Components of composites.....	48
<u>3.3 PP Nanocomposites fabrication</u>	51

<u>3.4 Samples preparation for testing</u>	54
<u>3.5 Nanocomposites characterization</u>	57
3.5.1 Dispersion behavior	57
3.5.1.1 <i>X-Ray Diffraction (XRD)</i>	57
3.5.1.2 <i>Scanning Electron Microscopy (SEM)</i>	60
3.5.2 Rheological behavior	63
3.5.3 Thermal properties	64
3.5.4 Mechanical properties	66
3.5.4.1 <i>Dynamic Mechanical Analysis (DMA)</i>	66
3.5.4.2 <i>Tensile and flexural tests</i>	69

4 Effects of clay on the formulation and properties of PP

nanocomposites	72
<u>4.1 Effect of types of clay in the absence of coupling agent</u>	72
4.1.1 Rheological Behavior	73
4.1.2 Dispersion behavior – SEM	77
4.1.3 Thermal properties	80
4.1.3.1 <i>Crystallization behavior</i>	80
4.1.3.2 <i>Melting temperature (T_m)</i>	81
4.1.4 Dynamic mechanical properties	83
4.1.5 Tensile properties	87
<u>4.2 Effect of types of clay in the presence of coupling agent CA3</u>	90

4.2.1 Rheological behavior.....	91
4.2.2 Dispersion behavior – XRD.....	92
4.2.3 Tensile and flexural properties.....	93
<u>4.3 Effect of types of clay in the presence of coupling agent CA4</u>	95
4.3.1 Rheological behavior.....	96
4.3.2 Dispersion behavior - XRD.....	96
4.3.3 Thermal properties.....	97
4.3.3.1 <i>Crystallization behavior</i>	97
4.3.3.2 <i>T_m</i>	97
4.3.4 Tensile and flexural properties.....	99
<u>4.4 Conclusions</u>	101

5 Effects of coupling agent on the formulation and properties of

PP nanocomposites.....	102
<u>5.1 Effect of coupling agent (alone) on PP matrix</u>	103
5.1.1 Rheological behavior.....	103
5.1.2 Thermal properties.....	105
<u>5.2 Effect of coupling agent in the presence of 15A clay</u>	107
5.2.1 Rheological behavior.....	107
5.2.2 Dispersion behavior.....	108
5.2.2.1 <i>XRD</i>	108
5.2.2.2 <i>SEM</i>	112

5.2.3 Thermal properties.....	115
5.2.3.1 Crystallization behavior.....	115
5.2.3.2 T_m	116
5.2.4 Dynamic mechanical properties.....	118
5.2.5 Tensile and flexural properties.....	122
<u>5.3 Effect of coupling agent in the presence of I31PS clay</u>	124
5.3.1 Rheological behavior.....	125
5.3.2 Tensile and flexural properties.....	126
<u>5.4 Effect of coupling agent in the presence of I30E clay</u>	127
<u>5.5 Conclusions</u>	129

6 Effect of processing parameters on the formulation

and properties of PP nanocomposites.....	131
<u>6.1 Effect of processing temperature</u>	131
6.1.1 Rheological behavior.....	132
6.1.2 Dispersion behavior.....	133
6.1.3 Mechanical properties.....	134
<u>6.2 Effect of residence time</u>	136
6.2.1 Rheological behavior.....	137
6.2.2 Dispersion behavior.....	138
6.2.3 Mechanical behavior.....	139
<u>6.3 Effect of processing rotor speed (shear rate)</u>	141
6.3.1 Rheological behavior.....	141

6.3.2 Dispersion behavior.....	142
6.3.3 Mechanical behavior.....	143
<u>6. 4 Conclusions</u>	145
7 Conclusions	146
8 Contributions	148
9 Suggestions for future work	150
References	151

List of Figures

Figure 2.1 The formula and structure of montmorillonite.....	10
Figure 2.2 Structure of 2:1 phyllosilicates layered crystals	10
Figure 2.3 TEM of MMT clusters.....	11
Figure 2.4 Schematic of chemistry on the clay surface.....	11
Figure 2.5 Effect of surface treatment	13
Figure 2.6 Effect of compounding operation	13
Figure 2.7 Scheme of different types of composite arising from the interaction of layered silicates and polymers.....	16
Figure 2.8 XRD curves.....	18
Figure 2.9 TEM micrographs of nanocomposites.....	18
Figure 2.10 Process steps for preparation of PA6 nanocomposites.....	20
Figure 2.11 Dispersion Mechanism of melt intercalation	22
Figure 2.12 Schematic representation of the clay dispersion process	31
Figure 3.1 The experimental procedure.....	41
Figure 3.2 C.W. PL2000 Brabender Mixer	52
Figure 3.3 The mixer bowl and screws of PL2000 Brabender Mixer	52
Figure 3.4 Schematic drawing of mixing in Brabender.....	53
Figure 3.5 Carver Laboratory Press	56
Figure 3.6 Molds for samples.....	56
Figure 3.7 A Philips X-ray generator with diffractometer.....	59
Figure 3.8 Scheme of Bragg's law.....	59
Figure 3.9 The JEOL 840A SEM machine.....	61
Figure 3.10 Scheme and structure of SEM.....	62
Figure.3.11 TA Instruments -DSC 2010	65
Figure 3.12 Dynamic Mechanical Analyzer	68

Figure 3.13 Du Pont 983 DMA	68
Figure 3.14 The schematic drawing of flexural test	69
Figure 3.15 Instron 5500 test machine.....	71
Figure 4.1 Torque – time curve of pure PP.....	74
Figure 4.2 Torque – time curve of PP with I31PS clay.....	74
Figure 4.3 Torque - time curves of mixtures with different types of clay.....	76
Figure 4.4 SEM photo of pure PP.....	78
Figure 4.5 SEM photo of mixture with Na - montmorillonite	78
Figure 4.6 SEM photo of mixture with 15A nanoclay.....	79
Figure 4.7 SEM photo of mixture with I30E nanoclay	79
Figure 4.8 Crystallization curves of the composites with different clays.....	81
Figure 4.9 Melting behavior curves of the composites with different clays.....	82
Figure 4.10 DMA curves (storage modulus E') for the mixtures.....	84
Figure 4.11 DMA curves (loss modulus E'') for the mixtures.....	84
Figure 4.12 Effect of types of clay on tensile properties.....	89
Figure 4.13 Effect of types of clay on tensile strain.....	89
Figure 4.14 Stress – strain curves of the composites with different clays.....	90
Figure 4.15 Torque – time curve of composites based on PP, CA3 and I31PS clay.....	91
Figure 4.16 Torque - time curves of the composites with CA3 and different types of clay.....	92
Figure 4.17 Effect of types of clay (with CA3) on the X-Ray results.....	93
Figure 4.18 Effect of types of clay on tensile properties (with the presence of CA3)	94
Figure 4.19 Effect of types of clay on flexural properties (with the presence of CA3).....	95
Figure 4.20 Torque - time curves of the composites with CA4 and different types of clay.....	96
Figure 4.21 Effect of types of clay on the X-Ray results.....	97
Figure 4.22 Crystallization curves of the composites with CA4 and different clays.....	98
Figure 4.23 Melting behavior of the composites with CA4 and different clays.....	99
Figure 4.24 Effect of types of clay on tensile properties (with the presence of CA4).....	100
Figure 4.25 Effect of types of clay on flexural properties (with the presence of CA4).....	100

Figure 5.1 Torque-time curves of blends with different coupling agents.....	104
Figure 5.2 Crystallization curves of the blends (PP with different coupling agents).....	106
Figure 5.3 Melting behavior curves of the blends (PP with different coupling agents).....	106
Figure 5.4 Torque – time curves of systems based on different coupling agents with clay 15A	108
Figure 5.5 Effect of coupling agent on the X-ray diffraction results.....	110
Figure 5.6 Schematic representation of the function of coupling agent in nanocomposites.....	111
Figure 5.7 SEM photo of nanocomposites with 15A nanoclay and coupling agent CA2P	113
Figure 5.8 (a) SEM photo of nanocomposites with 15A and coupling agent CA4 (area 1).....	114
Figure 5.8 (b) SEM photo of nanocomposites with 15A and coupling agent CA4 (area 2).....	114
Figure 5.9 Crystallization curves of the nanocomposites with 15A clay and different coupling agents.....	117
Figure 5.10 Melting behavior of the nanocomposites with 15A clay and different coupling agents.....	117
Figure 5.11 DMA curves (E') of the nanocomposites with 15A and different types of coupling agent.....	119
Figure 5.12 DMA curves (E'') of the nanocomposites with 15A and different types of coupling agent	120
Figure 5.13 Effect of coupling agent on tensile properties of 15A based nanocomposites.....	123
Figure 5.14 Effect of coupling agent on flexural properties of 15A based nanocomposites.....	124
Figure 5.15 Torque – time curves of the composites with different coupling agents and I31PS clay.....	125
Figure 5.16 Effect of coupling agent on tensile properties of I31PS based nanocomposites.....	126
Figure 5.17 Effect of coupling agent on flexural properties of I31PS based nanocomposites.....	127
Figure 5.18 Effect of coupling agent on tensile properties of I30E based nanocomposites.....	128
Figure 5.19 Effect of coupling agent on flexural properties of I30E based nanocomposites	129
Figure 6.1 Effect of processing temperature on the torque curves (PP+CA4+15A).....	133
Figure 6.2 Effect of processing temperature on XRD results.....	134
Figure 6.3 Effect of processing temperature on the tensile properties.....	135

Figure 6.4 Effect of processing temperature on the flexural properties.....	136
Figure 6.5 Effect of residence time on the torque curves.....	137
Figure 6.6 Effect of residence time on XRD results.....	139
Figure 6.7 Effect of residence time on the tensile properties.....	140
Figure 6.8 Effect of residence time on the flexural properties.....	140
Figure 6.9 Effect of shear rate on torque curves	142
Figure 6.10 Effect of shear rate (rpm) on the XRD results.....	143
Figure 6.11 Effect of shear rate on the tensile properties.....	144
Figure 6.12 Effect of shear rate on the flexural properties.....	144

List of Tables

Table 1.1 North American automobile consumption of polypropylene	5
Table 1.2 Polypropylene key applications in automobile	5
Table 2.1 Mechanical properties of Nylon 6 nanocomposites	8
Table 2.2 Compositions of PPCHs, PPCC, and PP/PP-MAs.....	28
Table 2.3 Comparison of tensile properties of PP nanocomposites.....	28
Table 2.4 Composition and mechanical properties of PP/MagPP/clay nanocomposites.....	31
Table 3.1 Study parameters.....	40
Table 3.2 Characteristics of coupling agent.....	45
Table 3.3 Characteristics of nanoclays.....	46
Table 3.4 Composition of samples.....	49, 50
Table 4.1 Variables and experimental conditions of Experiment Set 4.1.....	72
Table 4.2 Crystallization and melting behavior of the composites with different clays.....	82
Table 4.3 The glass transition temperature (T_g) and soften temperature (T_s) of mixtures	85
Table 4.4 Variables and experimental conditions of Experiment Set 4.2.....	90
Table 4.5 Variables and experimental conditions of Experiment Set 4.3.....	95
Table 4.6 Crystallization and melting behavior of the composites with different clays and CA4.....	98
Table 5.1 Variables and experimental conditions of Experiment Set 5.1.....	103
Table 5.2 Crystallization and melting behavior of PP and its blends.....	105
Table 5.3 Variables and experimental conditions of Experiment Set 5.2.....	107
Table 5.4 Gallery distances of the clays in the composites.....	111
Table 5.5 Crystallization and melting behavior of the nanocomposites with 15A clay and different coupling agent.....	118
Table 5.6 Effect of coupling agent on T_g and T_s	120

Table 5.7 Variables and experimental conditions of Experiment Set 5.3.....	124
Table 5.8 Variables and experimental conditions of Experiment Set 5.4.....	127
Table 6.1 Variables and experimental conditions of Experiment Set 6.1.....	131
Table 6.2 Variables and experimental conditions of Experiment Set 6.2.....	136
Table 6.3 Variables and experimental conditions of Experiment Set 6.3.....	141

List of nomenclatures

AA	acrylic acid
ABS	acrylonitrile butadiene styrene
AFM	Atomic Force Microscopy
CEC	cations exchange capacity
C18-Mt	octadecylammonium montmorillonite
DMA	Dynamic Mechanical Analysis
DSC	Differential Scanning Calorimetry
E'	storage modulus
E''	loss modulus
EPR	ethylene propylene rubber
HDPE	high-density polyethylene
MA	maleic anhydride group
MMT	montmorillonite
M _w	weight-average molecular weight
MT2EtOH	methyl, tallow, bis-2-hydroxyethyl, quaternary ammonium
MAgPP	maleic anhydride grafted polypropylene
OEM	original equipment manufacturer
PE	polyethylene
PC	polycarbonate
PNC	polymer nanocomposites

PP	polypropylene
rpm	screw rotating speed
SEM	Scanning Electron Microscope
T_c	peak crystallization temperature recorded during cooling
T_g	glass transition temperature
T_m	melting temperature
T_s	softening temperature
TEM	Transmission Electron Microscopy
TPO	thermoplastic olefins
X_c	the degree of crystallinity
XRD	X-ray diffraction
2M2HT	dimethyl, dihydrogenated tallow, quaternary ammonium

1 Introduction

Materials and their development are fundamental to society. Major historical periods of society are associated and described with materials, such as the stone age, bronze age, iron age, steel age (industrial revolution), silicon age and silica age (telecom revolution). Therefore, materials science represents a branch of the natural sciences that is becoming increasingly important in the world dominated by the choosing of the correct material. New materials are required for a wide variety of applications, which have to be extremely specialized and at the same time economically affordable. Nowadays, many technological efforts in material science are starting from the molecular and nano scale. Nano age is coming!

1.1 Polymer composites and polymer nanocomposites (PNC)

Composites materials are a significantly attractive part of materials science since their properties can be designed to tailor different applications depending on the demands. Among three types of matrix - metal, polymer and ceramics, polymer composites are one important and rapidly developing composite materials. Polymeric materials are characterized by long chains of repeated molecule units known as “mers”. These long chains intertwine to form the bulk of the plastic. The nature by which the chains intertwine determines the plastic's macroscopic properties.

Plastics can be classified as thermoplastic or thermoset, a label that describes the strength of the bonds between adjacent polymer chains within the structure. In thermoplastics, the polymer chains are only weakly bonded (van der Waals forces). The chains are free to slide past one another when sufficient thermal energy is supplied, making the plastic formable and recyclable. In thermosets, adjacent polymer chains form strong cross-links. When heated, these cross-links prevent the polymer chains from slipping past one another. As such, thermosets cannot be reshaped once they are cured (i.e. once the cross links form). Instead, thermosets can suffer chemical degradation if reheated excessively [1].

To form polymer composites, various types of reinforcement, i.e., mineral fillers, metals, and fibers, have been added to thermoplastics and thermosets for decades. Compared to neat resins, those composites reinforced by continuous fibers can generally have a number of improved properties including tensile strength, heat distortion temperature, and modulus; those composites reinforced by non-continuous reinforcement often provide decreased costs and good dimensional stability. Thus, for structural applications, composites have become very popular. However, the density of these composites is increased, typically by 50%, and the processing often becomes difficult and expensive [2]. More recently, advances in synthetic techniques and the ability to readily characterize materials on an atomic scale have led to interest in nanometer-size materials. Since nanometer-size grains, fibers and plates have dramatically increased specific surface area compared to their conventional-size materials, the chemistry of these nanosized materials is altered compared to conventional materials.

Polymer nanocomposites are such a new class of composites derived from the ultrafine inorganic particles with at least one dimension in the nanometer range which are dispersed in the polymer matrix homogeneously at a relatively low loading (often under 6% by weight). Therefore, polymer nanocomposites combine these two concepts, i.e., composites and nanometer-size materials. These materials are attracting the attention of government, academic, and industrial researchers more and more because of their outstanding properties [9], which include: (a) they are lighter compared to conventionally filled polymer because higher stiffness and strength are realized with far less high density inorganic material; (b) their mechanical properties are potentially superior to fiber reinforced polymers because reinforcement from the inorganic layers will occur in two dimensions rather than one dimension without special efforts to laminate the composites; (c) they possess outstanding diffusional barrier properties without requiring a multipolymer layered design; nanoclays are believed to increase barrier properties by creating a maze or “tortuous path” that slows the progress of gas molecules through the matrix resin; and (d) easy recycling. At the same time, these nano-platelets are only 1 nm thick, less than the wavelength of light, so they do not impede light’s passage [5]. Moreover, due to low filler content, painted parts were claimed to exhibit better surface appearance [10-11]. On the other hand, nano-particles (such as nanoclays, nanofibers, carbon nanotubes, etc.) are so small and their aspect ratio (L/D) is so high that properties improve with lower loading and fewer penalties (such as higher density, brittleness, or loss of clarity) than with conventional reinforcements like talc or glass.

1.2 Polypropylene (PP) and its nanocomposites

Most commercial interest in nanocomposites has focused on thermoplastics. Thermoplastics can be classified into two groups: less expensive commodity resins and more expensive (and higher performance) engineering resins. One of the goals of nanocomposites was to allow substitution of more expensive engineering resins with a less expensive commodity resin nanocomposite. Substituting a nanocomposite commodity resin with equivalent performance as a more expensive engineering resin should yield overall cost savings.

PP is among the most widely used and the fastest growing classes of thermoplastics due to its good balance of physical and chemical properties, its low cost, light-weight, favorable processing and recycling characteristics. Especially remarkable breakthroughs in catalyst and process development make polypropylene compete very successfully with other environmentally less friendly and less versatile plastics. Recently, PP has found many extensive applications in both packaging and engineering fields, especially automotive [3]. According to the American Society of the Plastics Industry's 1998 edition of Facts and Figures, PP is the largest volume thermoplastic used in automobiles. Table 1.1 shows the data on the amount and applications of polypropylene used in North American automobiles. Table 1.2 shows the key application of PP in automobiles.

Table 1.1 North American automobile consumption of polypropylene [5]

Year	1994	1999	2004	2009
Million Kilograms	240	295	345	427
Avg. Kgs./vehicle	16.5	18.8	21.5	26.2

Table 1.2 Polypropylene key applications in automobile [5]

Application	1999 Kgs./vehicle	2004 Kgs./vehicle
Bumper Systems	0.9	1.8
Electrical Components	1	1.1
Engine/Mechanical Components	1.1	1.2
Interior Trim Panels	7.1	7.5

However, like all plastics, PP has a few shortcomings in performance. For example, dimensional & thermal stability, relatively low modulus and poor gas barriers in packaging limit their range of application, especially in engineering field [4-5].

In order to improve PP's competition in engineering applications, it is an important objective in PP compounding to simultaneously increase dimensional stability, heat distortion temperature, stiffness, strength, and impact resistance without sacrificing easy processability. Currently, automotive and appliance applications also use conventional

glass or inorganic-mineral filler systems with loading levels ranging from 10-50% by weight. This approach improves most mechanical properties, i.e., dimensional and thermal stability, even the modulus, but it also makes the processing difficult and increases the products' weight, which is critical in automotive and some engineering applications. On the other hand, either addition of higher barrier plastics via a multilayer structure or high barrier surface coatings are employed to improve PP gas barrier, but the decreased transparency and increased cost make them less attractive for using PP in the first place [6-8].

The emerging field of polymer-layered nanocomposites makes up these shortcomings for both packing and engineering applications, and it does so with favorable cost, processing and weight profiles. Montell North America and General Motors Research and Development announced the development of thermoplastic olefin elastomer-based PP nanocomposites that are considered to compete with PC/ABS blends and other traditional thermoplastics. Since a low percentage of organophilic layered silicates is sufficient to achieve reinforcement, nanocomposites are up to 30% lighter than competitive resins. More recently, automotive OEMs (original equipment manufacturer) and molders have also turned their attention to PP and TPO (thermoplastic olefins) nanocomposites. Some experts estimated that about 30% of nano-PP usage by 2004 will be in autos, mostly cannibalizing existing PP applications. But replacement of metals and engineering thermoplastics will follow [5]. Therefore, PP nanocomposites have attracted significant research interest [9, 10, 31, 32, 35, 49, 50, 94-97] and become new and very promising materials.

2 Literature Survey

The significant improvement of PNC's mechanical properties can be attributed to the special structure and chemistry of nanoclays. Therefore, in this literature survey, a brief introduction of nanoclays is necessary. Moreover, researchers have applied many methods to obtain nanocomposites including applying various methods to modify the surface of nanoclay and matrix, using coupling agents to improve the interface, employing different equipment and processing methods, and so on. A review of these aspects is also included.

2.1 Development of PNC

In the late 1980s, PNC were developed in both commercial research organizations and academic laboratories. The first group to demonstrate the unprecedented mechanical properties of PNC was the Toyota research center [12-15]. The first company to commercialize these nanocomposites was also Toyota, which used nylon nanocomposite parts in one of its popular car models for several years. Following Toyota's lead, a number of other companies also began investigating nanocomposites. These great attractions were from the near 100% improvement of tensile and flexural modulus and 150% improvement of heat distortion temperature with only 6wt% nanoclay in Nylon 6 nanocomposites (Table 2.1) [16]. In general, the improvements in the properties may be

attributed to the following factors: (a) large surface area and aspect ratio, (b) sub-microscopic dispersion of the clay in the polymer matrix, (c) ionic bonds between the organic polymer and inorganic clay.

Table 2.1 Mechanical properties of Nylon 6 nanocomposites [16]

Nanomer (wt. %)	Flexural Modulus (MPa)	Tensile Modulus (MPa)	HDT (°C)
0%	3404	3117	56
2%	4374 (+35%)	4220 (+28%)	125 (+123%)
4%	4578 (+61%)	4897 (+65%)	131 (+134%)
6%	5388 (+90%)	5875 (+98%)	136 (+143%)

Amongst all the potential nanocomposite precursors, those based on clay and layered silicates have been more widely investigated probably because the starting clay materials are easily available and because their potentially high aspect ratio and unique intercalation/exfoliation characteristics have been studied for a long time. The most commonly used layered silicate is montmorillonite clay. And the use of clay as precursors for nanocomposites formation has been extended into various polymer systems including epoxies, polyurethanes, polyimides, nitrile rubber, poly (vinyl alcohol), polyesters, polypropylene, polystyrene, poly (methyl methacrylate), polyethylene, polycarbonate, and polysiloxanes, among others [11, 17-24]. Before further discussion, knowledge about montmorillonite clay will be briefly introduced.

2.2 Montmorillonite clay

Montmorillonite (MMT) clay belongs to the family of the 2:1 phyllosilicates [25]. In their natural form, these phyllosilicates consist of stacks of layered crystals. As shown in Figures 2.1 and 2.2, each layered crystal is a layered structure of aluminum octahedron sandwiched between 2 layers of silicon tetrahedron. These layered crystals, which are approximately 1 nanometer or 10 angstroms thick with lateral dimensions from 30nm to several microns, are stacked parallel to each other and are bonded by van der Waals forces. In Figure 2.3, the TEM of MMT shows a cluster of platelets, 1nm thick and 50-500 nm laterally. The aspect ratio of the layered crystals is about 1000 and surface area is in the range of 750 m²/g [26]. It has a large net negative charge, which will attract positive ions (cations) to its surface, most notably sodium and calcium, as Figure 2.4 shows. The purity level, the cation exchange capacity and the aspect ratio of the clay are the most critical factors that affect the performance of the nanocomposites [27].

The gap between layered crystals is called the interlayer or the gallery. The gallery is an important characteristic of the 2:1 phyllosilicates family allowing intercalation of polymers between the layered crystals and exfoliation of these crystals. During PNC processing, the gallery chemistry can be modified in order to promote chemical bonding between the polymer and the layered crystals, which is responsible for some of the effects of the addition of nanoparticles on the microstructure and mechanical properties. The modification can be through hydrogen ion exchange or cation interaction with organic molecules or polymer [28].

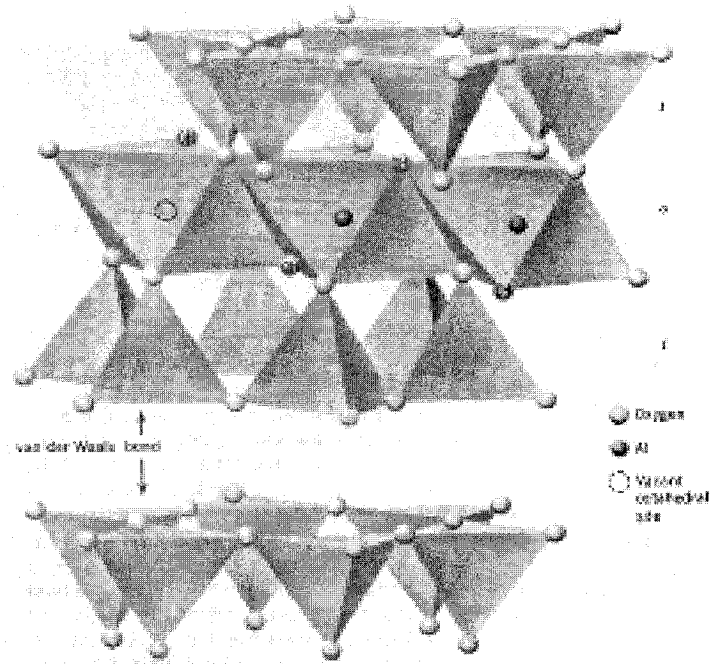


Figure 2.1 The formula and structure of montmorillonite [26]

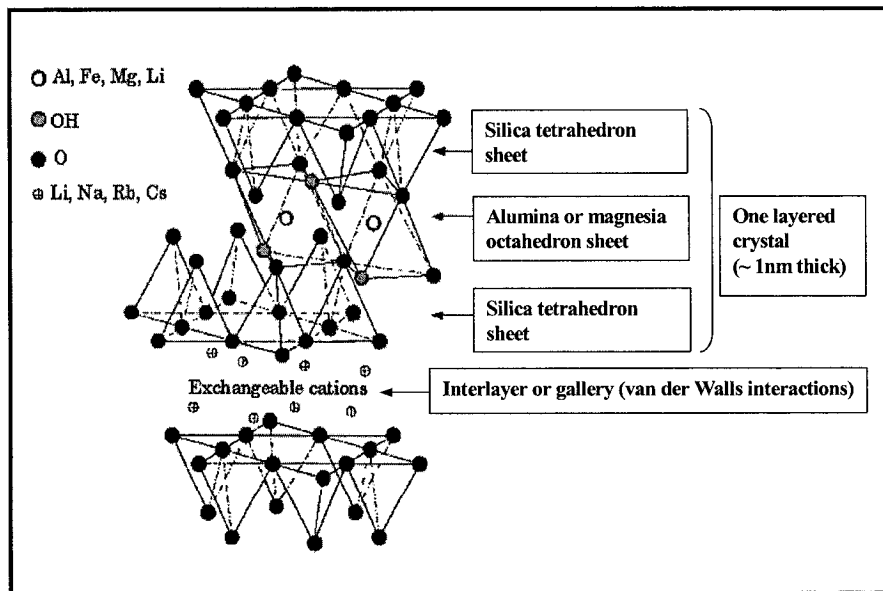


Figure 2.2 Structure of 2:1 phyllosilicates layered crystals [29]

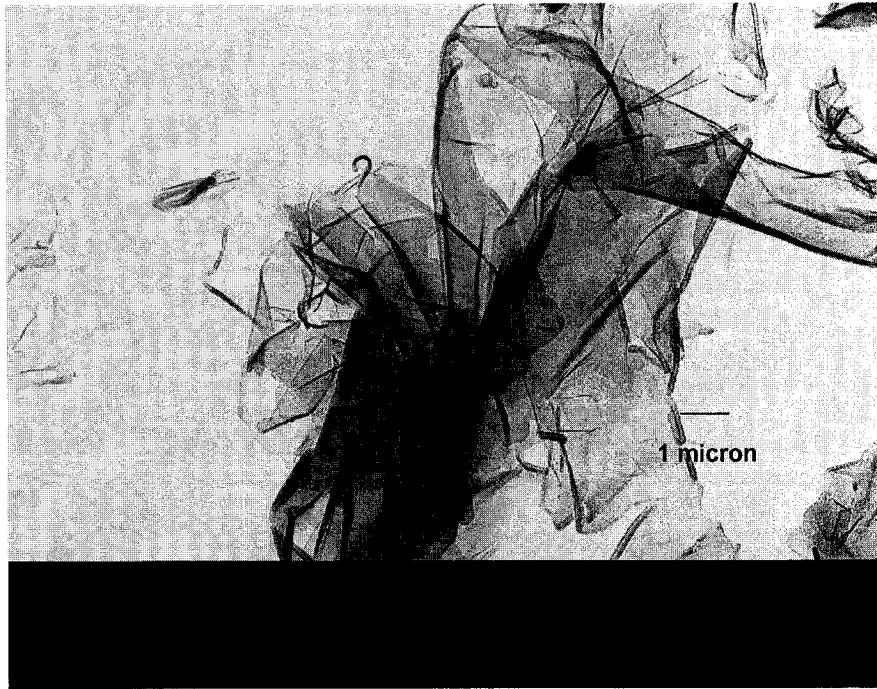


Figure 2.3 TEM of MMT clusters [30]

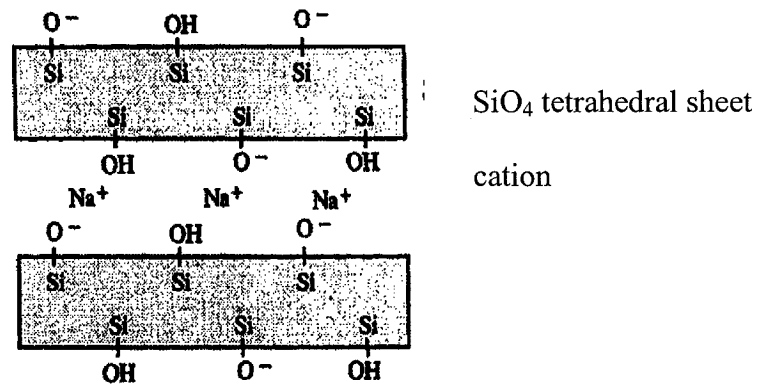


Figure 2.4 Schematic of chemistry on the clay surface

Na-montmorillonite is a specific type of montmorillonite, whose exchangeable cations located in the galleries are sodium cations. Na-montmorillonite is the most developed and commercialized clay. Since it has good affinity for water, this Na-montmorillonite and other layered clay structures are naturally hydrophilic. Therefore, they are incompatible with most polymers and hence difficult to get good mixing and dispersion. Another problem is that the clay platelets are held together tightly by electrostatic forces.

For these reasons the clay must be treated so it can be incorporated into a polymer. One way of modifying the clay surface to make it more compatible with a polymer is through ion exchanging (another way is ion dipole interaction). Since the cations on the clay surface are not strongly bound, they can be replaced by other cations, which are tailored to the polymer in which the clay would be incorporated. This process renders the clay more hydrophobic and helps to separate the clay platelets so that they can be easily intercalated and then subsequently exfoliated into the polymer.

As Figure 2.5 illustrates, montmorillonite particles are agglomerated to within a distance of about 3.5\AA . Surface treatment reduces particle-particle attraction, promoting an expansion of the distance (gallery) to above 20\AA . At this distance the particles can be separated further either by adsorbing monomer into the gallery prior to polymerization or in the case of high polymer by employing shearing force using an extrusion compounder or mixer [26]. Figure 2.6 depicts the case where dispersion occurs in the compounding operation. The modified clay sheets are separated completely and dispersed in the matrix to form nanocomposites using shear forces [26].

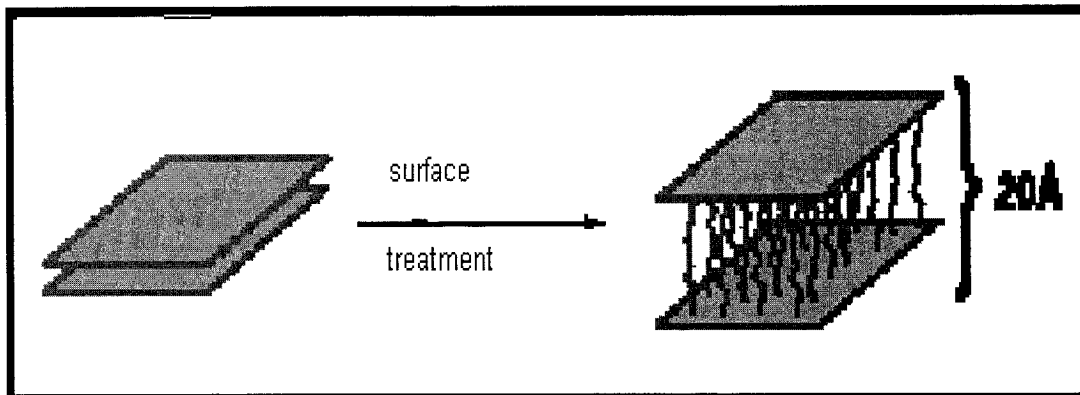


Figure 2.5 Effect of surface treatment [26]

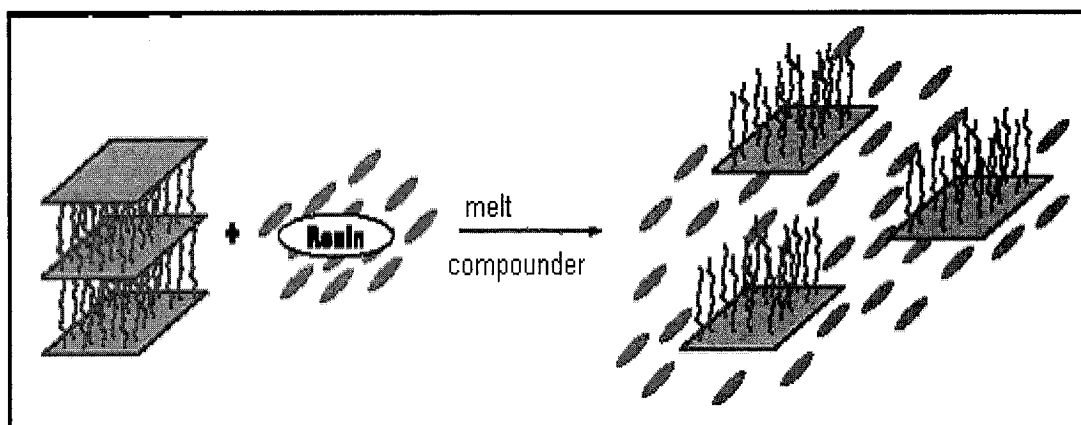


Figure 2.6 Effect of compounding operation [26]

The early work on polymeric nanocomposites was performed at Toyota Research Corporation's Central Research and Development Laboratories. In this work, the montmorillonite clay was exchanged with acid species in which a quaternary ammonium ion replaced cations on the clay surface. Many researchers have also used stearylamine and HCl [31, 63], hexadecyl-octadecyl trimethylammonium chloride [32], octadecylamine and HCl [26] to make organoclay. Since the negative charge existing in

the clay layer, the cationic head group of the alkylammonium molecule preferentially resides at the layer surface and the aliphatic tail will radiate away from the surface. The equilibrium layer spacing for organically modified clay depends both on the cation exchange capacity (CEC) of the clay, as well as on the chain length of the organic cation [33]. Toyota had demonstrated that under proper conditions, the spaces between the platelets could be filled with monomers; Nanocor Inc. and others have also found that the gallery space could be filled with oligamers and polymers as well [26].

M. Kawasumi et al [31] employed the following method to make organic clay: Sodium montmorillonite (80g, cation exchange capacity of 119meq/100g) was dispersed into 5000 ml of hot water (about 80°C) by using a homogemixer. Octadecylamine (31.1g) and concentrated HCl (11.5ml) were dissolved into hot water. It was poured into the montmorillonite-water solution under vigorous stirring by using the homogemixer for 5 min and yielded white precipitates. The precipitates were collected, washed with hot water 3 times, and freeze-dried to yield an organophilic montmorillonite intercalated with octadecylammonium (C18-Mt). The interlayer spacing of the C18-Mt was about 22 Å and the inorganic content of 69.2 wt% was found by measuring the weights before and after burning its organic parts.

2.3 PNC structures

Depending on the nature of the components used (layered silicate clay, organic cation and polymer matrix) and the process employed to associate these components, a microcomposite, an intercalated nanocomposite or an exfoliated nanocomposite can result [25]. These different types of composites are shown schematically in Figure 2.7. If no polymer is present between the crystal layers, the product is called a phase separated microcomposite (Figure 2.7 a) and it has properties in the range of traditional microcomposites. Consequently, the clay fraction in microcomposites plays little or no functional role and acts mainly as a filling agent for economic consideration. In the case of intercalated composites, the polymer is inserted between the layers of the clay and the interlayer spacing is expanded, but the layers still are in the well-ordered state (Figure 2.7 b). When the silicate layers are completely and uniformly dispersed in a continuous polymer matrix, an exfoliated or delaminated structure is obtained (Figure 2.7 c). Exfoliated nanocomposites have greater phase homogeneity than intercalated nanocomposites. More importantly, each layer in an exfoliated nanocomposite contributes fully to interfacial interactions with the matrix, which is the primary reason why the exfoliated clay state is especially effective in improving the properties of clay composites [34].

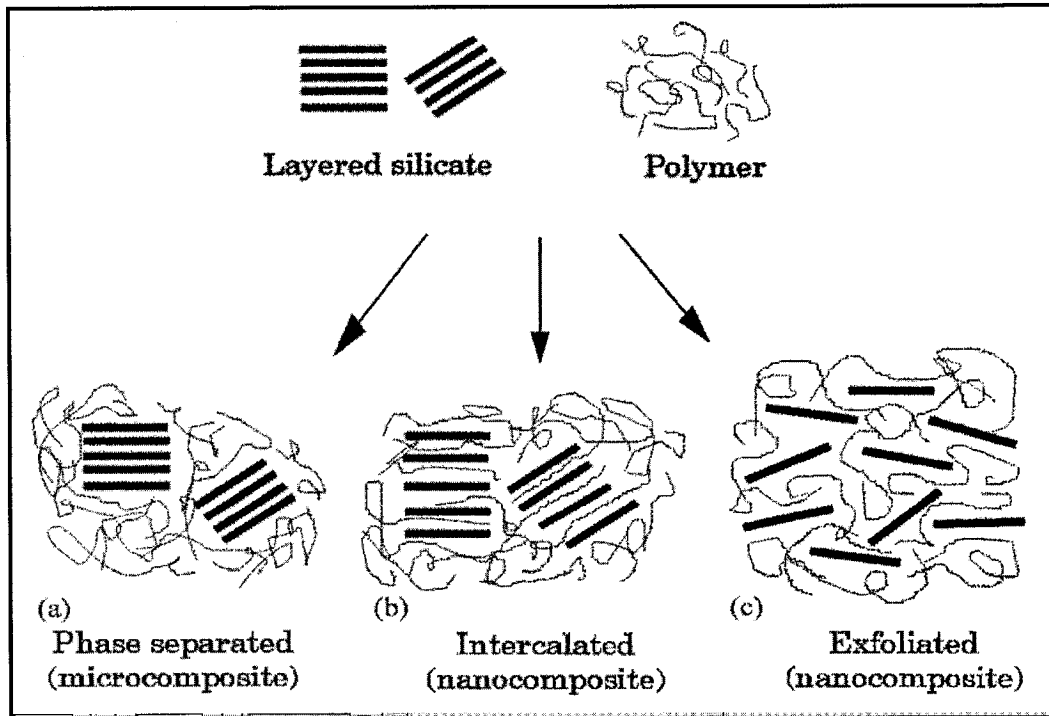


Figure 2.7 Schematic of different types of composite arising from the interaction of layered silicates and polymers: (a) phase-separated microcomposite; (b) intercalated nanocomposites and (c) exfoliated nanocomposites [25].

In practice, partially intercalated and exfoliated structures are generally observed. In the intercalated or exfoliated nanocomposites, the improvement in properties can often be observed, such as tensile and flexural properties, barrier properties, and thermal stability and flame retardance [35, 36].

Two methods are commonly employed to characterize these structures: X-Ray Diffraction (XRD) and Transmission Electron Microscopy (TEM).

XRD is used to identify intercalated structures. In such nanocomposites, the repetitive multilayer structure is well preserved, allowing the interlayer spacing to be determined. The intercalation of the polymer chains usually increases the interlayer spacing, which leads to a shift of the diffraction peak towards lower angle values (angle and layer spacing values related through the *Bragg's relation*: $n \lambda = 2d \sin \theta$, where λ is wavelength of X-ray radiation, d is the spacing between diffracted ionic lattice planes, and θ is the measured diffraction angle). Figure 2.8 show the XRD curves corresponding to different structures [25].

In the exfoliated structure, no more diffraction peaks are visible in the XRD curves either because of a much larger spacing between the layers (i.e. exceeding 8nm in the case of ordered exfoliated structure) or because the nanocomposites do not present ordering anymore [9]. TEM is used to characterize structures for intercalated and exfoliated nanocomposites. Figure 2.9 [37, 38] shows the TEM micrographs obtained for an intercalated and an exfoliated nanocomposite. Besides these two well defined structures, most nanocomposites present both intercalation and exfoliation structures. In this case, a broadening of the diffraction peak is often observed and one must rely on TEM observation to define the overall structure.

In addition, sometimes Atomic Force Microscopy (AFM) and Scanning Electron Microscopy (SEM) are also employed to identify the structures of PNC [39, 40].

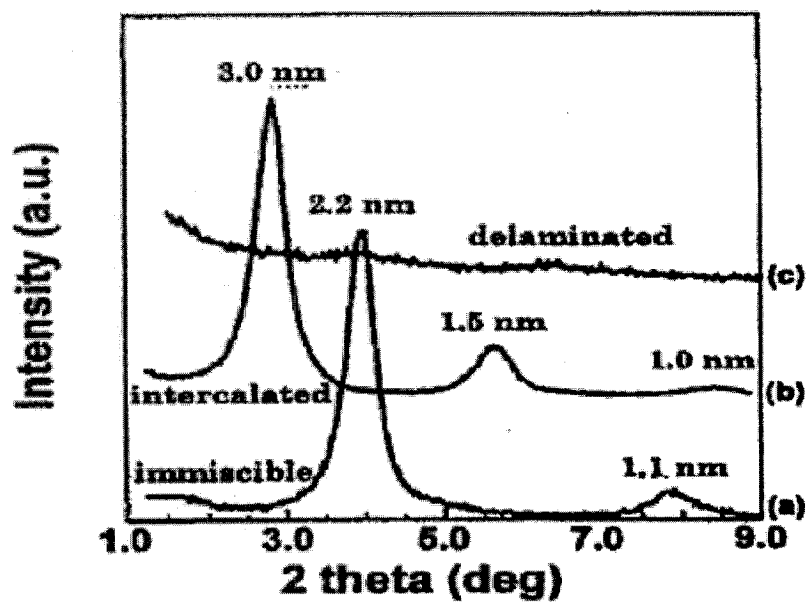


Figure 2.8 XRD curves [25]: (a) fluorohectorite in HDPE matrix (no intercalation, no exfoliation was achieved); (b) nanocomposite of fluorohectorite in polystyrene (intercalation was achieved); (c) nanocomposite of fluorohectorite in silicon rubber (exfoliation was achieved; diffraction peaks are not visible).

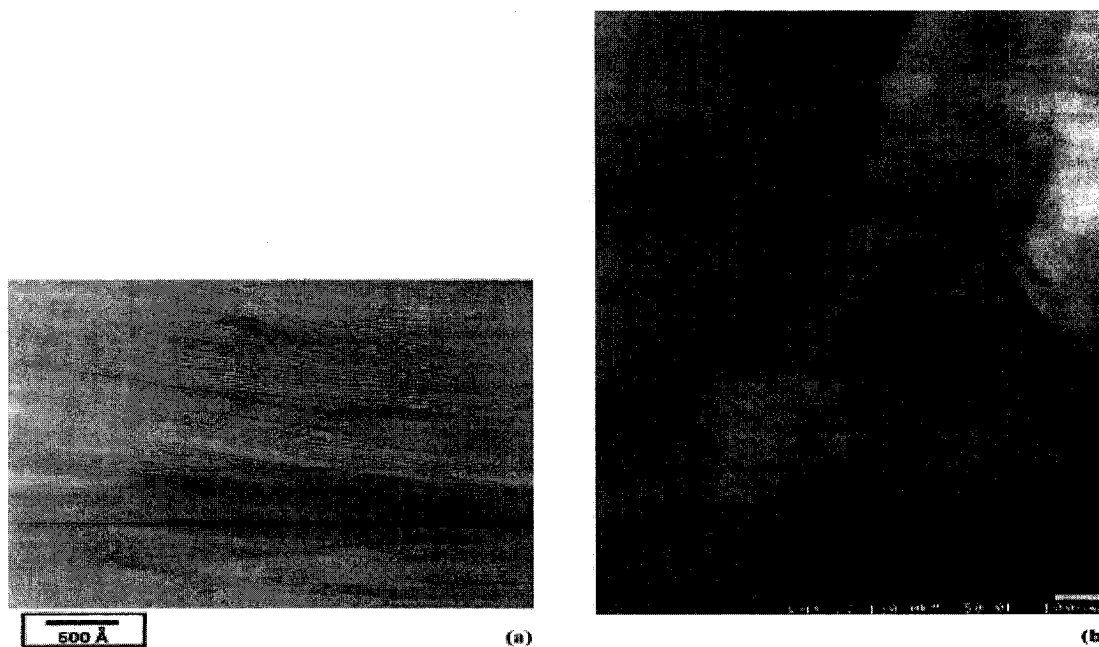


Figure 2.9 TEM micrographs of nanocomposites: (a) intercalated nanocomposite; (b) exfoliated nanocomposite [37, 38]

2.4 PNC fabrication

This subsection intends to describe how the nanocomposites are produced. Fabrication is an important step to obtain nanocomposites and there are many factors that need to be considered in the process. In general, researchers developed three processes to fabricate PNC: In-situ polymerization process, solution process, and melt intercalation (or compounding) process [29].

2.4.1 In-situ polymerization process

In-situ polymerization is a method in which fillers or reinforcements are dispersed in monomer first and then the mixture is polymerized using a technique similar to bulk polymerization. Using this method, inorganic particles may be evenly dispersed in the polymer matrix, creating composites with good processability as a result of their flow properties. This method has been industrialized by Ube Industries to produce the commercial grade 1015C2 of the PA6/montmorillonite nanocomposites.

The process employed for the preparation of PA6 nanocomposites of commercial grade 1015C2 is summarized in Figure 2.10 [101]. Na-montmorillonite clays are modified through the first processing step. Na-montmorillonite is hydrated in the presence of hydrochloric acid (HCl) and aminolauric acid ($\text{H}_3\text{N}^+(\text{CH}_2)_{11}\text{COOH}$) (ALA). During this submersion, the cations of sodium located in the interlayers are substituted by the cations of the ALA and ALA-montmorillonite was obtained. In the second processing step, the

ALA-montmorillonite is mixed with ϵ -caprolactam monomers. A small amount of polymerization catalyst is added and mixture is stirred and heated up. The cooled and solidified product is crushed, washed and dried. For less than 15% of ALA-montmorillonite, an exfoliated structure is obtained as evidenced by XRD and TEM [13].

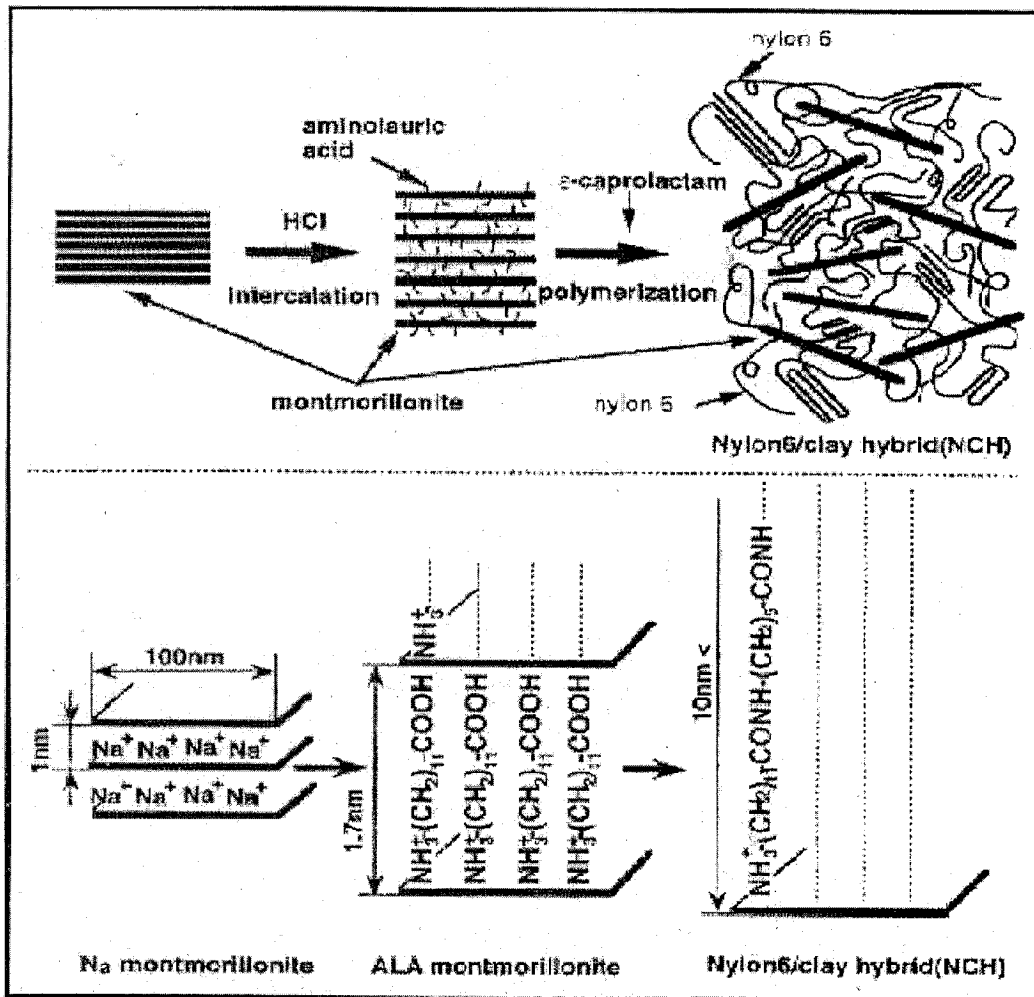


Figure 2.10 Process steps for preparation of PA6 nanocomposites [101]

In a very recent work, J.S. Ma et al [41] discussed the synthesis of polypropylene/clay nanocomposites by using the in-situ intercalative polymerization. The Na-montmorillonite was modified by hexadecyl-octadecyl trimethylammonium and activated by the Ziegler-Natta catalyst ($\text{TiCl}_4/\text{MgCl}_2$), the activated montmorillonite served as a

catalyst for propylene polymerization. During the polymerization, the clay structure would be destroyed and exfoliated by the growing PP molecules. The XRD patterns and TEM image showed that the clay in the nanocomposites was exfoliated into nanometer size and dispersed uniformly in the PP matrix. The storage modulus of the nanocomposites increased with increasing clay content, particularly at temperatures higher than T_g , where the storage modulus was about three times that of the pure PP.

The biggest drawback to this route is that large materials suppliers thus far have not been willing to invest in capacity to produce nanocomposites.

2.4.2 Solution process

In this process, the layered clays are exfoliated into single layers using a solvent in which the polymer or the prepolymer is soluble. The polymer added to the solvent is then adsorbed on to the delaminated sheets. This technique has been widely used with water-soluble polymers: poly (vinyl alcohol), poly (ethylene oxide), etc.

2.4.3 Melt intercalation (compounding) process

In this process, the layered clays are mixed with the polymer matrix in the molten state (usually under shear force) and the polymer extends into the interlayer space if the compatibility between the interlayer treated surfaces and the polymer is sufficient. The stacked layer structure of the clay might be expected to separate when subjected to

mechanical shear, particularly after expanding the interlayer space through intercalating organic modifiers (intercalants). This approach would allow nanocomposites to be formulated directly using ordinary compounding devices such as extruders or other mixers according to need without the necessary involvement of resin producers. It is a promising new approach for forming nanocomposites that would greatly expand the commercial opportunities for this technology. If technically possible, melt compounding would be significantly more economical and simple than in situ polymerization processes. Figure 2.11 shows the dispersion mechanisms of melt intercalation.

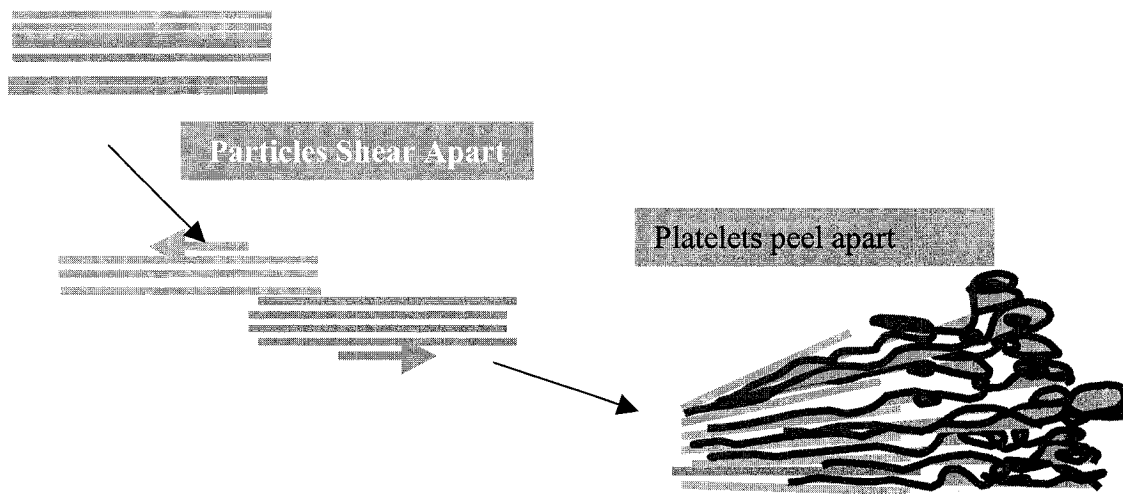


Figure 2.11 Dispersion Mechanism of melt intercalation [30]

2.5 PP nanocomposites

2.5.1 Challenges in formulation of PP nanocomposites

As mentioned above, MMT has negatively charged surfaces and is naturally hydrophilic while PP does not have any polar groups in its backbone and is one of the most hydrophobic polymers. Therefore, they repel each other and no direct intercalation happens between them when PP and clay are simply mixed together, and the properties are in the microcomposites' range. Actually, the nanometer dispersion of silicate layers in a PP matrix was not realized even by using a montmorillonite treated with a dioctadecyldimethylammonium ion (DSDM-Mt), in which the polar surfaces of the clay mineral should be covered with one of the most hydrophobic alkylammonium ions [42].

Vaia and Giannelis [43-45] found that, in general, the outcome of polymer intercalation is determined by an interplay of entropic and enthalpic factors. Entropy is a measurement of the amount of disorder in a system, and natural processes will tend to go in a direction of greater entropy or greater disorder. Enthalpy is the total kinetic and potential energy of a system under constant pressure, and its changes can be determined from the energy changes of the surroundings. Dispersion of MMT in a polymer requires sufficiently favorable enthalpic contributions to overcome any entropic penalties (Polymer molecules may have more randomness outside the galleries than inside the galleries). Favorable enthalpy of mixing for the polymer/organic MMT can be achieved when the polymer/MMT interactions are more favorable compared to the surface modifier/MMT interactions [43-45]. The challenge existing between PP and clay is that the entropic

barriers can prevent any dispersion of the inorganic fillers in such polymers. In addition, since no excess favorable interaction exists in the PP-clay system compared to the alkylmodifier-clay system, the miscibility of PP and alkyl modified clay is also difficult [33].

2.5.2 Miscibility strategies

Researchers have found many ways to improve the miscibility of hydrophobic polymers and hydrophilic clay [25, 46- 47]. These ways can be classified in three routes:

2.5.2.1 Modifying clay surface

This method is to make the inorganic (polar) surface of clay become organic to be more miscible with nonpolar polymer. The usual way to do this is ion exchanging which uses the cationic-organic surfactants, such as alkyl-ammoniums to replace the unbound cations (such as Na^+) on the clay surface. This aspect has been introduced in Section 2.2.1. Currently, many types of modified clays are available from nanoclay manufacturers, such as the Cloisite and Nanomer series.

Another way is using an organic swelling agent (whose boiling point is situated between 100~200°C, such as ethylene glycol, naphtha or heptanes) to increase the interlayer spacing. The swollen organo-modified clay was then compounded with PP in a twin-screw extruder at 250°C. The swelling agent was volatized during extrusion process [25].

2.5.2.2 *Modifying matrix*

1) Matrix functionalization In this technique, very small amounts of functional groups (0.5–2 mol%) are added randomly across the polymer [47]. For example, in the case of polypropylene, just 0.5 mol% of functional groups (methyl-styrene, maleic anhydride, or 3-hydroxyl-butylene-styrene) is sufficient to promote miscibility with clays. And at such levels the functional group is not enough to change in any measurable extent the polymer characteristics, such as crystallinity, melting point, etc. However, this method needs the resin manufacturers involved to synthesize the functionalized polymer, and this becomes the major impedance to research and widen this technology.

2) Using coupling agent is the most popular way to modify the matrix because it is simple, economical and can be processed by the usual mixing instruments. Coupling agent is polyolefin oligomer modified with either maleic anhydride (MA) or hydroxyl groups (OH) or other functional groups, which should include a certain amount of polar groups (i.e. –OH, –COOH) to intercalate between silicate layers through hydrogen bonding or other chemical bonding to the oxygen group or negative charges of the silicate layers. In addition, coupling agent should have long molecular chains that are compatible with polyolefin matrix. As in the production of conventional composites, grafted polyolefins are frequently used as coupling agents. Among them, polyolefin containing grafted maleic anhydride (MA) or acrylic acid (AA) are the most attractive candidates because of their high reactivity and ready availability. Coupling agents usually used in PP matrix is maleic anhydride grafted polypropylene (MAgPP) [31, 32, 48-50, 93].

2.5.2.3 Modifying matrix and clay surface

Most researchers have used both ways (modifying matrix and clay surface at the same time) to improve the miscibility of clay and nonpolar polymers, especially for PP because using only one way is not enough to overcome the typical nonpolarity of PP [31, 32, 48-50, 93]. However, the results varied with the types of intercalant and functional group. In the next subsection some research in the field of PP nanocomposites will be described.

2.5.3 Research in polypropylene nanocomposites

PP nanocomposites have been studied widely due to their commercial importance, but exfoliation of the nanoclays appears to be more difficult to achieve than in the case of polyamides, which might be due to several issues related with thermodynamic interactions in the modified clay-matrix-coupling agent system. Some research works are introduced below.

R. Peter et al [51] used synthetic sodium fluoromica as water swellable layered silicate, which was rendered organophilic by means of cation exchange with various protonated alkyl amines such as butyl (C₄), hexyl(C₆), octyl(C₈), dodecyl(C₁₂), hexadecyl(C₁₆), and octadecyl(C₁₈) amine. Interlayer spacing of the organophilic silicates increased with increasing alkyl chain length of the amine. Only C₁₂, C₁₆, and C₁₈ amine modifiers in conjunction with MAgPP as coupling agent promoted exfoliation and self-assembly of individual silicate layers within the polypropylene matrix. Interlayer distance increased

with increasing content and increasing anhydride functionality of MAgPP. Only 10 wt% of fluoromica modified with C₁₆ amine in conjunction with 20 wt% of MAgPP containing 4.2 wt% maleic anhydride grafts was sufficient to achieve effective polypropylene matrix reinforcement, as reflected by increase of Young's modulus from 1490 MPa to 3460 MPa and increase of yield stress from 33 MPa to 44 MPa with respect to bulk PP.

M. Kawasumi et al [31, 32] researched the three components (PP, MAgPP and modified clay) which were melt-blended in a twin-screw extruder at 210°C to obtain nanocomposites. The clay concentration is 5 wt%. It is found that there are two important factors to achieve the exfoliated and homogeneous dispersion of the clay layers in the hybrids: (1) the intercalation capability of the coupling agents in the layers and (2) the miscibility of the coupling agents with PP. To form an exfoliated structure requires (1) relatively high MAgPP content—typically 22 wt%, (2) sufficient polar functionalization of MAgPP chain (acid value=26mg KOH.g for Mw=40,000). They found the composites exhibit higher storage modulus compared to those of PP especially in the temperature range from T_g to 90°C. The highest relative storage modulus at 80°C of the composites based on a mica and the miscible MAgPP is as high as 2.0 times to that of PP and is 2.4 times to that of the PP/ MAgPP mixture. However, the relative content in maleic anhydride cannot exceed a given value in order to keep some miscibility between MAgPP and PP chains. When too many carboxyl groups are spread along the polyolefin chains (e.g. acid value=52mg KOH/g), no further increase in the interlayer spacing was obtained in clay/PP/MAgPP blends, leading rather to the dispersion of MAgPP

intercalated clay in the PP matrix. The mechanical properties they obtained are shown in Tables 2.2, 2.3.

Table 2.2 Compositions of samples [31,32]

Sample	C18-Mt/PP-MA [C18-Mt + PP-MA] (Wt %)	PP-MA (Wt %)	PP (Wt %)
PPCH-1/3	C18-Mt/PP-MA-1/3	[7.2 + 21.6]	—
PPCH-1/2	C18-Mt/PP-MA-1/2	[7.2 + 14.4]	—
PPCH-1/1	C18-Mt/PP-MA-1/1	[7.2 + 7.2]	—
PPCC	C18-Mt	6.9	—
PP/PP-MA-22	—	21.6	78.4
PP/PP-MA-7	—	7.2	92.8

Notes: PPCH denotes the composites based on PP with clay and coupling agent; PPCC denotes the composites based on PP with only clay; PP/PP-MAs denotes the blends based on PP with coupling agent.

Table 2.3 Comparison of tensile properties of PP nanocomposites[31,32]

Sample	Modulus (MPa)	Strength (MPa)	Elongation (%)
PPCH-1/3	1010 ⁺²⁵ ₋₄₈ (1.29)	31.7 ^{+0.2} _{-0.2} (0.98)	5.6 ^{+0.3} _{-0.3}
PPCH-1/2	964 ⁺¹³ ₋₁₂ (1.23)	34.6 ^{+0.2} _{-0.2} (1.06)	8.6 ^{+0.5} _{-0.5}
PPCH-1/1	838 ⁺²² ₋₄₅ (1.07)	29.5 ^{+0.5} _{-0.2} (0.91)	7.5 ^{+0.4} _{-0.5}
PPCC	830 ⁺²² ₋₄₅ (1.06)	31.9 ^{+0.1} _{-0.2} (0.98)	105 ⁺³⁵ ₋₃₀
PP/PP-MA-22	760 ⁺²⁴ ₋₅₇ (0.97)	32.6 ^{+0.2} _{-0.3} (1.00)	40.3 ⁺¹⁶ ₋₁₁
PP/PP-MA-7	714 ⁺²⁰ ₋₃₂ (0.92)	31.4 ^{+0.2} _{-0.1} (0.97)	> 150
PP	780 ⁺¹⁸ ₋₁₀	32.5 ^{+0.1} _{-0.2}	> 150

*The values in parentheses are the relative values of the hybrids to those of PP.

N. Hasegawa et al [52] prepared polyolefin-clay hybrids by using maleic anhydride modified polyolefins (PP, PE, EPR (ethylene propylene rubber)) and organophilic clay during melt blending, wherein the silicate layers of the clay were exfoliated and homogeneously dispersed at the monolayers. The schematic representation of the clay dispersion process is shown in Figure 2.12. The driving force of the intercalation

originates from the strong hydrogen bonding between the maleic anhydride groups of the silicate layers. The polyolefin-clay hybrids exhibited remarkable reinforcement compared to conventional composites filled with talc which were dispersed at the micrometer level. The relative storage modulus of MAgPP/C18-Mt is 2.3 times higher than that of the matrix polymer at 60°C.

M. Kato et al [49] modified the Na-montmorillonite by octadecyl ammonium (C18-Mt) and applied them with different weight ratios of coupling agent (MAgPP) to melt-mix under shearing (at 200°C for 15min) to obtain nanocomposites. The mixing weight ratio of MAgPP and C18-Mt changed from 1:3 to 3:1. The results displayed that as the weight of MAgPP in the mixtures increased, the dispersion became better and the basal spacing of the clay layers expanded. When the ratio reached to 3:1, the average of the basal spacing could be 7.2nm, but the structure was still intercalated. In addition, MAgPP with a low maleic anhydride content (acid value=7mg KOH/g for $M_w=12000$) did not intercalate under the same conditions, showing that a minimal functionalization of the PP chains has to be reached for intercalation to proceed.

In a U.S patent published as WO 01/85831 A2 [53], M. Ladika et al also suggested the use of an organic cation (compatibilizer) having a pendent polymer chain (a polymer chain extending from a cation site that does not terminate with a cation site) which is miscible with the bulk polymer and the average molecular weight should be more than 3000. Ordinarily, the polymer of the pendent polymer chain is the same polymer type as the bulk polymer. The organic cation can be a polymer having a plurality of cationic sites

or a single cation site such as an amine hydrochloride group, a quaternary ammonium group, a sulfonium group or a phosphonium group and have a pendent polymer chain which may be linear or branched. They use amine terminated 15,000 molecular weight polypropylene as the compatibilizer and get ideal result. They suggest that in polyolefin nanocomposites, the organic cation content is 0.1%-10% and the layered silicate content is 2%-20%.

M. Mehrabzadeh et al [54] used melt processing to get the HDPE/clay and HDPE/nylon-6/clay nanocomposites. They observed that the intensity of the characteristic peak of X-ray curve in HDPE/organic-clay (5%) is reduced and a broad peak is observed at about $2\theta=2.8^\circ$ ($d_{001}=3.16$ nm) compared with the clay's peak $2\theta=3.67^\circ$ ($d_{001}=2.41$ nm), which suggests that the structure is both intercalated and exfoliated. In the blend of HDPE/nylon-6: 80/20 with 5% modified clay, the characteristic peak of the clay disappeared, indicating that the structure is exfoliated, apparently due to incorporation of the polar nylon-6 in the HDPE. DSC results showed that the clay does not have an effect on melting temperature (T_m), crystallization temperature (T_c), and crystallinity of HDPE although the clay plays an important role in enhancement of the crystallization.

P. Kodgire et al [55] carried out the melt intercalation of PP and organically modified clay by a single screw extruder. They verified that the expansion of the gallery distance of the clay was governed by the interaction between the clay treatment and the coupling agent. A partially exfoliated nanocomposites was obtained. And with 4% clay and 12wt% coupling agent, 35% and 10% increases in the tensile modulus and tensile strength, respectively.

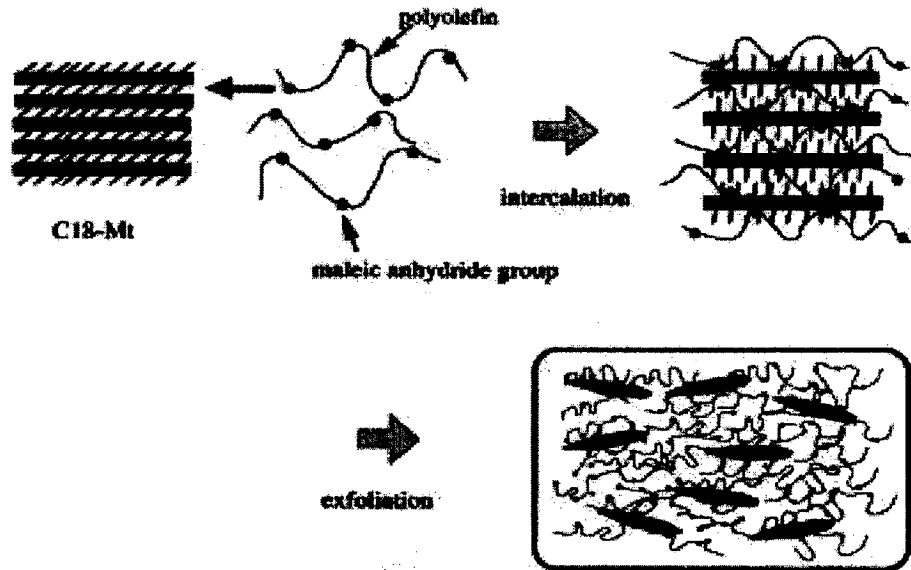


Figure 2.12 Schematic representation of the clay dispersion process [52]

Table 2.4 Composition and mechanical properties of PP/MAGPP/clay nanocomposites [56]

PP (wt%)	MAGPP (wt%)	Type of clay	Clay (wt%)	TGA clay content (wt%)	Modulus (MPa)	Tensile strength (MPa)
100	-	-	-	-	1828 ± 33	34.3 ± 0.9
91	9	-	-	-	1797 ± 81	36.0 ± 0.4
79	21	-	-	-	1672 ± 36	35.4 ± 0.2
88	9	Bentonite	3	2.6	2024 ± 43	36.8 ± 0.2
72	21	Bentonite	7	4.8	2130 ± 56	35.5 ± 0.3
88	9	Nanomer I30.TC	3	2.4	2282 ± 27	36.8 ± 0.4
72	21	Nanomer I30.TC	7	4.5	2597 ± 34	36.2 ± 0.1

* Bentonite and Nanomer I30.TC were two types of clay with different surface treatment.

D. Garcia-Loez et al [56] investigated the effect of coupling agent on clay dispersion in PP/clay nanocomposites using an intermeshing twin screw extruder operating at 190-210°C and 50rpm. They found clay modification and processing conditions are not enough to provide an appropriate nanometric dispersion of clay layers and a homogeneous distribution of the clay in the PP matrix. The mechanical properties varied with the types and content of coupling agent. They used the ratio of coupling agent and clay of 3:1. When 9wt% MAgPP and 3% clay applied, the tensile modulus and strengths increased only 20% and 5%, as shown in Table 2.4. The XRD results displayed that not too much expansion happened in the galleries of the clay.

M. T. Ton-That et al [57] prepared PP nanocomposites by melt processing using Brabender mixer in the presence of MAgPP as a coupling agent. They reported an increase in Young's modulus and tensile strength of approximately 24% and 7% respectively as a result of the addition of 6% of nanoclays and partially optimized melt intercalation conditions.

2.6 Summary

Combining the significant improvement of thermo-mechanical properties (attained at very low filler content (5% or less)) and the ease of production (simply employed conventional equipment, i.e. extruder or mixer or injection molding machine), the polymer - layered silicate nanocomposites are becoming a very promising new class of materials. They are already commercially available and applied in car and food package

industries. Undoubtedly, their competitive properties and low costs are paving ways to much boarder range of application.

From previous works, the melt intercalation method to prepare nanocomposites has been accepted and widened in the research due to its simple, economic and good results. However, a large number of parameters can influence nanocomposites formation: (1) molecular architecture of alkyl ammonium used in ion exchange; (2) additives present during silicate modification; (3) processing temperature; (4) shear rates; (5) coupling agent's type and content, and (6) polymer molecular weight, etc. Among them, clay modification (factor 1, 2) and matrix modification (factor 5, 6) have a direct influence on mechanical properties of the obtained nanocomposites [65]. Processing parameters also have an important influence on the results. Based on the above survey of literature, of the matrix modifications, the coupling agent is one crucial factor that is directly related to the quality of adhesion of matrix with clay (interface) and dispersion of the clay. Currently, most research still uses coupling agents based on maleic anhydride (MAgPP) or hydroxyl (PP-OH) groups and focuses on the effect of concentration of coupling agent. However, the properties of nanocomposites based on these types of coupling agent were not satisfactory, as shown above. Therefore, it is desirable to develop a new type of coupling agent having a suitable structure and chemistry for the formation of nanocomposite systems.

2.7 Objectives of the thesis

The main objective of this thesis was to study the effect of the chemistry (modification of clay and matrix) and processing conditions on the formation of PP nanocomposites using melt process in order to optimize the mechanical properties through maximizing the clay dispersion in PP matrix and promoting the interface between them.

PP has received a lot of attraction because of its high properties/cost. The research in PP nanocomposites is providing wide application for PP. Since PP is typically hydrophobic, it is impossible to disperse the hydrophilic clay well. Therefore, the use of coupling agent (matrix modification) is always essential for the production of PP nanocomposites. Fabrication of PNC can be done by different processes, including in-situ, solvent and melt process. Among them, melt process is more economical and simple and widely used for the fabrication of PP nanocomposites. In this study, the different clays, the different coupling agents and the different processing conditions were investigated using the melt process to understand the factors which affect the formation of PP nanocomposites.

Samples were prepared by Brabender and compression molding. Specimens were tested by various experimental methods, including X-ray diffraction (XRD), Differential Scanning Calorimetry (DSC), Dynamic Mechanical Analysis (DMA), Scanning Electron Microscope (SEM), and mechanical testing machines.

The first step of the experiments was to study five types of commercial clay (15A, 20A and 30B from Southern Clay Products Inc.; I30E and I31PS from Nanocor Inc.), which had been treated by different types and concentration of modifiers, and to find the effect of modifiers on the properties.

Second step was to research five types of coupling agents (CA1, CA2 and CA2P were coupling agents with maleic anhydride group; CA3 was coupling agent with amine group; and CA4 was coupling agent with ammonium ion group), which had different molecular weights and functional groups and could interact with the clay surface and PP matrix. The goal of this step is to find the effects of functional groups and more effective coupling agents for PP.

Third step was to detect the effect of processing parameters on the formulation and the mechanical properties of PP nanocomposites, including processing temperature, mixing time and shear force (screw rotating speed rpm).

These three steps form the integrated procedure to research and prepare PP nanocomposites. The results were verified by various experiments and discussed from different angles. The discussions attempt to integrate the results and to establish relationships between the experimental results and concepts presented in the literature survey. In general, this thesis presented the knowledge on polymer nanocomposites, a clear way to obtain PP nanocomposites that have optimal properties, and the guide for further research.

3 Materials and Experiments

3.1 Selection of materials and experimental design

Based on literature survey, clay, matrix modification and processing parameters are three major factors which influence the formulation of PP-clay nanocomposites. Therefore, this thesis experimental design has mainly considered these three aspects:

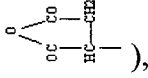
- Clay: using different intercalants (organic modifiers)
- Matrix: adding different coupling agents
- Processing conditions: temperature, residence (mixing) time, rpm

3.1.1 Clay

Surface treatment of MMT clay is a difficult work and the quality is affected by many factors. A lot of researchers have been studying this topic [31-38] and those that have resulted in commercial benefits have been developed by manufacturers. Currently many types of organo-clay are commercially available in the market, which are mainly from Nanocor Inc. and Southern Clay Products Inc. Since these two manufacturers have strong technology and have developed several types of organo-clay that are more or less compatible with PP, the work on surface treatment was not considered in this project. What was done was to select the most effective type with our selected coupling agents

among the commercial clays. In the products of Southern Clay, Cloisite 15A and 20A, which are modified by alkyl ammonium and have relatively large gallery distances, are considered to be most suitable with PP. Cloisite 30B clay has hydroxyl group which is different from Cloisite 15A and 20A, but may have a great potential for the interaction with certain coupling agent. It was therefore selected. For products of Nanocor Inc., Nanomer I31PS, which is surface-treated by octadecylamine and silane modifier, and Nanomer I30E, which is modified by octadecylamine group, were also considered. All of them are from Na-montmorillonite clay, which are briefly called clay or nanoclay in following experiments.

3.1.2 Coupling agents

The coupling agent is crucial to create better interfaces and dispersion between matrix and clay. Since it has to be miscible with the matrix and have affinity with the clay surface, some oligomers that have alkyl chains that are like PP and have functional groups, such as maleic anhydride () , hydroxyl (-OH), amine (NH₂-) or ammonium (NH₃⁺-), should be used. Among them, maleic anhydride grafted PP (MAgPP) has been widely used. In principle, the desired nanoscale dispersion of org-MMT in PP matrix may be achieved with MAgPP via strong hydrogen bonding between the hydroxyl groups of the silicates and the MA groups of the MAgPP, while the chemical similarity of the PP backbone of MAgPP and the PP ensure a good compatibility between the matrix and coupling agent [31].

On the other hand, considering clay nature, amine and ammonium ions may interact with clay surface effectively. These types of coupling agent are not commercially available. Researchers [64] from IMI (Industrial Materials Institute of National Research Council of Canada) have developed an amine - terminated coupling agent which was made through reactive extrusion of maleic anhydride grafted PP and Jeffamine. Such amine groups can also be transferred to ammonium ions by acid environment, so ammonium - terminated coupling agent can be obtained without difficulty. Therefore, it is desirable to detect the effects of these two new types of coupling agents.

In this study, three types of coupling agents with maleic anhydride groups were also studied in order to find the effects of MA contents, molecular weight and the purity of coupling agent on the formation of nanocomposites.

3.1.3 Composition

From the literature survey, the relative content of MAgPP cannot exceed a certain value depending on the molecular weight and grafting amount of MA in order to ensure the miscibility between MAgPP and PP chains and minimize the cost. It has been found that even the addition MAgPP as high as 22 wt% (the clays loading was 5 wt %) cannot produce a fully exfoliated structure [33, 34], while it caused the loss of ductility and toughness. Therefore, lower content of coupling agent and clay tend to be more attractive in terms of cost effectiveness and efficiency [53-57]. As a result, the coupling agent has been kept as low as 6 wt% in this study.

Similarly, it has been reported that the modulus of PP nanocomposites increased with nanoclay loading [32], while strength, ductility and toughness decreased. Therefore, the clay content has been kept as low as 3wt % in all samples, while the ratio of coupling agent to nanoclay was kept constant at 2:1.

3.1.4 Processing parameters

In melt intercalation (Figure 2.11), clay particles are mixed with polymer matrix in the molten state by shear force which is produced by the screw rotating in mixers or extruders. In this procedure, products are often affected by processing parameters, such as temperature, shear rate, residence time and even screw configuration [65]. However, how these factors affect the formulation of nanocomposites has seldom been reported. Therefore, some experiments were necessary in this thesis with the aim of maximizing the interaction between matrix and organo-nanoclay, while minimizing the degradation and oxidation of the materials at the same time.

3.1.5 Equipment

As the crucial step to disperse the nanoclay into the matrix in melt intercalation, the mixtures or systems have to be mixed in an extruder or a mixer. Most researchers employed twin - screws extruder rather than single screw extruder because twin-screws extruders have stronger shear forces that are beneficial to exfoliate the clay. Although most work was done in an extruder, it is difficult to change one single processing

parameter while other parameters are kept constant. For example, to increase residence time, one has to lower the feeding rate and/or reduce the screw speed. In this aspect, another mixer – Brabender- can give us more flexibility in changing different parameters that may affect the dispersion. In Brabender, the residence time can be varied while the rotating speed (rpm) of screws does not need to be changed. At the same time, when rpm is changed, residence time can be kept constant. Therefore, in this thesis, the Brabender mixer was employed to mix the nanoclay, coupling agent and matrix.

3.1.6 Study parameters

In order to fulfill the objective described in Section 2.7, the experiments have been designed as described in Table 3.1.

Table 3.1 Study parameters

Objectives	Effect of clay types	Effect of coupling agent	Effect of processing parameters
Variables	Five types of clay: Cloisite*: Na, 15A, 20A and 30B Nanomer: I30E and I31PS	Five types of coupling agent*: CA1, CA2, CA2P (functional group: maleic anhydride), CA3 (functional group: amine), CA4 (functional group: onium ion)	Three parameters: temperature (170°C, 180°C, 200°C), residence time (2.5 min, 5min, 10min), rpm (40, 60, 80).

* The details can be found in Section 3.2.

3.1.7 Experimental procedure

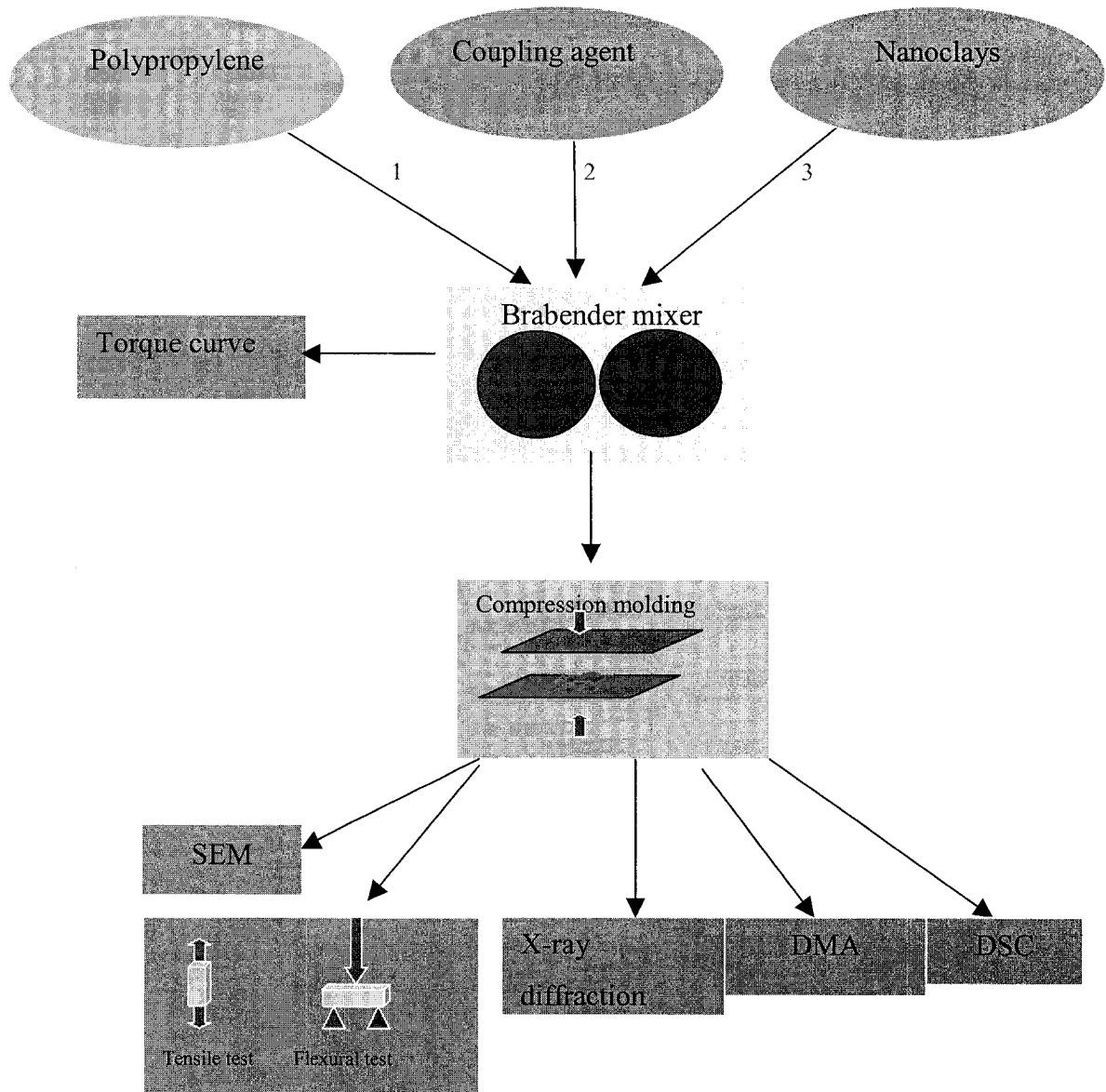


Figure 3.1 The experimental procedure

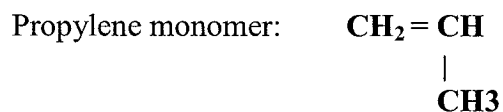
Note: 1, 2, and 3 in Figure 3.1 refer to the sequence of adding materials to Brabender: First, introduce PP and wait until it melts; second, add coupling agent (around 2minutes after introducing PP); finally add nanoclay after coupling agent melts (around 1min after adding coupling agent).

Figure 3.1 shows the experimental procedure. First, PP, coupling agent and clay were mixed together to fabricate nanocomposites with the Brabender mixer. Then, samples for various tests (including tensile and flexural, DMA, XRD) were molded in a press. Finally, tests on samples were performed to obtain properties.

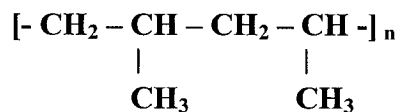
3.2 Materials

3.2.1 Polypropylene

Polypropylene (PP) used in this study was PP6100SM from Montell for injection and general purpose. The chemical formula of PP is shown as follows:

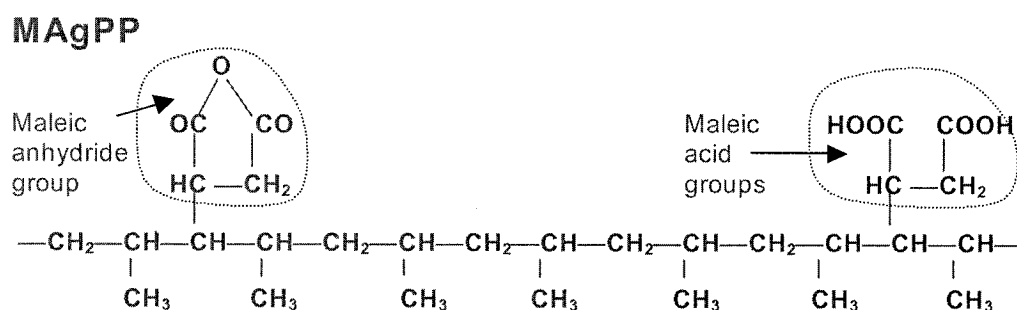


Polypropylene polymer:



3.2.2 Coupling agents

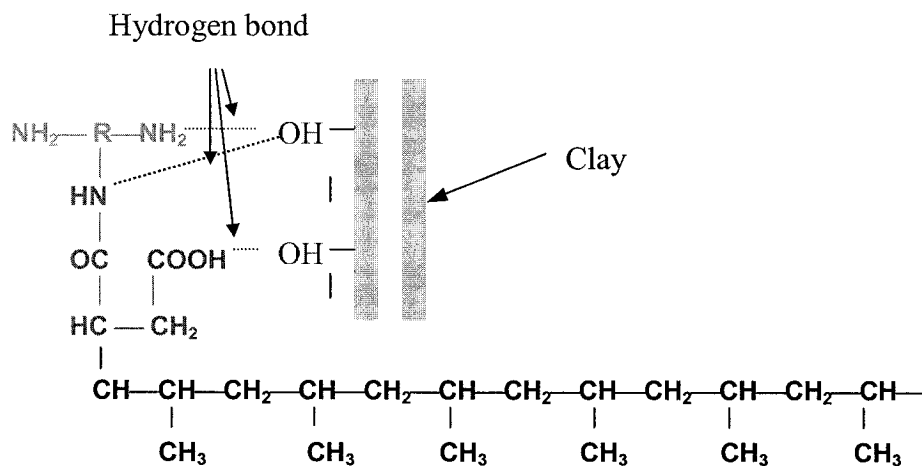
Two different types of coupling agent, namely CA1 (Polybond 3150), CA2 (Epolene 3015), based on maleic anhydride grafted PP (MAgPP) were obtained from Uniroyal Chemical and Eastman Chemical, respectively. The grafting process of MA into PP is based on a free radical reaction with an excess amount of reactants, and it is impossible to remove all the residuals and radicals from the material. CA2P was purified CA2. Since the CA2 has high impurities (more than 0.5%), it has been purified by dissolving in hot toluene, followed by precipitation in acetone. The chemical structure of MAgPP is as follows and more information is listed in Table 3.2.



CA3 is a new type of coupling agent that was developed by IMI (Industrial Materials Institute of National Research Council of Canada). CA3 is an amine-terminated (NH_2 -t) coupling agent which was prepared by reacting Polybond 3150 and Jeffamine T-403 (1.5 wt %) by reactive extrusion. As the result of the reaction, in CA3, the functional maleic anhydride group of the Polybond has been replaced by the amine group.

CA4 was produced from CA3 by immersing the CA3 thin film in HCl solution (20 wt %) at 80°C for 12h; the amine functional group was transformed to onium ion (NH_3^+). The chemical structure of CA3 and CA4 and the possible reaction with the clay surface can be simply described as follows:

CA3 (NH_2 -t-PP)



CA4 (NH_3^+ -t-PP)

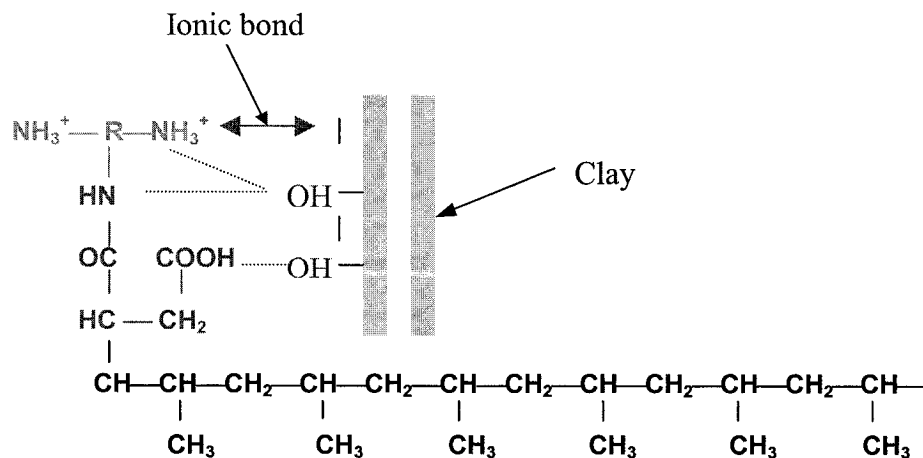


Table 3.2 gives information of each type of coupling agent.

Table 3.2 Characteristics of coupling agent

Experimental name	Commercial name	Supplier	Functional group	Acid number	Other technical information
CA1	Polybond 3150	Uniroyal Chemical	MA	22	$M_w=330,000$; MA=0.5wt%; $T_m=157^\circ\text{C}$ [66]
CA2	Epolene 3015	Eastman Chemical	MA	15	$M_w=47,000$; MA= ~1.0 wt%; $T_m=156^\circ\text{C}$ [67]
CA2P	-	Eastman Chemical	MA	-	Purified from CA2
CA3	-	-	Amine		Modified from CA1
CA4	-	-	Onium ion		Modified from CA3

MA: maleic anhydride group; M_w : weight-average molecular weight; T_m : melting point.

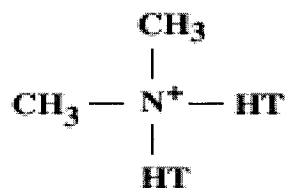
3.2.3 Nanoclays

Na, Cloisite 15A, 20A and 30B were provided by Southern Clay Products Inc. Nanomer I30E and I31PS were supplied by Nanocor Inc. Table 3.3 provides the technical details of nanoclays used in this study [26, 68].

Table 3.3 Characteristics of nanoclays

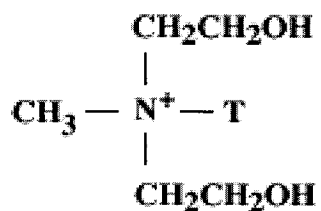
Sample	Intercalant	Modifier concentration (meq/100g)	Gallery distance (X-Ray Results) (Å)	Supplier
Na	-	-	-	Southern Clay Products Inc.
15A	2M2HT	125	28.5	Southern Clay Products Inc.
20A	2M2HT	95	24.2	Southern Clay Products Inc.
30B	MT2EtOH	90	18.5	Southern Clay Products Inc.
I30E	octadecylamine	-	-	Nanocor Inc.
I31PS	octadecylamine + silane	-	-	Nanocor Inc.

Note: 1) 2M2HT: dimethyl, dihydrogenated tallow, quaternary ammonium [68]



Where HT is Hydrogenated Tallow (~65% C18; ~30% C16; ~5% C14)

2) MT2EtOH: methyl, tallow, bis-2-hydroxyethyl, quaternary ammonium [68]



Where T is Tallow (~65% C18; ~30% C16; ~5% C14)

3) Typical dry particle sizes of 15A, 20A and 30B [68]: (microns, by volume)

10% less than:	50% less than:	90% less than:
2	6	13

4) Information about nanoclays was from the website of Southern Clay Products Inc.

(www.nanoclay.com) and of Nanocor Inc. (www.nanocor.com).

3.2.4 Composition of the composites

PP was used as a reference and as matrix in composites. The composites have been prepared with and without coupling agent. Blends of PP with coupling agent were also made for comparison purpose. The total weight of materials was 40grams, which was the appropriate volume for the Brabender mixer. In all samples, the concentration of nanoclay was kept at 3 wt%, and the coupling agent was 6wt% where applicable. Table 3.4 describes the composition of the prepared samples. Mixture refers to the composite containing PP and nanoclay (no coupling agents), while blend is a combination of PP and coupling agent (no clay). System refers to the nanocomposites consisting of PP, coupling agent and clays.

Table 3.4 Composition of samples

Sample	Coupling agent		Nanoclay	
	Type	Concentration (wt %)	Type	Concentration (wt %)
Reference				
PP	-	-	-	-
Mixtures				
15A	-	-	15A	3
20A	-	-	20A	3
30B	-	-	30B	3
I30E	-	-	I30E	3
I31PS	-	-	I31PS	3
Systems				
CA1-15A	CA1	6	15A	3
CA2-15A	CA2	6	15A	3
CA2P-15A	CA2P	6	15A	3
CA3-15A	CA3	6	15A	3
CA4-15A	CA4	6	15A	3
CA1-I30E	CA1	6	I30E	3
CA3-I30E	CA3	6	I30E	3

Table 3.4 Composition of composites (continued)

Sample	Coupling agent		Nanoclay	
	Type	Concentration (Wt %)	Type	Concentration (Wt %)
Systems (continue)				
CA4-I30E	CA4	6	I30E	3
CA1-I31PS	CA1	6	I31PS	3
CA3-I31PS	CA3	6	I31PS	3
CA4-I31PS	CA4	6	I31PS	3
CA4-20A	CA4	6	20A	3
CA4-30B	CA4	6	30B	3
Blends				-
CA1	CA1	6	-	-
CA2	CA2	6	-	-
CA3	CA3	6	-	-
CA4	CA4	6	-	-

3.3 PP Nanocomposites fabrication

In this thesis, the melt compounding process was employed to prepare PP nanocomposites. Mixing took place in a C.W. PL2000 Brabender Plasticorder (Figures 3.2, 3.3) and samples for testing were molded by compression molding in a hot press (Figure 3.5).

Brabender mixer was employed to disperse the nanoclay and coupling agent into the PP matrix. The measuring mixers consist of a mixer backstand with gear unit and a detachable mixer bowl. In addition to the electronic safety systems, they are connected to the drive unit through a shear pin coupling protecting both mixer and drive unit from damage due to overload. At the same time, a computer can record the torque (shear rate) of the screws during mixing.

Figure 3.2 illustrates the photo of this machine. Figure 3.3 shows the mixer bowl (with heating and cooling instruments) and the screws of PL2000 Brabender Mixer. Figure 3.4 shows the schematic of screws' rotation.

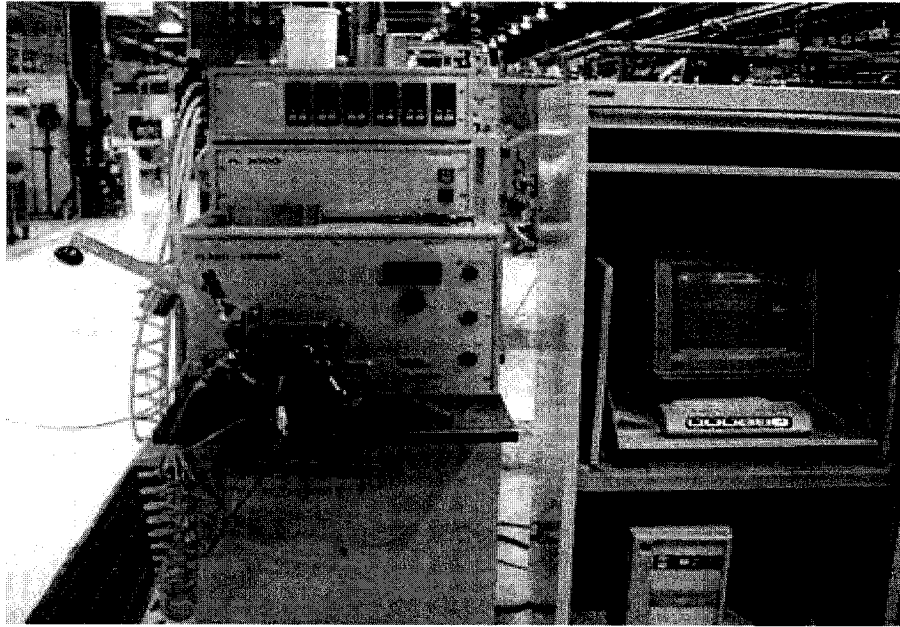


Figure 3.2 C.W. PL2000 Brabender Plasticorder *(from IMI lab)*

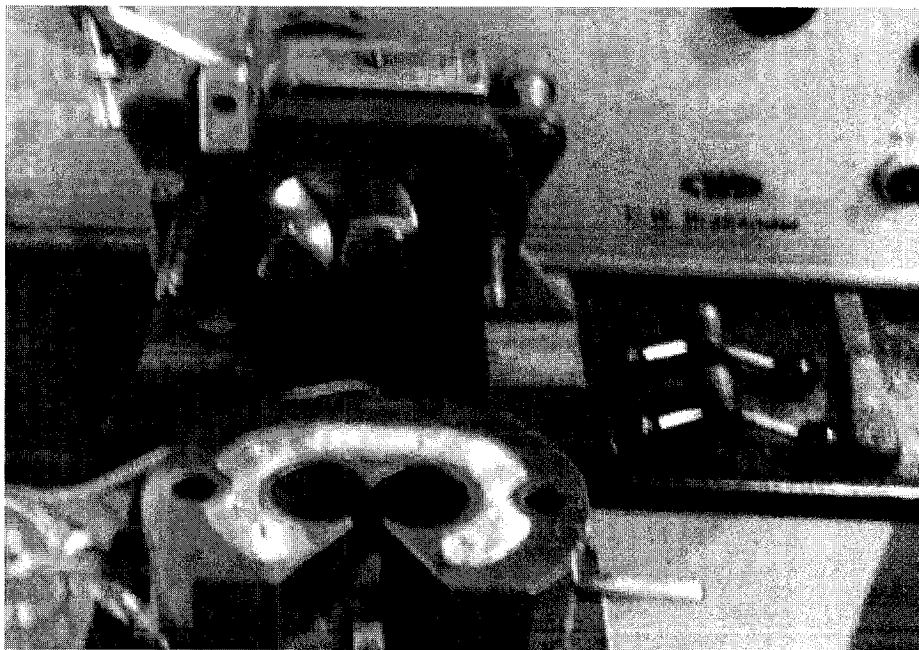


Figure 3.3 The mixer bowl and screws of PL2000 Brabender Mixer *(from IMI lab)*

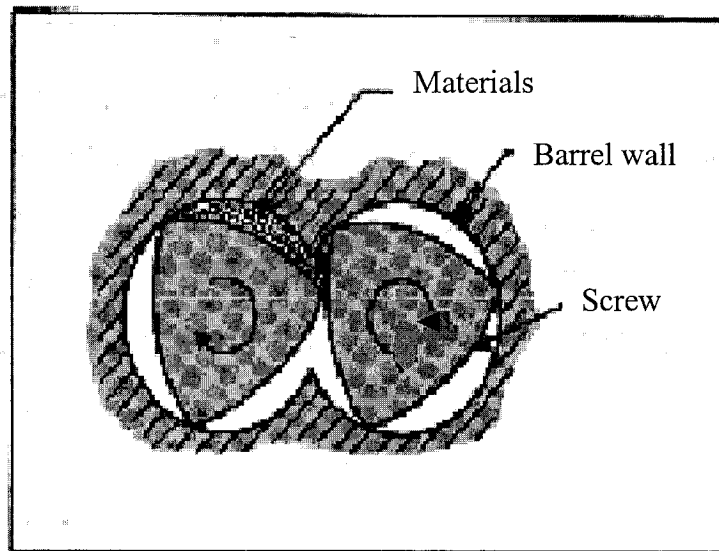


Figure 3.4 Schematic drawing of mixing in Brabender

According to references [57, 69], the following parameters were selected for step 1 and step 2 (Table 3.1). The mixing temperature was kept at 180°C in order to ensure good viscosity for the mixing and minimize the degradation at the same time. The rotation speed (RPM) was 60rpm, which is a standard mixing speed for most polymers. Mixing time (counting after all ingredients have been introduced into the Brabender and melt) was kept at 5 minutes.

After choosing the best formulation, the effect of processing conditions on the dispersion and thus the performance was conducted in step 2 (Table 3.1). In this step, only one parameter (among temperature, residence time and rpm) was changed each time while the other two were kept constant as in step 1. For example, while the residence time was kept at 5 min and rpm was 60rpm, the same composition samples were mixed under different processing temperatures: 170°C, 180°C and 200°C.

Before mixing a new sample each time, the Brabender was cleaned two times with high density polyethylene (HDPE). The steps of mixing include:

- 1) Add PP first when the mixing chamber reached the desired temperature;
- 2) After PP melted, add coupling agent;
- 3) After the coupling agent melted completely, slowly and slightly add the clays to avoid clays from aggregating together;
- 4) Then continue to mix until the desired residence time is reached;
- 5) Finally, stop the motor and take out the sample with a copper knife.

3.4 Sample preparation for testing

Specimens for tensile and flexural testing, DMA, and X-ray were prepared with a Carver Laboratory Press (Model M), as shown in Figure 3.5, at temperature of 180°C for both platens (upper and lower) under a pressure of 275 MPa (40,000 psi).

Since the materials taken out from the Brabender were large pieces, to facilitate the molding step, they were crushed in smaller pieces manually and then lined in the mold. The molds used to prepare the samples are shown in Figure 3.6. To ensure the uniformity of the specimens, the weight of raw materials for each molding was weighed carefully before putting into the mold, while the heating and cooling time were also kept the same for all cases. The procedure was:

- 1) Put the materials (in the mold) on the lower platen when the temperature of the platen reached 180°C;
- 2) Wait about 4-5 minutes to ensure that the materials melted, then close the mold with the upper platen;
- 3) Apply pressure quickly to 275 MPa (40,000 psi);
- 4) Wait 10-15 seconds, then open the cooling water valve to cool down the mold;
- 5) After the temperature reached 30°C, take out the mold and the specimens;
- 6) Check the quality of specimens to make sure there are no defects (not fully filled, voids, holes, etc.) and trim off the edges.

The specimens for X-ray diffraction were prepared using a Carver press at 180°C followed by molding on a clean glass slide in order to assure the flat surface and optimize the accuracy for the comparison of the X-ray results. Since the intensity of the XRD peaks is sensitive to the surface, in order to obtain more quantitative results, the specimens should not be deformed or have bubbles and defects.

SEM observation was conducted on the samples which had been fractured in the tensile test (mechanical rupture).

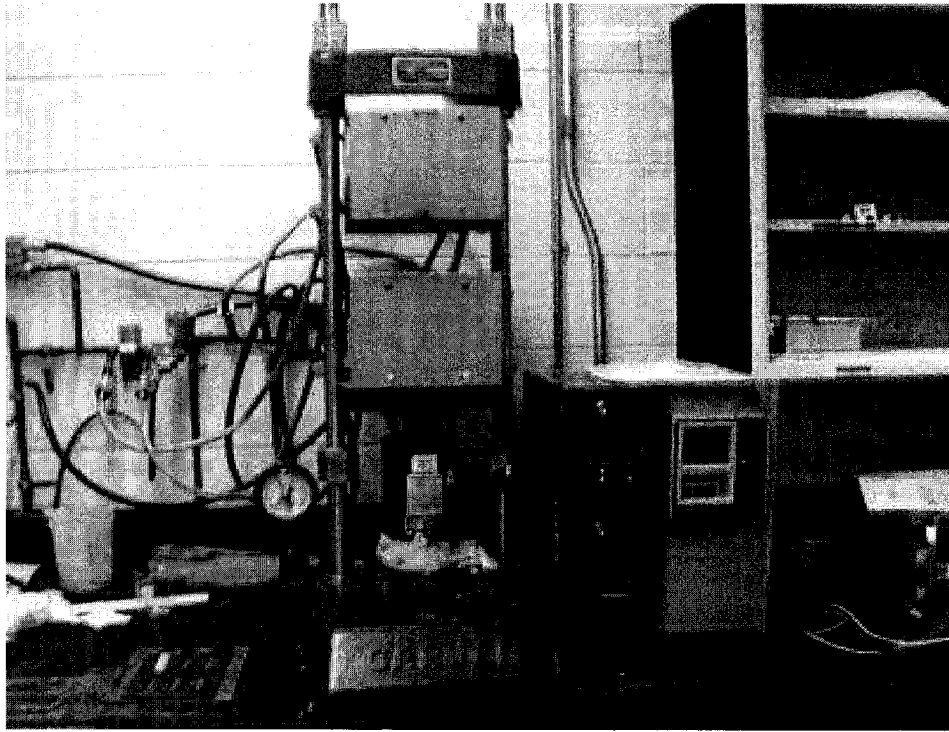


Figure 3.5 Carver Laboratory Press (*from IMI lab*)

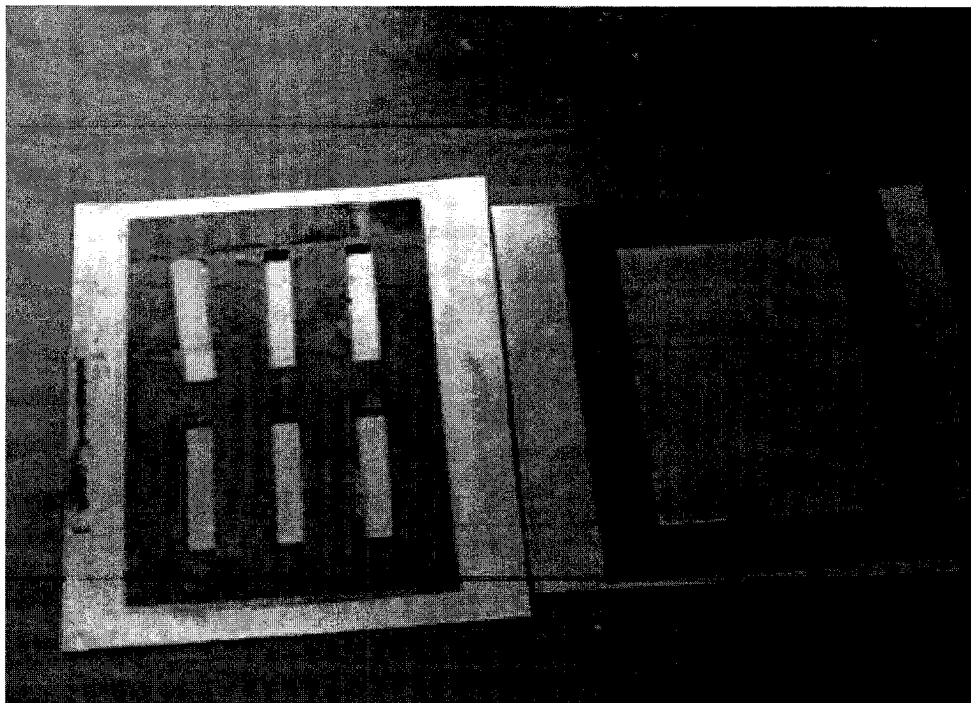


Figure 3.6 Molds for samples

3.5 Nanocomposites characterization

PNC produced from different types of clay and coupling agent may have different properties and behavior. Various methods have been considered to characterize these differences. The following methods were employed in the experiment.

3.5.1 Dispersion behavior

As described earlier (Chapter 2), dispersion behavior determines the nanocomposite structure, which can be either microcomposites, intercalated or exfoliated nanocomposites. Therefore, it is very important to estimate the degree of clay dispersion in PP matrix. From literature survey, XRD, TEM, AFM and SEM are the most popular tools for this purpose. Due to the time restraint and facility limitations, only XRD and SEM were used in this project. XRD can detect the degree of dispersion via the gallery distance; SEM can give the direct image of dispersion and fracture state.

3.5.1.1 X-ray diffraction

To evaluate the dispersion of the nanoclays in the polymer matrix, X-ray diffraction analysis was carried out using a Philip PW1710 X-ray diffractometer (Figure 3.7). The generator power was 40 kV and 20 mA. The scanning uses radiation from a copper target tube (CuK α radiation, $\lambda=1.54250 \text{ \AA}$) with the 2θ scan range from 1° to 10° . The scanning

speed was 1° /min. To ensure accuracy, the measurement was repeated two times for some samples.

The X-ray diffraction method gives an easy way to measure the interlayer distance d . From Figure 3.8, assume that an X-ray beam incident on a pair of parallel planes (clay layers) P1 and P2, separated by an interlayer spacing d . The two parallel incident rays 1 and 2 make an angle (THETA= θ) with these planes. A reflected beam of maximum intensity will result if the waves represented by 1' and 2' are in phase. The difference in path length between 1 to 1' and 2 to 2' must then be an integral number of wavelengths, (λ). We can express this relationship mathematically in *Bragg's law*:

$$n \lambda = 2d \sin \theta$$

Where λ is wavelength of X-ray radiation, d is the spacing between the diffracted layer planes, and θ is the measured diffraction angle [71]. Since λ is a constant after the target tube is selected and θ can be controlled and recorded automatically, d can be calculated.

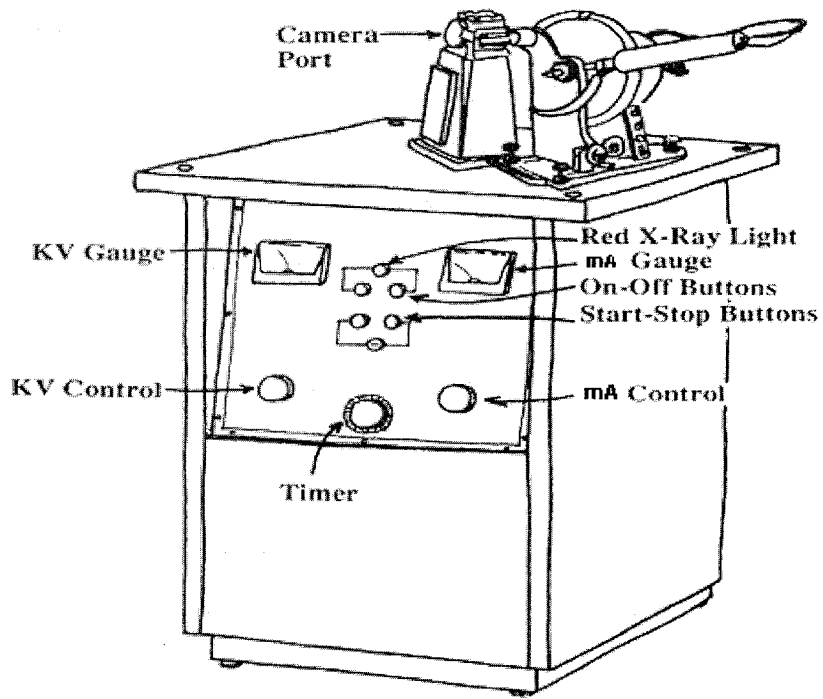


Figure 3.7 A Philips X-ray generator with diffractometer

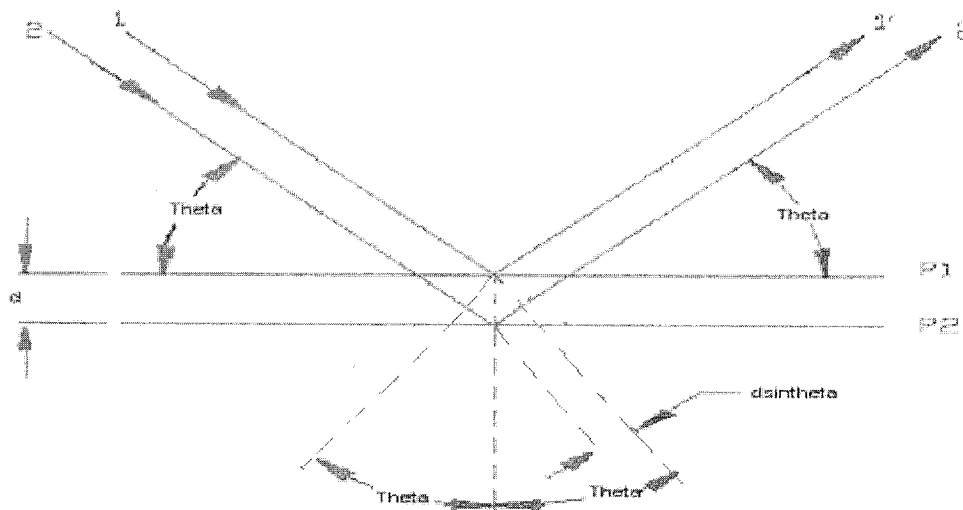


Figure 3.8 Scheme of Bragg's law ($n \lambda = 2d \sin \theta$)

3.5.1.2 Scanning electron microscopy (SEM)

The SEM is an instrument that produces a largely magnified image by using electrons instead of light to form an image. A beam of electrons is produced at the top of the microscope by an electron gun. The electron beam follows a vertical path through the microscope, which is held within a vacuum. The beam travels through electromagnetic fields and lenses, which focus the beam down toward the sample. Once the beam hits the sample, electrons and X-rays are ejected from the sample; detectors collect these X-rays, backscattered electrons, and secondary electrons, and convert them into a signal that is sent to a screen similar to a television screen. This produces the final image. Figure 3.10 is the schematic drawing of SEM. SEM is very useful in the identification of textures and shapes of mineral grain aggregates. The definition or resolution of the image is of the order of $0.01\mu\text{m}$ [72].

The SEM has many advantages over traditional microscopes. It has a large depth of field, which allows more of a specimen to be in focus at one time. The SEM also has much higher resolution, so closely spaced specimens can be magnified at much higher levels. Because the SEM uses electromagnets rather than lenses, the researcher has much more control on the degree of magnification. All of these advantages, as well as the actual strikingly clear images, make the SEM one of the most useful instruments in research today.

A JEOL JSM-840A scanning microscope was employed to evaluate the fracture surfaces and dispersion behavior. Figure 3.9 shows a photo of the SEM machine. Because the

SEM utilizes vacuum conditions and uses electrons to form an image, special preparations must be done to the sample.

All water must be removed from the samples because the water would vaporize in vacuum. Samples need to be made conductive by covering the sample with a thin layer of conductive material which is usually gold. This is done by using a device called a "sputter coater" in which an electric field and argon gas are applied. The sample is placed in a small chamber that is in a vacuum. Argon gas and an electric field cause electrons to be removed from the argon, making the atoms positively charged. The argon ions then become attracted to a negatively charged gold foil. The argon ions knock gold atoms from the surface of the gold foil. These gold atoms fall and settle onto the surface of the sample producing a thin gold coating. Then these samples are placed in sequence on platform and put into the chamber of the microscope. Adjusting various parameters, different magnifications from different areas will be obtained and recorded.

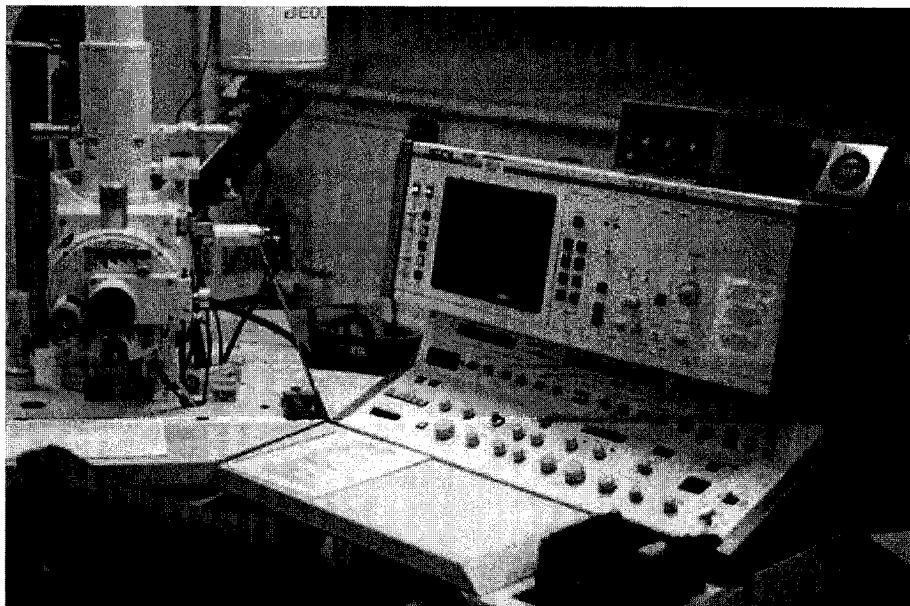


Figure 3.9 The JEOL 840A SEM machine *(from Microscopy lab of McGill University)*

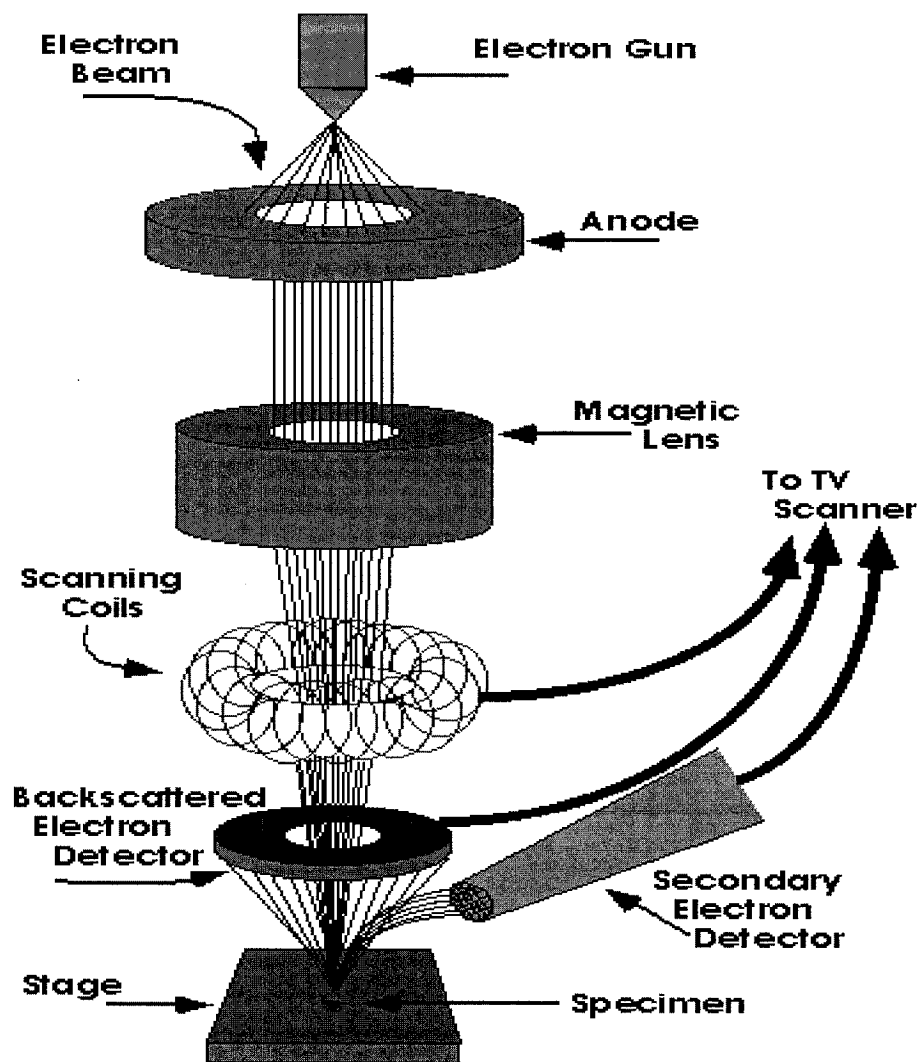


Figure 3.10 Scheme and structure of SEM (Diagram courtesy of Iowa State University SEM Homepage)

3.5.2 Rheological behavior

The data of the rheological behavior was collected by computer during mixing in the Brabender. The data included torque, time and temperature. The motor in the Brabender rotates the two co-rotating screws (Figures 3.2, 3.3, 3.4) and results in strong shear to mix all the compositions in the homogeneous state. Torque is proportional to the shear stress ($\tau = Tr/J$, where: τ is the shear stress; T is the applied torque; r is the radius; and J is polar moment of inertia). The shear stress transmitted to the system is proportional to the melt viscosity of the material because the viscosity is the ratio of the shear stress to the shear rate ($\eta = \tau / \dot{\gamma}$, η is the viscosity (Pa·s), τ is the shear stress (Pa), and $\dot{\gamma}$ is the shear rate (s^{-1})). On the other hand, the viscosity of the material varies with temperature and residence time. Therefore, the torque-time curves can also display the shear stress that is applied to the material and the viscosity of material during mixing so that it can help to detect any changes in the mixture which can cause changes in viscosity (crosslink, degradation, level of dispersion, etc.).

In this thesis, a CL. W. PL2000 Brabender mixer (Figure 3.2) was used to disperse materials together and at the same time a computer connected with the Brabender recorded the data of these parameters. Excel was employed to process these data and to produce time-torque and time-temperature curves.

3.5.3 Thermal properties

Thermal properties refer to polymer properties that are related to the temperature and heat flow, such as glass transition temperature (T_g), melting temperature (T_m), crystallization temperature (T_c), etc. Differential scanning calorimetry (DSC) is such an instrument to determine the temperature and heat flow associated with physical and/or chemical phenomena that can release or absorb heat as a function of time and temperature. It also provides quantitative and qualitative data on endothermic (heat absorption) and exothermic (heat evolution) processes of materials during physical transitions and chemical process that are caused by phase changes, melting, oxidation, and other heat-related changes. From this information, one can determine the important transition temperatures, the degree of crystallization, heat capacity, heat of formation and sample purity. Since PP is a semi-crystalline material, which has high crystallinity (60-70%), the energy step responding with T_g is very weak in the DSC curve. In comparison with DSC, DMA is more sensitive for detecting T_g .

A TA Instruments – DSC 2010 (Figure 3.11) was employed to obtain the thermal data in this experiment. Around 10 milligrams of material was sealed in an aluminum pan using the sample encapsulating press (Figure 3.11). The sample pan was loaded and a similarly prepared empty reference pan was placed into the cell (Be sure that they are centered on the platforms). After entering sample and instrument information, samples were heated to 200°C under nitrogen atmosphere and kept at this temperature for 5min before cooling down in order to assure the materials melt uniformly and eliminate the thermal history.

The sample was then cooled down to room temperature at a cooling rate of 10°C/min. T_m was detected under the same conditions at a heating rate of 10°C/min.

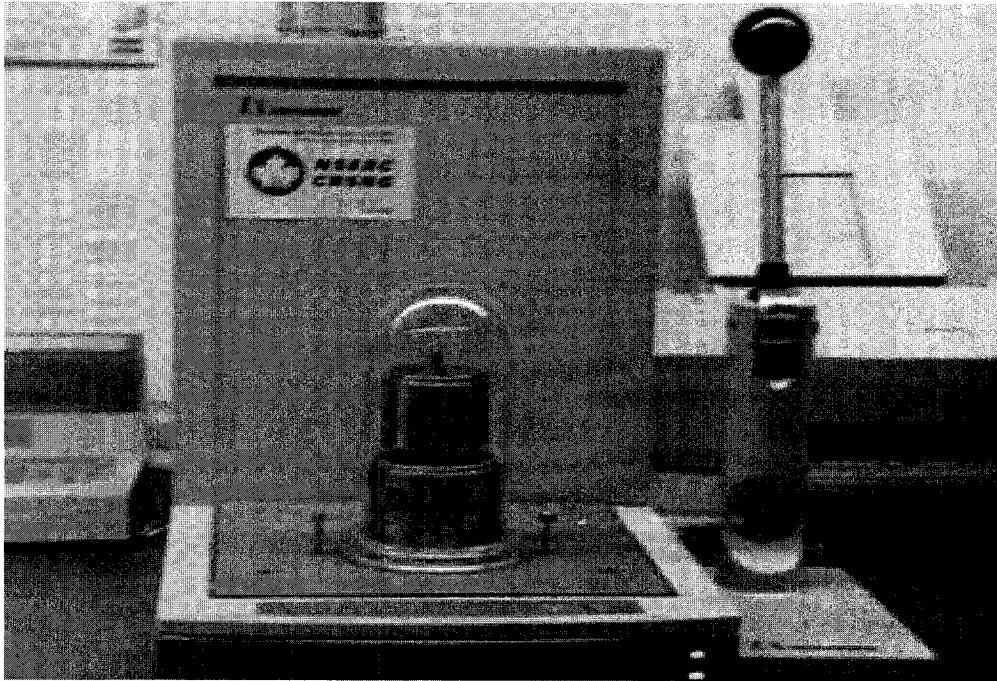


Figure 3.11 TA Instruments -DSC 2010 (from Composite Centre of Concordia University lab)

From the curves obtained from DSC, T_c , T_m , and X_c can be determined (T_c denotes the peak crystallization temperature recorded during cooling; X_c denotes the degree of crystallinity; T_m denotes the peak melting temperature). X_c can be calculated from the equation:

$$X_c(\%) \text{ Crystallinity} = \frac{\text{Area of sample melting peak}}{\text{Area of standard sample melting peak}}$$

The area of melting peak, which is the enthalpy of fusion, can be calculated from these curves. With reference to [73], a value of 209 J/g was accepted as the enthalpy of fusion for a fully crystalline polypropylene (area of standard sample melting peak).

3.5.4 Mechanical properties

3.5.4.1 Dynamic Mechanical Analyzer (DMA)

Dynamic Mechanical Analysis (DMA) characterizes the viscoelastic properties of materials and simultaneously determines the elastic modulus (stiffness) and energy absorbing (toughness) characteristics of a material as a function of temperature, frequency or time as well. To measure viscoelastic properties, DMA applies a sinusoidal force to a sample then measures the resulting sample deformation or strain. The sample strain response lags behind the input stress wave with respect to time and the lag is known as the phase angle. The ratio of the dynamic stress to the dynamic strain provides the complex modulus that includes both the storage modulus (E') and the loss modulus (E''). The E' , which is the elastic component, refers to the ability of a material to store energy and represents the change in stiffness of the sample with regard to temperature. The E'' , which is the viscous component, reflects the damping or energy absorbing characteristics which are related to molecular motions [74]. The tangent of phase difference is another common parameter that provides information on the relationship between the elastic and inelastic component. These parameters can be calculated as a function of time, temperature, frequency, or amplitude (stress or strain) depending on the application. [75]. DMA can detect the coefficient of expansion, glass transition

temperature (T_g), softening temperatures, phase transitions and sintering. Figure 3.12 shows a schematic of the DMA [76].

The results of the DMA tests include large amounts of information on the sample. The modulus value below the glass transition can indicate levels of molecular orientation and crystallinity. Transition initialization can be related to the polymer's structure and may be particularly useful where a multiple component composite is under investigation. Dynamic mechanical methods are most sensitive for measuring the glass transition, which is one of the key properties of a polymer from both the structural and processing viewpoint [77].

A Du Pont 983 DMA (TA Instruments) was employed in this experiment. Figure 3.13 shows the exterior of the machine. Samples, whose dimensions are $L/T > 10$ (L is the length and T is the thickness and T is between 1.5 mm and 3.5 mm), were prepared using compression molding. The dynamic properties were studied under fixed frequency mode at frequency of 1Hz, and the amplitude was 0.2mm. The samples were analyzed from -40°C to 160°C at a heating rate of $5^\circ\text{C}/\text{min}$.

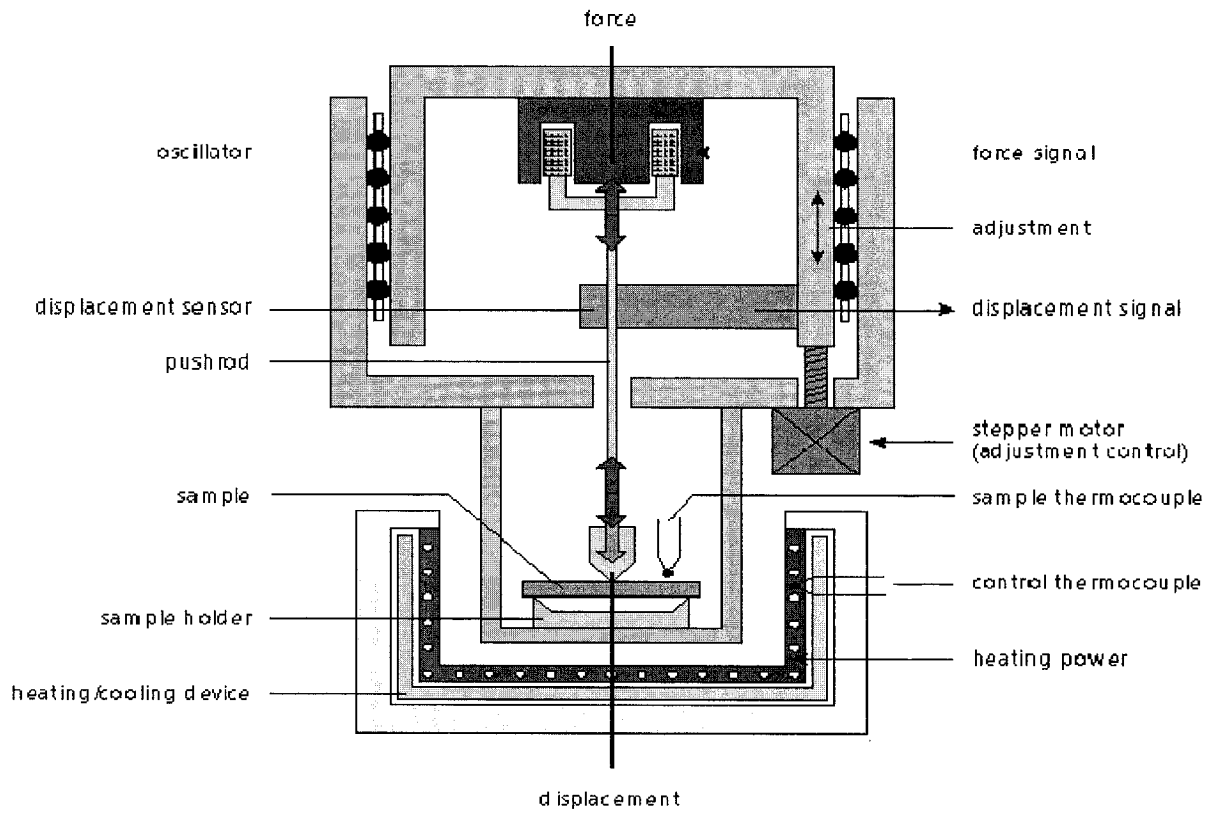


Figure 3.12 Dynamic Mechanical Analyzer [85]

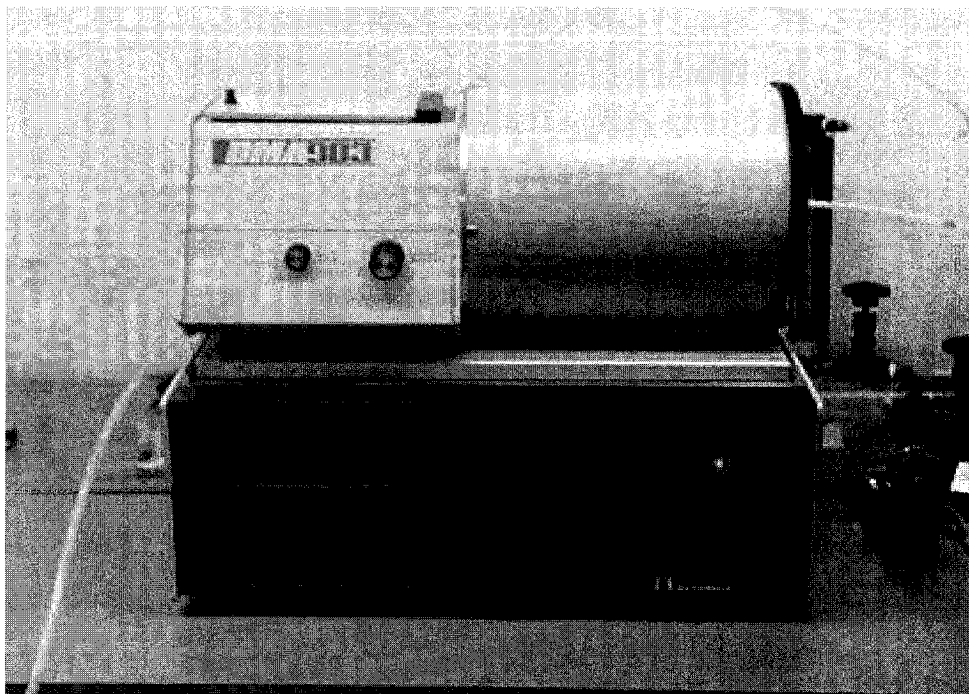


Figure 3.13 Du Pont 983 DMA

3.5.4.2 Tensile and flexural tests

The flexural strength of a material is its ability to resist deformation under load. Figure 3.14 shows the test geometry. These tests also give the procedure to measure a material's flexural modulus (the ratio of stress to strain in flexural deformation).

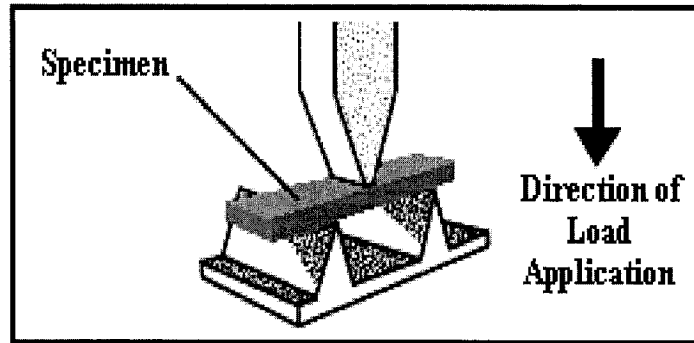


Figure 3.14 The schematic drawing of flexural test

According to standard D790-99 [78], for all tests, the support span shall be 16 (tolerance ± 1) times the depth (thickness) of the beam. The thickness of the samples in this project for flexural test was 2.8-2.9mm, so a 45mm span was used for the test. The rate of crosshead motion is calculated by the equation:

$$R = ZL^2/6d$$

Where R= rate of crosshead motion, mm/min; L= support span, mm; d= depth of beam, mm; Z= rate of straining of the outer fiber, mm/mm/min.

After calculation, the crosshead speed for flexural test was determined to be 1.2 mm/min.

Tensile property, the ability of a material to resist breaking under tensile stress, is one of the most important and widely measured properties of plastics used in structural applications. Tensile strength is the force per unit area (MPa) required to break a material in such a manner. The elongation of a plastic is the percentage increase in length that occurs before it breaks under tension. The combination of high ultimate tensile strength and high elongation leads to materials of high toughness. The tensile modulus is the ratio of stress to elastic strain in tension. A high tensile modulus means that the material is rigid - more stress is required to produce a given amount of strain. In polymers, the tensile modulus and compressive modulus can be close or may vary widely. This variation may be 50% or more, depending on resin type, reinforcing agents, and processing methods.

During the tensile testing, the machine pulls the sample from both ends and measures the force required to pull the specimen apart and how much the sample stretches before breaking. According to ASTM D638 [79], the speed of crosshead at which a sample is pulled apart in the test can range from 1mm to 500mm per minute and will influence the results. In this project, the crosshead speed for tensile test was 5mm/min and the gauge length was 25mm. The video extension meter was applied during the tensile testing.

In this project, tensile and flexural tests were performed on an Instron 5500R. Figure 3.15 is the photo of this machine. All tests were at room temperature (23°C), humidity 50%. For each test at least three defect - free specimens were tested.

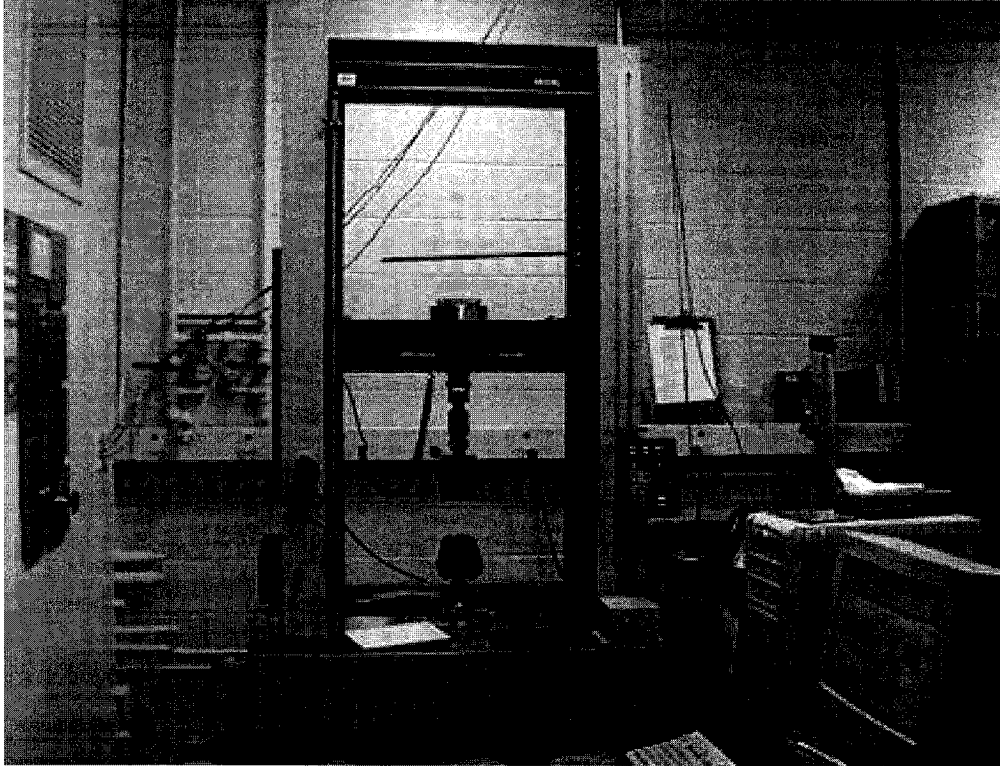


Figure 3.15 Instron 5500 test machine

4 Effects of clay on the formulation and properties of PP nanocomposites

The objective of this part was to investigate the performance of PP nanocomposites with different types of clay. The experiments were organized in three series: PP with different types of clay, with different clays in the presence of coupling agent CA3, with different clays in the presence of coupling agent CA4. Pure PP was also used as a reference. Different analysis techniques were used to characterize the dispersion and the properties of the nanocomposites.

4.1 Effect of clay types in the absence of coupling agent

The variables and experimental conditions of this set are listed in Table 4.1.

Table 4.1 Variables and experimental conditions of for Experiment Set 4.1

Variables Sample	Types of clay	Types of coupling agent	Processing parameters		
			Temperature (°C)	Mixing time (min)	rpm
Na	<i>Na</i>	-	180	5	60
15A	<i>15A</i>	-	180	5	60
20A	<i>20A</i>	-	180	5	60
30B	<i>30B</i>	-	180	5	60
I30E	<i>I30E</i>	-	180	5	60
I31PS	<i>I31PS</i>	-	180	5	60

4.1.1 Rheological behavior

During mixing, adding materials in the Brabender chamber can result in variations of torque curves depending on their amount and type. Figures 4.1 and 4.2 show the torque-time curves for pure PP and a mixture based on PP and I31PS clay, respectively. At first, when PP was introduced into the chamber, the torque increased significantly as shown by the strong sharp peak at the first stage of the curve in Figures 4.1 and 4.2. After that, the PP melted down, therefore the torque decreased. After 4 minutes, the PP melted completely, as a consequence the torque stabilized. In the preparation of the mixture of PP with clay, the PP was melted first and clay was added into the melt PP (approximately after 2 minutes) as shown in Figure 4.2. The system stabilized after 4 minutes, similarly as in the pure PP in Figure 4.1. Therefore, during mixing, in the first 5 minutes the system was not stable, since it took some time to introduce the ingredients one by one into the chamber and also some time to heat and melt the materials. It is more reasonable to look at the change of the torque in the later step after all ingredients have been added, melted, and well mixed. Curve segments after 5 minutes will therefore be plotted later on.

In general, it is difficult to compare the torque value between each sample because it is strongly determined by the volume of the whole material occupied in the mixing chamber. Since it is difficult to control the volume of the system, the amount of sample introduced into the chamber was controlled by weight. Each ingredient has different density, even though the amount of all samples used was the same in weight, it may not be the same in volume. It is therefore more meaningful to compare the trend of the torque curve during mixing.

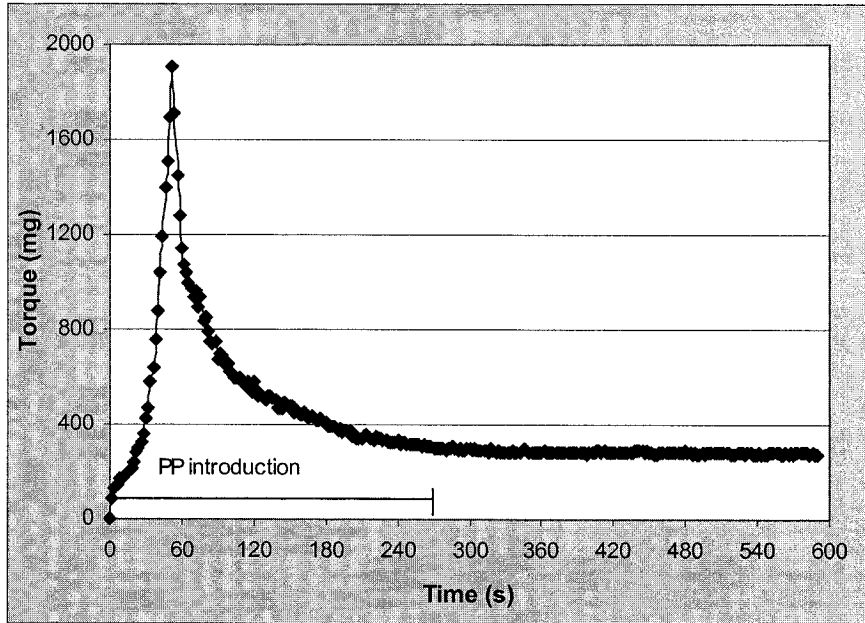


Figure 4.1 Torque–time curve of pure PP (mixing temperature 180°C; rpm 60rpm; residence time 5 min.)

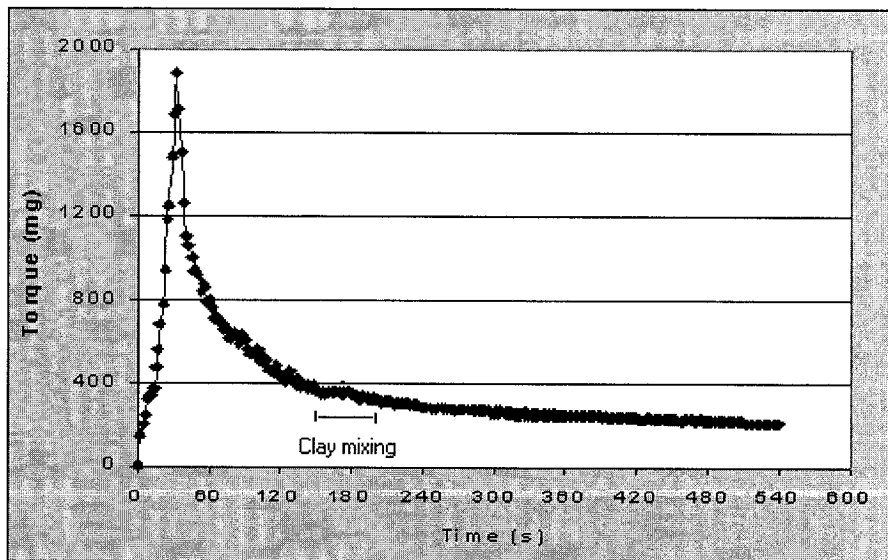


Figure 4.2 Torque – time curve of PP with I31PS clay (mixing temperature 180°C; rpm 60rpm; residence time 5 min.)

Different types and concentration of intercalants that are used to modify the clay surface may have effects on the rheological behavior of mixtures. Figure 4.3 shows the torque curves of the PP and its composites with different clays. Some obvious differences in the trend of the curves can be observed. The temperature of the chamber was very stable in all experiments; therefore, these changes are likely due to the change in the materials themselves. The torque curve of PP became relatively stable after 5 min of mixing and showed only a slight downward trend with time, indicating little change in the viscosity of the sample. However, the presence of nanoclays in the mixtures has different impact on the torque as seen in Figure 4.3. The torque curves of the mixtures with Na clay, 15A clay, 20A clay and 30B clay, are nearly parallel with the PP curve. These stable curves mean almost constant viscosity of the systems during mixing. However, the I30E- and I31PS-mixtures curves have a significantly downward trend compared with the PP curve. In other words, the viscosity of these composites reduced greatly during mixing, which can be caused by evaporation of low molecular weight materials or reduction in molecular weight due to oxidation or/and degradation of the matrix. Moreover, during the Brabender mixing, the color of composites based on I30E and I31PS turned brown and gave out some odious smell as the residence time increased. This can be another sign that degradation or/and oxidation has happened. The degradation/oxidation should be related to the differences in organic surface modification. 15A, 20A and 30B were modified by alkyl ammonium, whereas I30E and I31PS were modified by alkyl amine. The residual amine in I30E and I31PS can greatly affect the oxidation and the degradation, resulting in poor thermal stability of mixtures. From the curves, the order of the effect of the clay on the oxidation or/and degradation is $I30E > I31PS > 15A \approx 20A \approx 30B \approx Na \approx \text{None (PP)}$.

Although torque curves of Na, 15A, 20A and 30B are stable, there are some differences between them. Among them, Na, 20A and 30B curves are higher than PP one and Na is the highest; 15A curve is lower than PP curve. These differences indicate the mixtures viscosity was different. Introduction of pure clay can cause the increase of viscosity because clay is rigid particles. However, the low molecular weight intercalant used to modify the clay surface can result in the decrease of system viscosity. And the reduction of viscosity becomes more significant with the increase of the intercalant concentration. 15A, 20A were modified with the same type of intercalant (Table 3.3), but the intercalant amount decreases from 15A to 20A. As a result, the torque of the 20A was higher than that of 15A. 20A and 30B have similar intercalant and concentration, their torque curves are nearly same. The general order of the composites viscosity with different clays is thus $Na > 20A \approx 30B > PP > 15A > I31PS > I30E$.

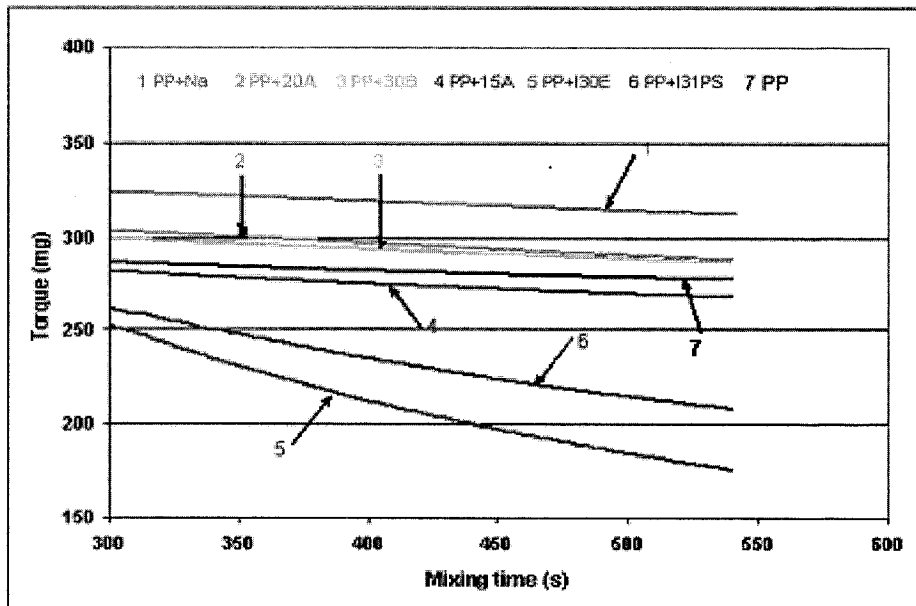


Figure 4.3 Torque-time curves of mixtures with different types of clay

4.1.2 Dispersion behavior - SEM

Figure 4.4 to Figure 4.7 show the SEM photos of the samples fracture surfaces after tensile testing. The magnification was 1500x for all samples. From the photos, the fracture mode of the samples and the dispersion quality of the clays, such as concentration and size of aggregates, can be seen. SEM observation showed that the clays were dispersed into the PP matrix in the form of large and small aggregates. Figure 4.5 is the photo of the mixture with nanoclay Na-montmorillonite (without surface treatment), in which the relatively large aggregates and poor interface between matrix and aggregates are observed. The size of some observed aggregates could reach to over 5 μ m. The fracture mode became more brittle than pure PP because the big aggregates stopped the elongation of the matrix. 15A and I30E are organic nanoclays that have been surface-treated by different intercalants (Table 3.3). The size of the nanoclay aggregates is reduced significantly, which can be observed from their SEM photos (Figure 4.6 and Figure 4.7). Almost all aggregates are under 2 μ m. That means the dispersion of nanoclay is improved considerably by the surface treatment. Compared to Figure 4.5, the interface between aggregates and matrix are also improved apparently. Therefore, surface treatment for nanoclay is very important to improve the affinity between nanoclay and matrix and to break down the large aggregates. This can be attributed to the surface treatment reducing particle-particle attraction, promoting an expansion of the distance (gallery) [26]. The intercalant can open up the gallery distance of clay from 1 nm (for Na-montmorillonite) to 2.8 nm (for 15A). At the same time, the intercalant makes the clay become more hydrophobic and increases the compatibility with the matrix.

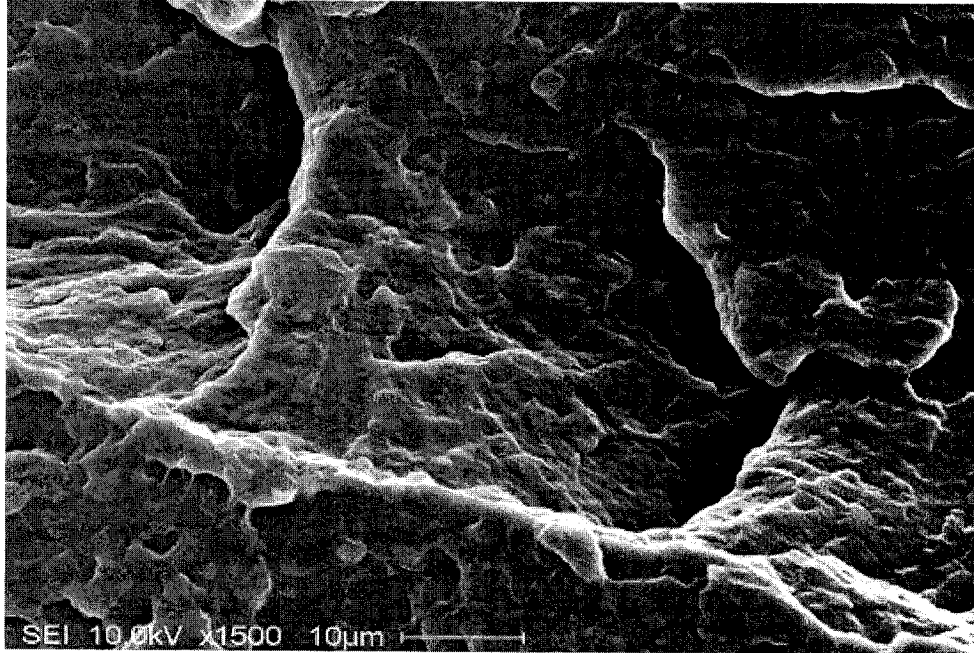


Figure 4.4 SEM photo of pure PP

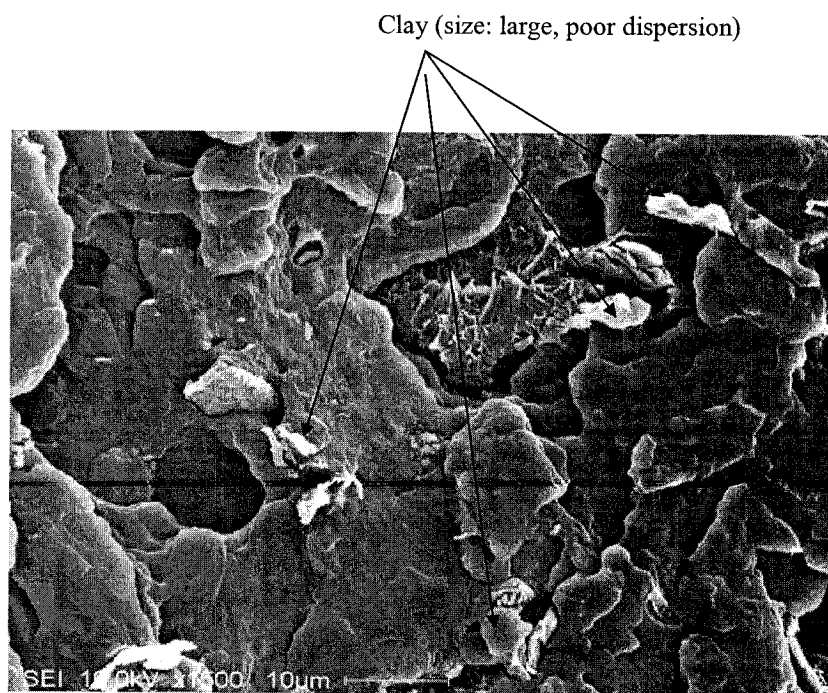


Figure 4.5 SEM photo of mixture with Na- montmorillonite

Clay (size: mixture of small & large, better dispersion)

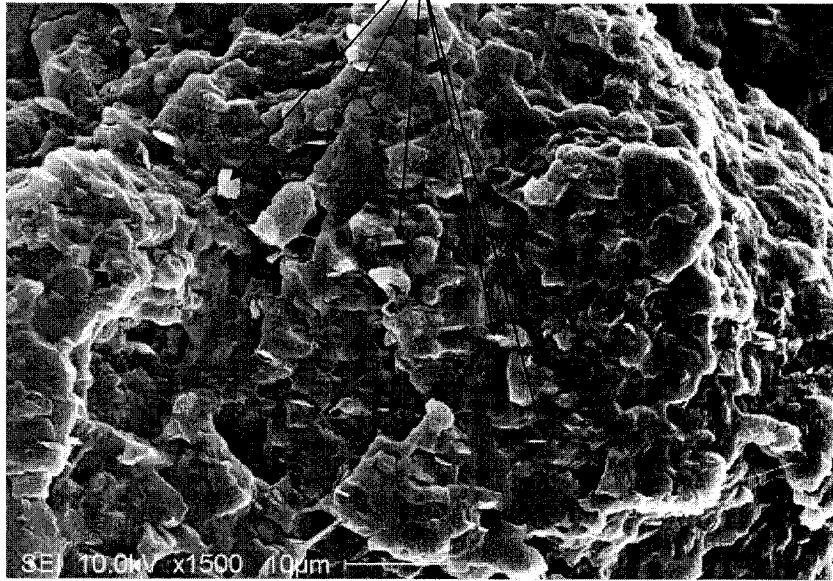


Figure 4.6 SEM photo of mixture with 15A nanoclay

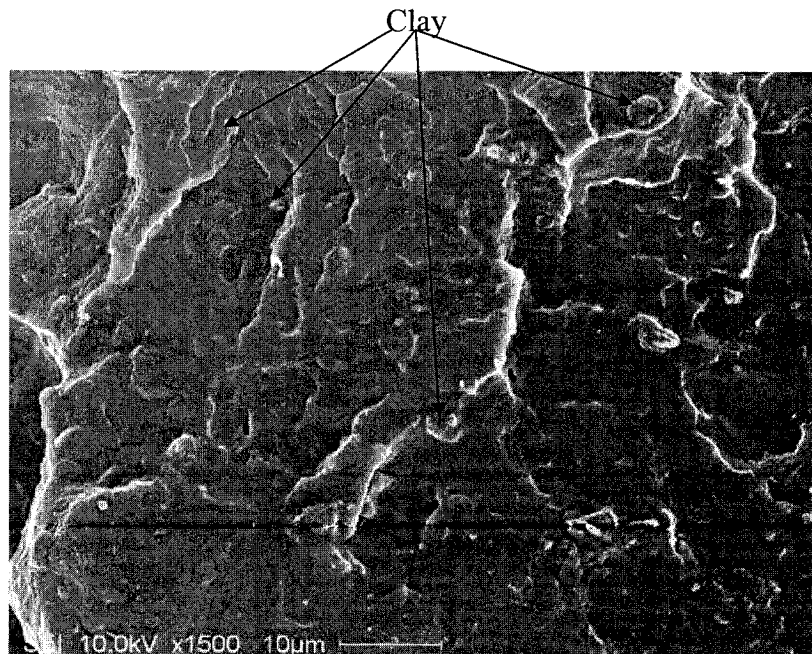


Figure 4.7 SEM photo of mixture with I30E nanoclay

4.1.3 Thermal properties

4.1.3.1 Crystallization behavior

The crystallization of polymers with nanoclay has been studied extensively. Many studies have shown a nucleating effect of nanoclay for different polymers [62, 83-85]. This effect can be used to enhance the mechanical and thermal properties of the polymer, since the surface-nucleated crystalline phase has better mechanical and thermal characteristics than the pure polymer crystal phases. In these cases, using fillers with large surface area maximizes the filler-induced enhancements of the material properties; a dramatic manifestation of such a response was found in nylon-6/clay nanocomposites [86, 87].

In this study, crystallization of all samples was performed at the same cooling rate of 10°C/min for comparison purposes. Figure 4.8 and Table 4.2 show the crystallization behavior of samples obtained from a DSC test. The crystallization temperature (T_c) of pure PP was found to be 107.4°C. The presence of the nanoclay in the mixtures increased the T_c significantly, from 107°C (PP) to about 115°C. These increases indicated the nucleating effect of the nanoclays in the crystallization of PP. The extent of increase of T_c varied slightly with the types of clay. The magnitude of T_c of the different clays is 15A \approx 20A > I31PS \approx I30E \approx 30B > PP. The degree of crystallinity (X_c) also varied with the types of clay. 15A had a higher X_c than PP, while other clays had the lower X_c than PP. The magnitude of X_c of these clays is 15A > PP > 20A \approx I30E > 30B > I31PS. These differences between clays may result from the different types and concentration of intercalants.

4.1.3.2 Melting temperature (T_m)

T_m was detected at the same heating rate of 10 °C/min. Figure 4.9 and Table 4.2 show the melting curves and values of T_m of the different mixtures. The T_m of all mixtures decreased compared to pure PP. This can be a result of the introduction of low molecular weight surface modifiers. Among the five types of clays, 15A, 20A and 30B, which are modified by onium ion based intercalants, had higher T_m than I30E and I31PS, which are modified by the amine based intercalants. This difference confirms that I30E and I31PS are less stable than other types of clays /or they degrade PP into smaller molecules as discussed earlier. The magnitude of T_m of these clays is PP \approx 15A > 20A \approx 30B > I31PS = I30E.

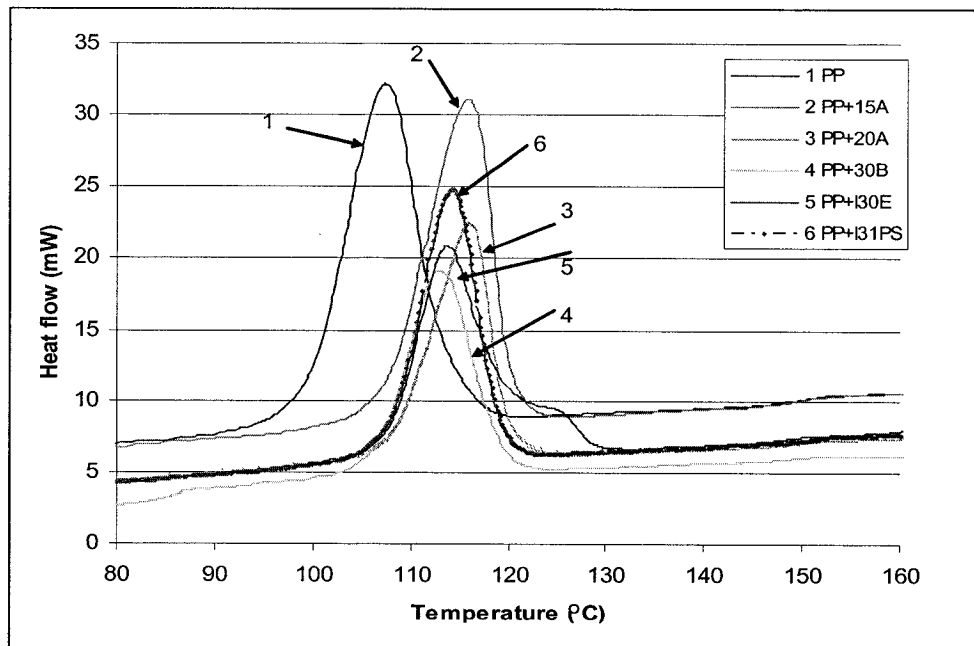


Figure 4.8 Crystallization (cooling) curves of the composites with different clays

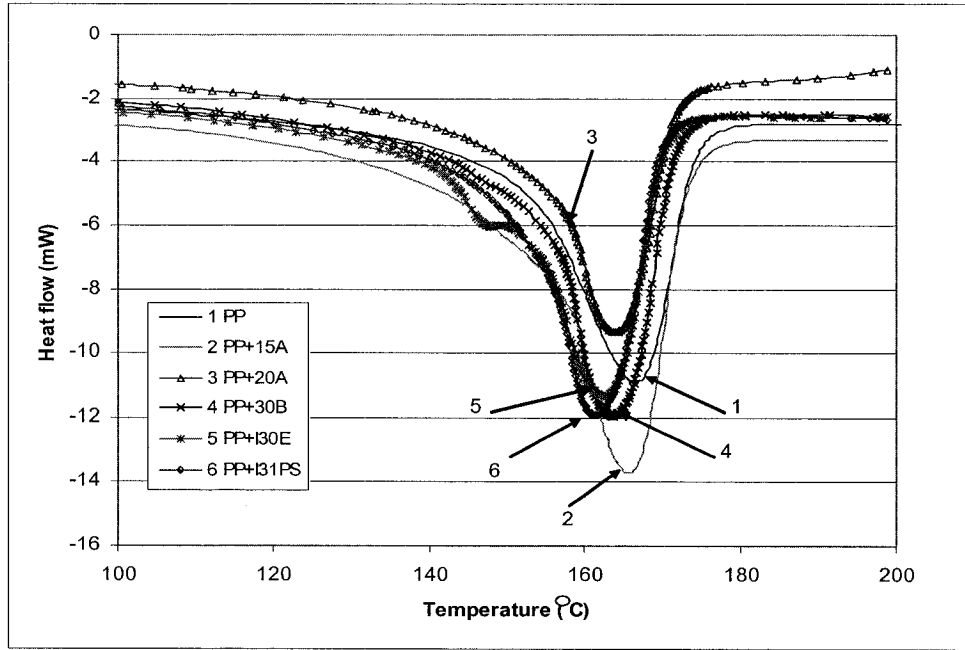


Figure 4. 9 Melting behavior (heating) curves of the composites with different clays

Table 4.2 Crystallization and melting behavior of the composites with different clays

Sample	T_c (°C)	T_m (°C)	X_c (%)
PP	107.6 ± 0.3	165.9 ± 0.2	43.9 ± 0.8
PP+15A	116 ± 0.2	165.6 ± 0.2	46.1 ± 0.7
PP+20A	115.9 ± 0.2	164 ± 0.4	43.0 ± 1.2
PP+30B	113.9 ± 0.6	163.5 ± 0.3	41.5 ± 0.6
PP+I30E	114.2 ± 0.3	162.5 ± 0.3	42.3 ± 1.5
PP+I31PS	114.5 ± 0.4	162.5 ± 0.5	40.5 ± 0.7

Note: T_c denotes the peak crystallization temperatures recorded during cooling characterization. T_m denotes the peak melt temperature recorded during heating characterization. X_c denotes the degree of crystallinity determined from the DSC curve.

4.1.4 Dynamic mechanical properties

Dynamic properties reflect the viscoelastic properties of materials and the change of stiffness and energy absorbing with temperature variation. The analysis of the storage modulus (E'), loss modulus (E''), and the tangent of phase difference ($\tan\delta$) curves are very useful in ascertaining the performance of the sample under stress and temperature. The E' refers to the ability of a material to store energy and represents the change in stiffness of the sample with regards to temperature. The E'' reflects the damping or energy absorbing characteristics which are related to molecular motions [74].

For comparison purpose, all samples were examined at the same increasing temperature rate of $5^\circ\text{C}/\text{min}$ from -40°C to 160°C . Figure 4.10 shows the change in storage modulus E' at different temperatures for mixtures based on different types of clay and pure PP. All the mixtures with nanoclay possessed higher storage modulus than pure PP all through the temperature range. The mixtures of 20A and 15A have the higher storage modulus than ones of I30E and I31PS over the entire temperature range.

Two apparent changes of E' with temperature can be observed for all the mixtures in Figure 4.10: a sharp drop in E' from -10°C to about 20°C and a reduction in the rate of drop in E' with temperature above 75°C . The first change between -10°C and 20°C may be associated with the relaxation of the amorphous phase (β relaxation). In this case, the glassy state of the amorphous phase goes through its glass transition and there is a sharp drop in E' [88]. At about 15°C , E' continues to fall and slope is flatter than before. From 70°C to 80°C , the reduction in E' is less severe.

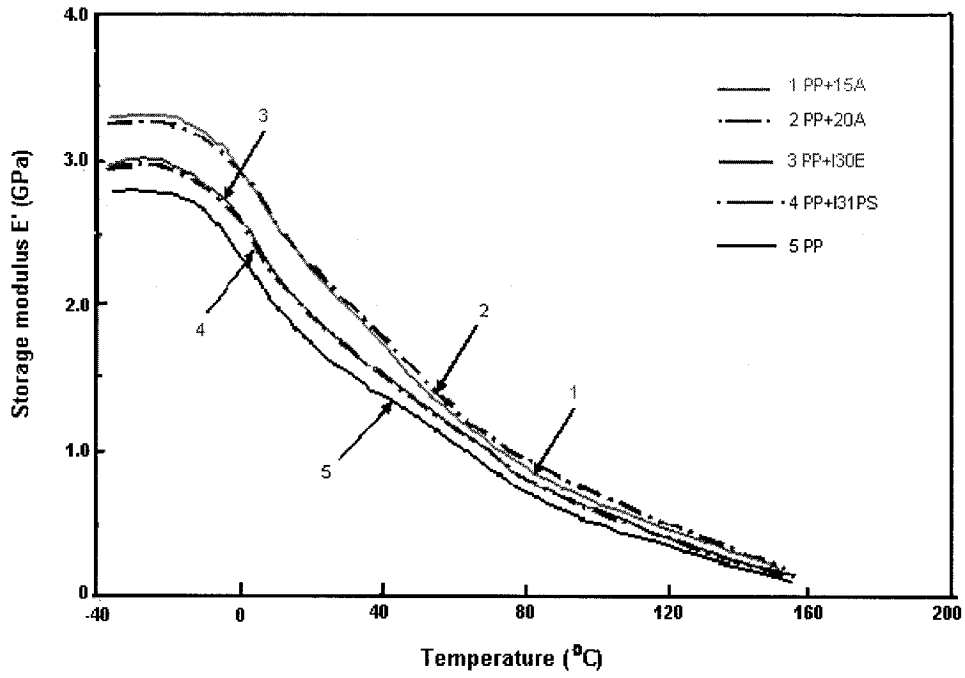


Figure 4.10 DMA curves (storage modulus E') for the mixtures

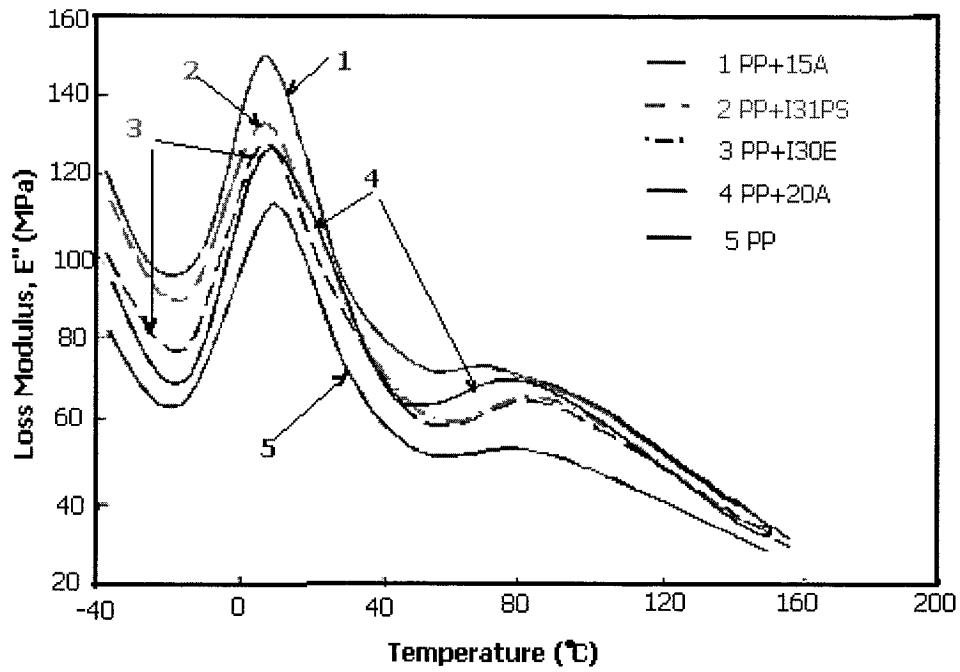


Figure 4.11 DMA curves (loss modulus E'') for the mixtures

Table 4.3 The glass transition temperature (T_g) and soften temperature (T_s) of mixtures

Samples	T_g (°C)	T_s (°C)
PP	6.2 ± 0.2	86.6 ± 0.6
15A	5.6 ± 0.2	85.3 ± 1.2
20A	6.0 ± 0.1	85.7 ± 1.6
I30E	4.7 ± 0.5	88.9 ± 2.1
I31PS	4.6 ± 0.3	94.0 ± 1.8

Figure 4.11 shows the loss modulus E'' of PP and its clay based mixtures and the dependence on temperature. The two major relaxations that are corresponding with the E'' curve can be easily seen. The β transition (the first big peak observed between -10°C to 20°C) results from the relaxation of the amorphous phase in mixtures and the ability of energy absorbing becoming stronger. The peak of β relaxation can be considered as the glass transition (T_g), at around 5 to 10°C range for pure PP and all mixtures. The α transition (the second peak between 70°C and 90°C) is related to the relaxation of restricted PP amorphous chains in the crystalline phase and is believed to be due to the movement of small crystallites [98]. The peak of α transition can be seen as the softening point (T_s).

In general, the increase in peak temperature indicates decrease in chain mobility, and the E'' peak amplitude is directly related to the amount of amorphous PP chains involved in the transition [90]. All these four types of clay have been modified by low molecular weight intercalants. The molecular weight of these modifiers is similar, while the amount

of loading is different. Among them, 15A has the biggest and excessive amount of loading (Table 3.3), so the excessive modifiers in the PP matrix would improve the mobility of the amorphous phase of PP molecules and contribute to the highest β peak than other mixtures and pure PP.

Since the peak of β can be considered as T_g , from Figure 4.11 and Table 4.3, the mixtures have lower T_g than PP. However, the extent of decrease varied with the types of clay. The mixtures of 15A and 20A had similar T_g to PP (the reductions were 0.64°C and 0.27°C respectively) while ones of I30E and I31PS had much lower T_g (the reduction were 1.52°C and 1.63°C respectively). Conversely, the T_s of mixtures of I30E and I31PS were higher than pure PP, 2.3°C and 7.4 °C respectively. The mixtures of 15A and 20A still had similar T_s to pure PP. Since the increase in peak temperature indicates decrease in chain mobility, the decrease of T_g in these four mixtures indicates that the amorphous molecules become more mobile at lower temperature than ones in PP due to the presence of low molecular weight intercalant. The increase of T_s in the mixtures of I30E and I31PS implies that the mobility of rigid amorphous molecules in the crystal was limited to higher temperature. The increase of T_s is beneficial to the application of these materials in high temperature environment. The difference of T_g and T_s between Cloisite (15A and 20A) and Nanocor (I30E and I31PS) should be also attributed to the different types of modifier applied to the surface of nanoclay. 15A and 20A were modified by long alkyl chain with quaternary ammonium group while I30E and I31PS were modified by long alkyl chain with amine group. It seems that amine group modifier can form more perfect crystals in the PP matrix than ammonium modifier, so the softening temperature increases for mixtures of I30E and I31PS. The mechanisms need more detailed research.

4.1.5 Tensile properties

Figures 4.12 and 4.13 show tensile results of nanocomposites made of 3wt% of five types of nanoclays. The tensile moduli were improved by about 10% to 20% depending on the types of the clays. 15A, I30E and I31PS had better performance than others. Almost no change was observed in tensile strengths (except I30E-mixture which showed increase). The significant improvement of modulus should be due to the high aspect ratio of the clay and the much higher modulus of the clay than PP matrix. Because nanoclay approaches the scale of resin molecules, a very close encounter can be made between the matrix and the clay when the nanoclay is properly surface modified and under ideal dispersion. And since the nanoclay has very high aspect ratio that can be 1000 to 1, the particle-molecule interaction creates a constrained region at the clay surface, which fixes a portion of the resin matrix. With so many particles available for interactive association, the total percent of constrained polymer can become large. Then the mechanical properties can be improved when perfect adhesion exists between matrix and nanoclays surface. Therefore, the main problems here are the ideal dispersion and adhesion.

Among three types from Southern Clay Products, 15A, 20A and 30B, 15A gave better properties than the other two. This can be explained by the different treatment of the clay surface that leads to different gallery distances. Although 15A and 20A have the same modifier, 15A has a higher concentration (Table 3.3) that made the clay more hydrophobic and more compatible with the PP matrix so that better dispersion can be expected. In addition, 15A has a larger gallery distance (2.8 nm) than the other ones

which allowed PP molecules to intercalate more easily. The properties (except tensile elongation) of clays from Nanocor, I30E and I31PS, were better than ones from Southern Clays Products, 15A, 20A and 30B. From Figure 4.13, the elongations of all the mixtures decreased significantly as compared to PP. The 15A-mixture gave better elongation and toughness than others. I30E and I31PS based mixtures became more brittle which can be related to degradation of these samples during mixing as discussed earlier. Figure 4.14 shows the stress-strain curves of the mixtures with different clays, which are good agreement with Figure 4.12 and Figure 4.13.

Based on the above results, we can see that the difference in distance of gallery of clay among 15A, 20A and 30B does not affect the mechanical properties a lot. According to the technical data from Southern Clay Products Inc., the gallery of 15A is 28.5Å, of 20A is 24.2Å, and of 30B is 18.5Å. From the figures, nanocomposites of 20A and 30B nearly had the same performance. The improvement of 15A mixture was not very apparent. Therefore, although organic-modification of the clay surface can make the clay more hydrophobic and increase the gallery distance, it is still difficult to get ideal dispersion in PP. To introduce an agent that can be accepted by PP and clays is one effective way to overcome this challenge [33, 46-48].

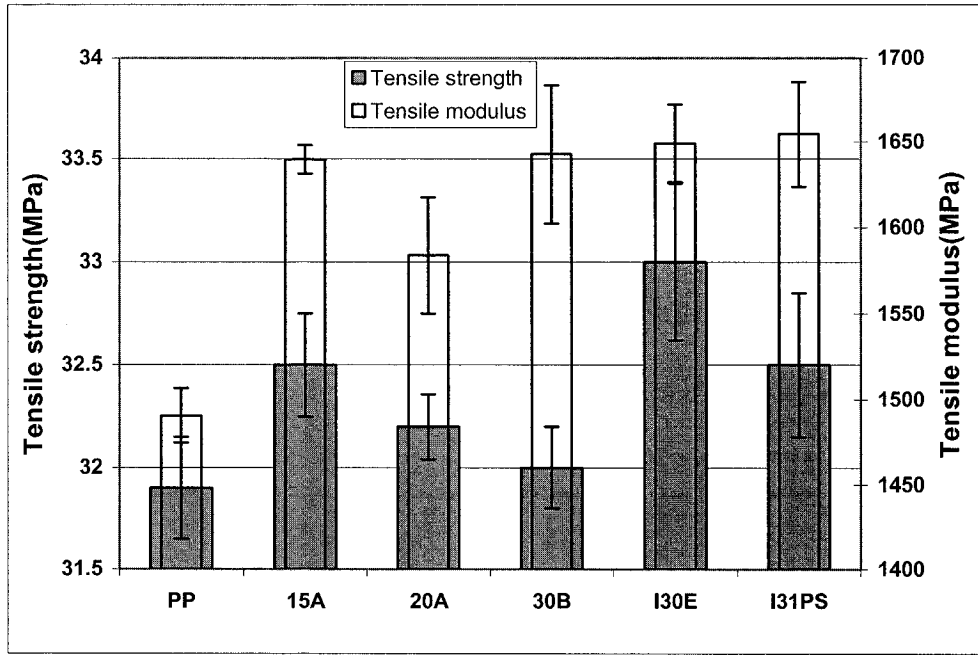


Figure 4.12 Effect of types of clay on tensile properties

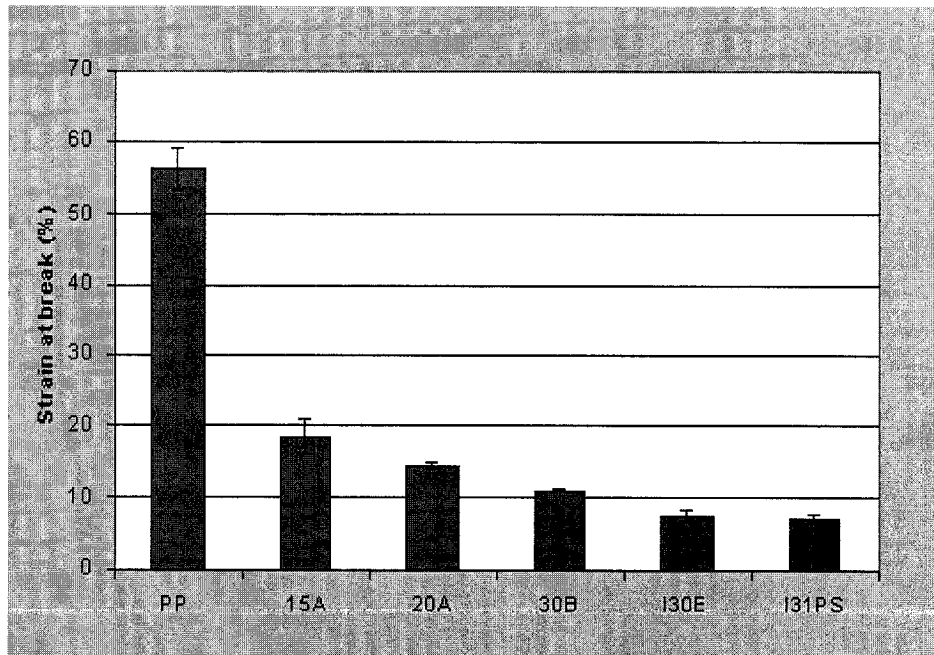


Figure 4.13 Effect of types of clay on tensile strain

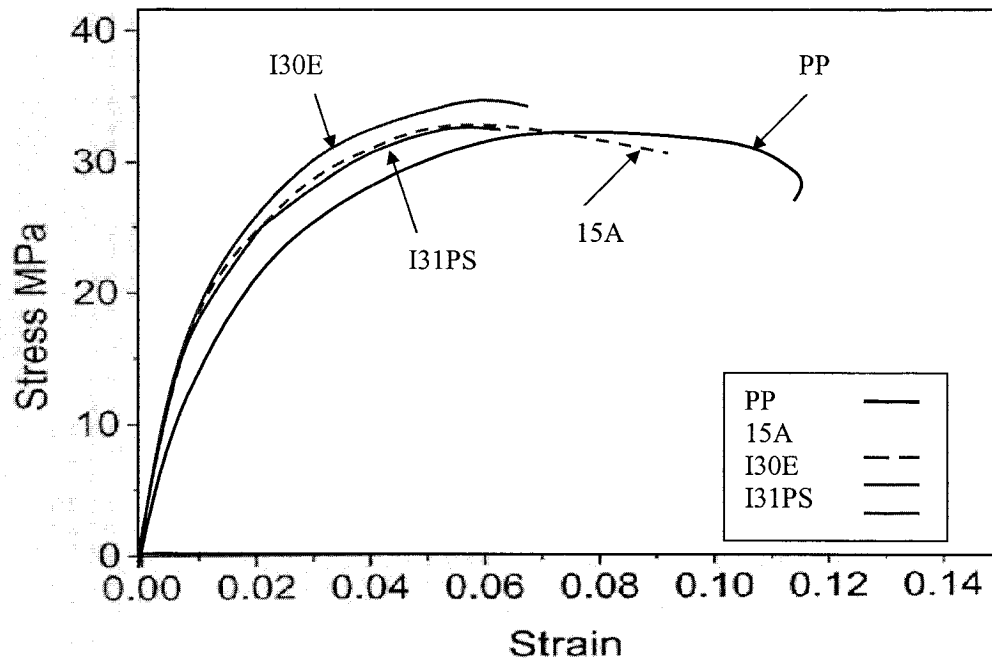


Figure 4.14 Stress – strain curves of the composites with different clays

4.2 Effect of types of clay in the presence of coupling agent CA3

Table 4.4 shows the variables and experimental conditions of this experiment set.

Table 4.4 Variables and experimental conditions of Experiment Set 4.2

Variation Sample	Types of clay	Types of coupling agent	Processing parameters		
			Temperature (°C)	Mixing time (min)	rpm
CA3+15A	15A	CA3	180	5	60
CA3+20A	20A	CA3	180	5	60
CA3+30B	30B	CA3	180	5	60
CA3+I30E	I30E	CA3	180	5	60
CA3+I31PS	I31PS	CA3	180	5	60

4.2.1 Rheological behavior

Figure 4.15 shows the torque – time curve of the composites containing coupling agent CA3 and clay. The curve can also become stable after 5 minutes as in Figures 4.1 and 4.2. Therefore, the curve segments after 5 minutes were also used to compare the change of the torque in these systems. Figure 4.16 shows the torque curves of the composites prepared with different clays in addition to the same coupling agent CA3. The torque curves confirm the observation in Section 4.1.1 (Figure 4.3): the composites with I30E and I31PS have poor thermo- stability, especially I30E, where the composite torque (viscosity) curve has a sharp downward trend as residence time increased, while 15A, 20A and 30B composite have better stability because their torque curves are nearly parallel with pure PP's during mixing.

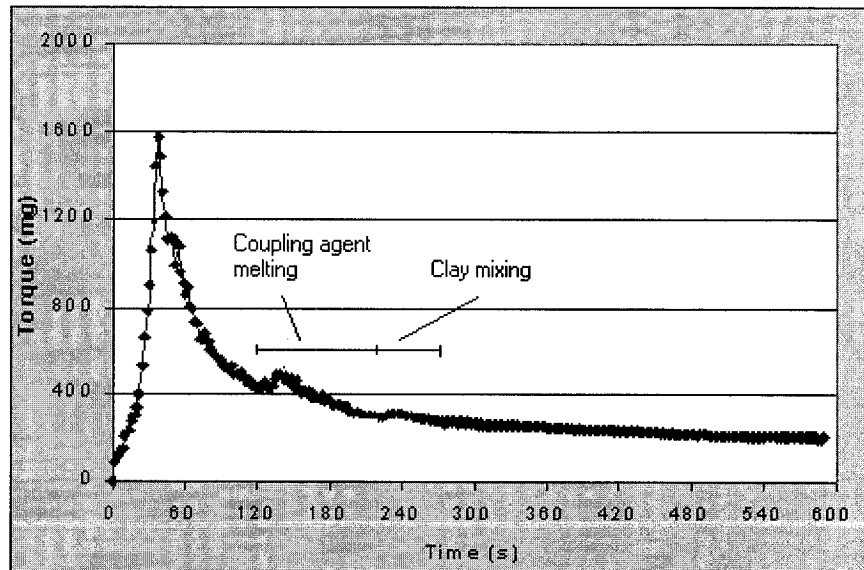


Figure 4.15 Torque – time curve of composites based on PP, CA3 and I31PS clay

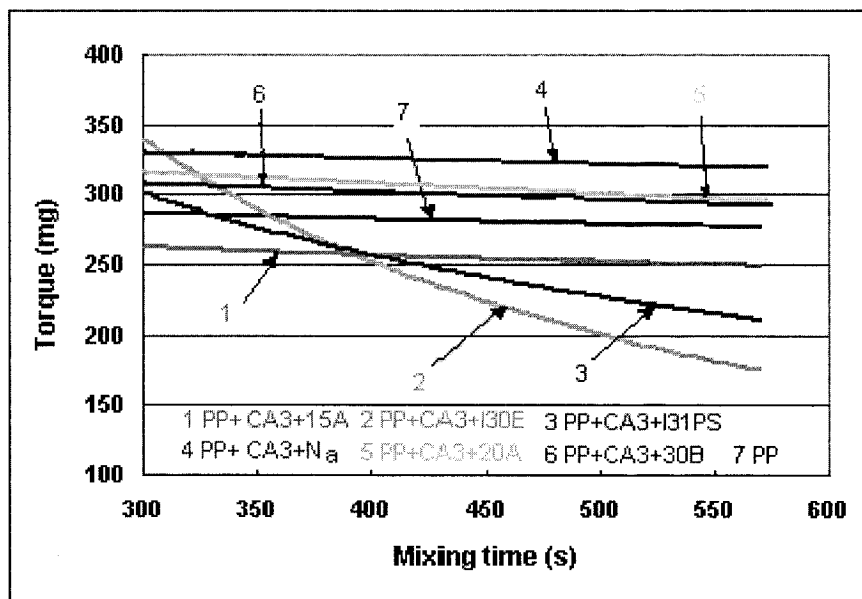


Figure 4.16 Torque-time curves of the composites with CA3 and different types of clay

4.2.2 Dispersion behavior - XRD

XRD curves are widely used to determine the structure of PNC due to its simple preparation and good results. In XRD curves, the peak location (peak at angle 2θ), which relates to the gallery distance, can indicate the intercalation degree; the intensity or area of peaks, which relates to the amount or the size of clay clusters, can indicate the exfoliation degree or the size of cluster [57]. Figure 4.17 shows X-Ray curves of the composites containing different types of clay and the same coupling agent CA3. On X-Ray curves of I30E and I31PS nanocomposites, the second and third peaks almost disappeared and their intensities are lower than ones of 15A, suggesting that I30E and I31PS have better exfoliation or dispersion than 15A. In other words, I30E and I31PS can easily disperse in matrix or have better interaction with coupling agent so that the bigger clay cluster can break easily into small pieces. This probably is because their degradation and/or extended PP degradation produced lower molecular weight materials (according to

the torque-time curve), then these small size molecules can easily enters into the gallery of clays.

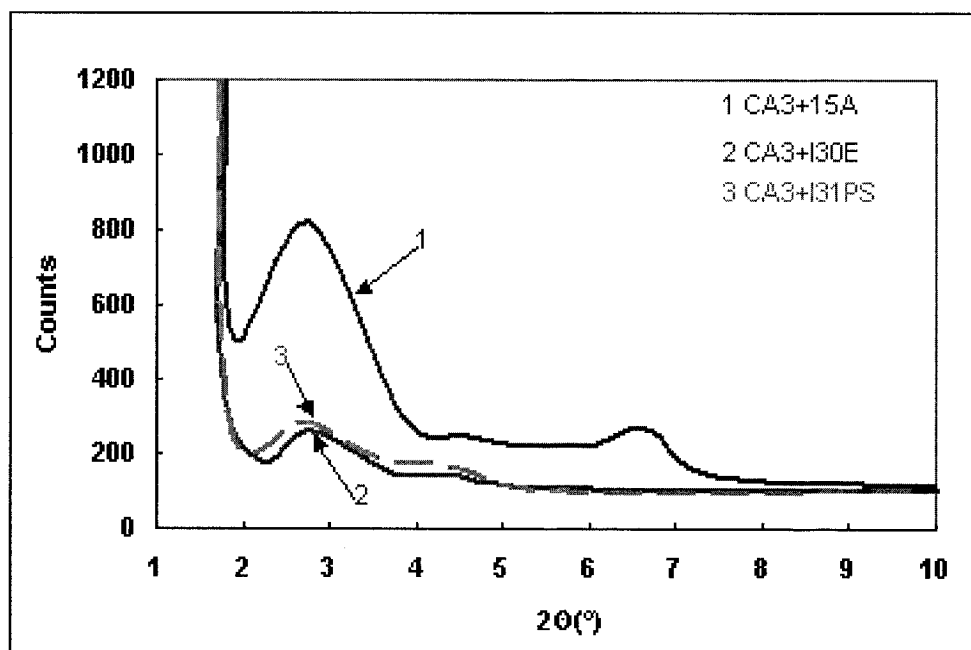


Figure 4.17 Effect of types of clay (with CA3) on the X-Ray results

4.2.3 Tensile and flexural properties

Figures 4.18 and 4.19 show the performance of nanocomposites filled by five types of clays in addition to the same coupling agent CA3. 15A, I30E and I31PS composites also gave better performance than others. Their tensile moduli were improved by about 35-45%; flexural moduli were improved by about 25% as compared to pure PP. At the same time, their flexural strength were also improved a little as well as the tensile strength of 15A composites. Compared to Figure 4.12, which showed the properties of the composites with clay alone, significant property improvements have been achieved with

the presence of coupling agent CA3, especially for 15A clay. Because the same process conditions and concentration of clay were applied in the composites, the improvement of tensile and flexural properties should be attributed to the better dispersion of clay in matrix or better interface between clay and matrix with the cooperation of CA3. Due to the degradation effect of I30E and I31PS, their improvement in properties should have more relation with their better exfoliation under the same conditions than 15A as shown in Figure 4.17.

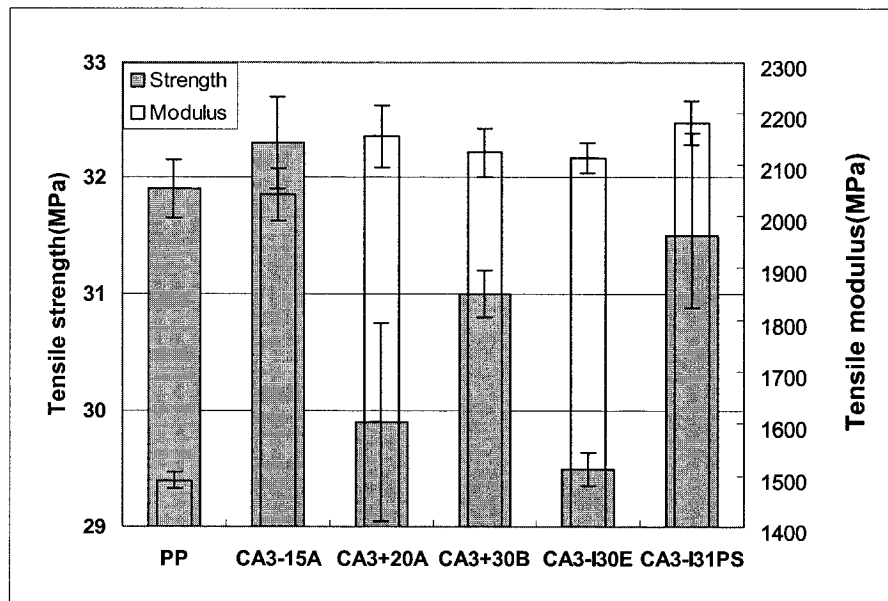


Figure 4.18 Effect of types of clay on tensile properties (with the presence of CA3)

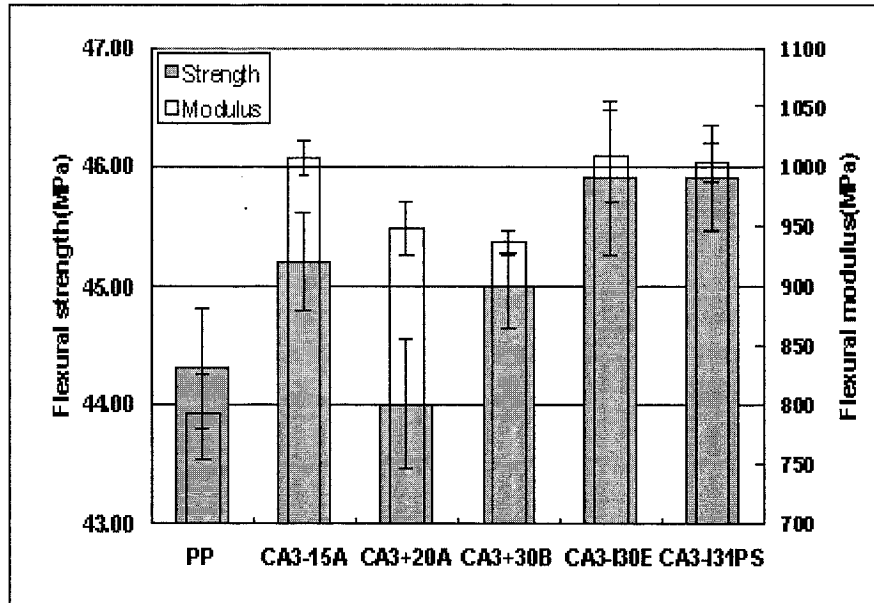


Figure 4.19 Effect of types of clay on flexural properties (with the presence of CA3)

4.3 Effect of types of clay in the presence of coupling agent CA4

The variables and experimental conditions of this experiment set are listed in Table 4.5.

Table 4.5 Variables and experimental conditions of Experiment Set 4.3

Variation Sample	Types of clay	Types of coupling agent	Processing parameters		
			Temperature (°C)	Mixing time (min)	rpm
CA4+15A	15A	CA4	180	5	60
CA4+20A	20A	CA4	180	5	60
CA4+30B	30B	CA4	180	5	60
CA4+I30E	I30E	CA4	180	5	60
CA4+I31PS	I31PS	CA4	180	5	60

4.3.1 Rheological behavior

Figure 4.20 is the torque-time curves of the composites containing three different clays and the same coupling agent CA4. They have the same trends as observed in Figure 4.3 and 4.16.

4.3.2 Dispersion behavior- XRD

Figure 4.21 illustrates X-Ray curves of the composites containing different types of clay and same coupling agent CA4. These curves are similar to those in Figure 4.17. I30E and I31PS have lower peaks than 15A. However, with addition of CA4, 15A composites first peak apparently shifted to a lower angle compared to other composites curves, which means better intercalation has taken place due to CA4 presence.

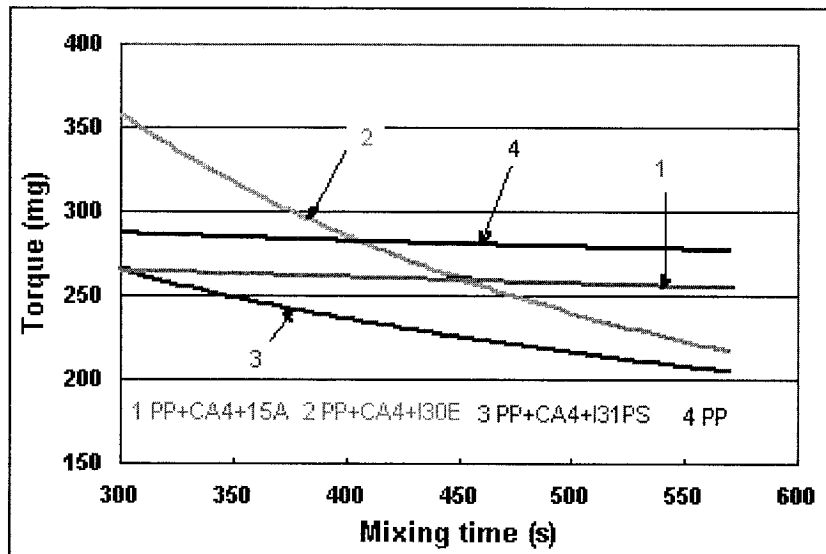


Figure 4.20 Torque-time curves of the composites with CA4 and different types of clay

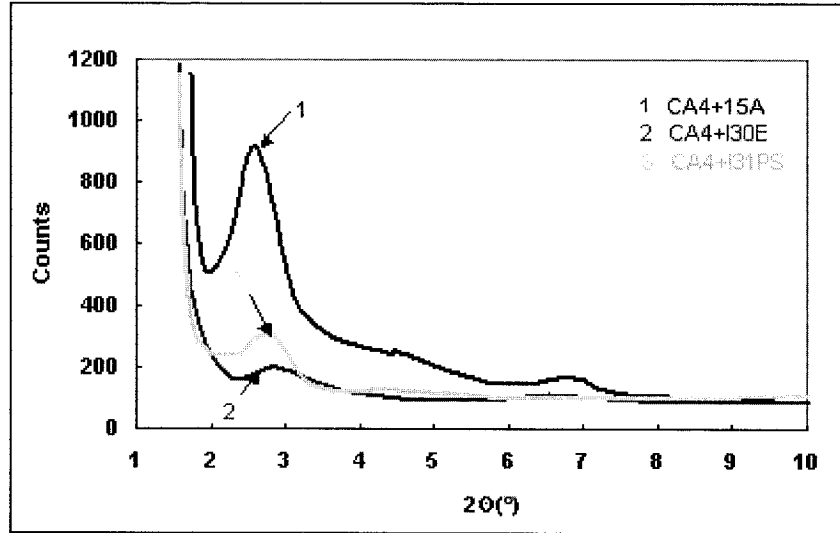


Figure 4.21 Effect of types of clay on the X-Ray results

4.3.3 Thermal properties

4.3.3.1 Crystallization behavior

Figure 4.22 and Table 4.6 show the crystallization behavior of the composites containing CA4 and different clays. T_c of the composites with CA4 increased compared to the composites without CA4. The magnitude of T_c of the different clays is 15A > 20A > I30E > I31PS > PP. The degree of crystallinity (X_c) also varied with the types of clay. The magnitude of X_c of these clays is 15A > 20A > I30E > PP > I31PS. This is generally similar to the order without coupling agent.

4.3.3.2 T_m

Figure 4.23 shows the melting curves of the composites with coupling agent CA4 and different clays. Their T_m , which are listed in Table 4.6, decreased as compared to pure PP

(except 15A composite had higher T_m than PP). The order of their T_m is 15A > PP > 20A > I31PS > I30E, which is also similar to the order without coupling agent.

Table 4.6 Crystallization and melting behavior of the composites with different clays and CA4

Sample	T_c (°C)	T_m (°C)	X_c (%)
PP	107.4 ± 0.3	165.9 ± 0.2	43.9 ± 0.8
PP+CA4+15A	121.4 ± 0.2	167.4 ± 0.3	45.5 ± 0.8
PP+CA4+20A	119.6 ± 0.3	164.9 ± 0.4	44.6 ± 0.6
PP+CA4+I30E	118.3 ± 0.2	161.7 ± 0.6	44.07 ± 1.6
PP+CA4+I31PS	117.3 ± 0.5	163.1 ± 0.3	42.44 ± 0.9

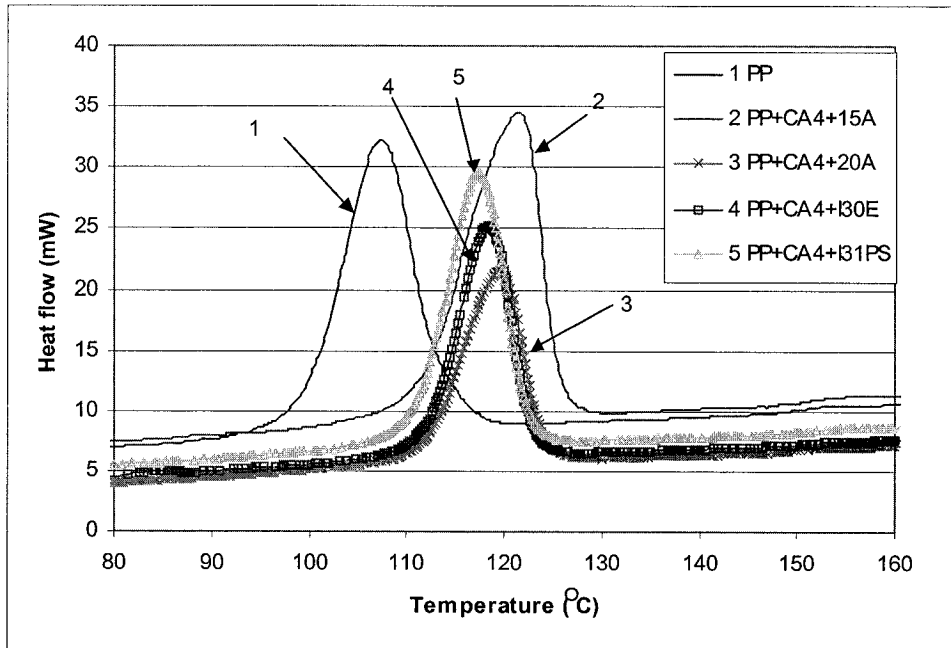


Figure 4.22 Crystallization curves of the composites with CA4 and different clays

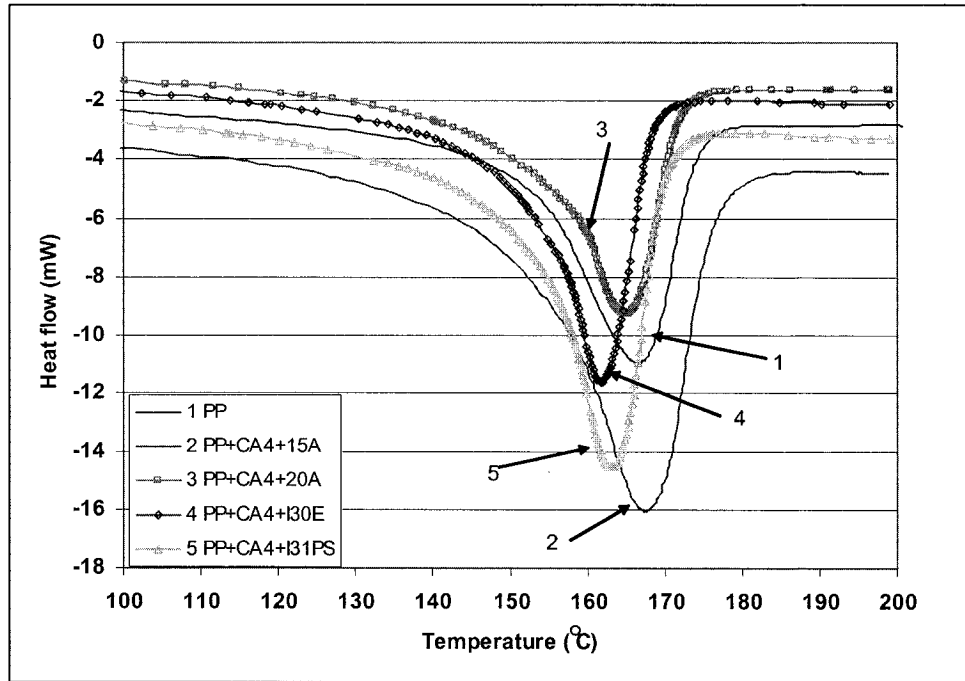


Figure 4.23 Melting behavior of the composites with CA4 and different clays

4.3.4 Tensile and flexural properties

Figures 4.24 and 4.25 show the mechanical properties of nanocomposites filled by different types of clay using the same coupling agent CA4. 15A gave the best performance among them. The increase of the tensile modulus and the flexural modulus in 15A-CA4-nanocomposites was 52% and 31%, respectively. The properties of I31PS nanocomposites were also good. The excellent properties of 15A-CA4 nanocomposites indicate that CA4 has good interaction with 15A or makes 15A disperse better in PP. This was proved by X-ray results (Figure 4.21) - the first peak of the curve shifted to a lower degree than other composites.

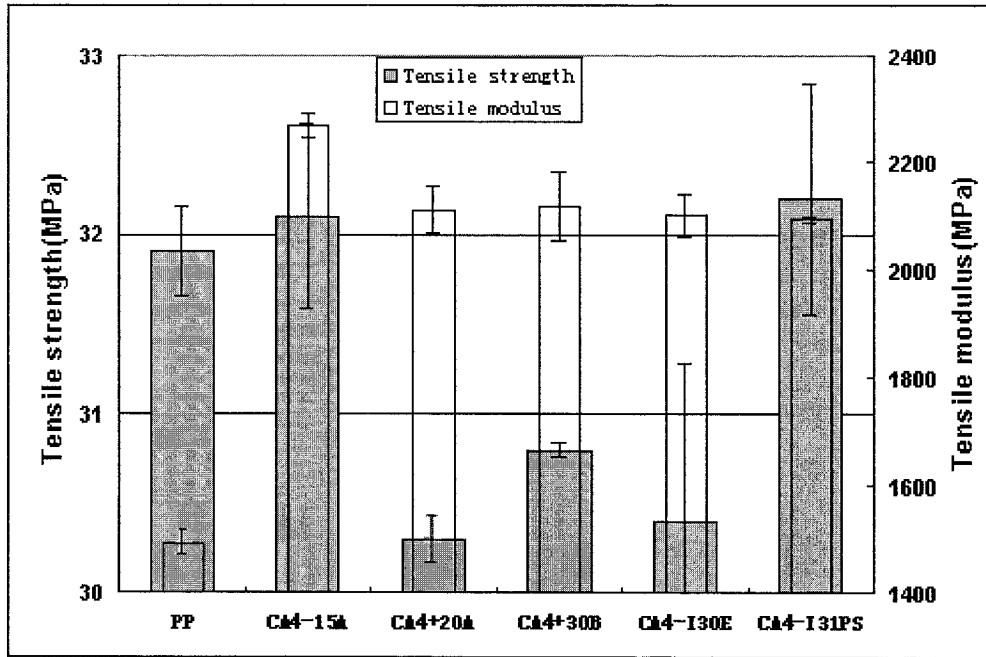


Figure 4.24 Effect of types of clay on tensile properties (with the presence of CA4)

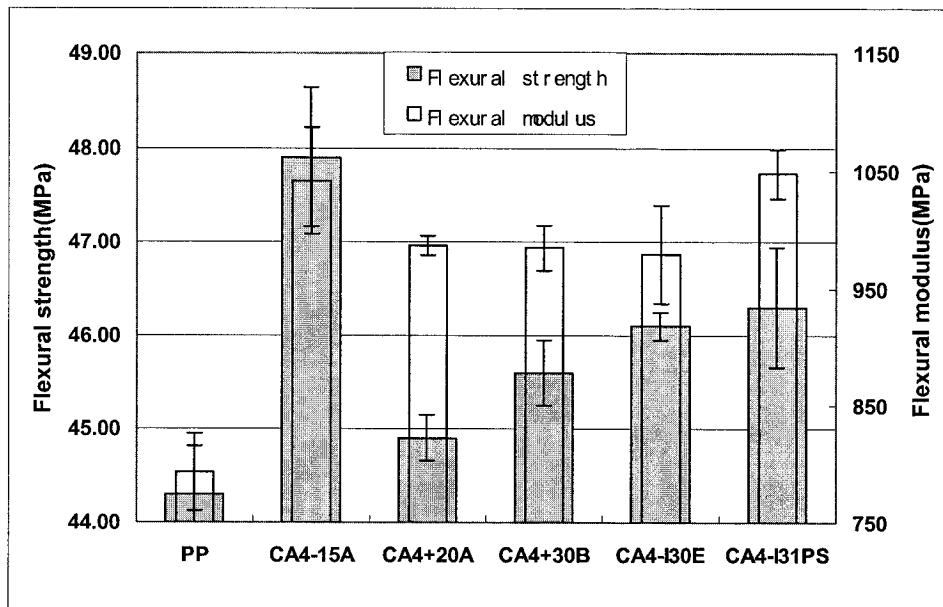


Figure 4.25 Effect of types of clay on flexural properties (with the presence of CA4)

4.4 Conclusions

Modification of the montmorillonite surface by intercalants significantly improves the interface between the clay and the matrix and the dispersion of the clay. The effects of modification on PP nanocomposites varied with the types of clay that are different in the types and concentration of intercalants. Among the five types of clays, 15A, 20A and 30B, which were from Southern Clay Products Inc, had better torque (thermal) stability than I30E and I31PS, which were from Nanocor Inc. The mixtures (with 3% nanoclay, without coupling agent) of 15A, I30E and I31PS had better mechanical performance than the others. 15A mixture had better elongation than other mixtures. On the other hand, mixtures of I30E and I31PS had lower T_g and higher T_s than the other mixtures and pure PP. In addition, nanoclay had an apparent nucleating effect and can improve T_c .

However, mixtures (with only organic-modified clay without coupling agent) cannot give good dispersion and ideal performance compared with PP matrix. 3% nanoclay without coupling agent can only improve 10% tensile modulus and flexural modulus as compared to neat PP. But with 6% coupling agent CA4 present, the improvement of 15A nanocomposites in tensile and flexural modulus can reach 52% and 31%, respectively. Therefore, the use of coupling agent is essential in the formation of PP nanocomposites.

5 Effects of coupling agent on the formulation and properties of PP nanocomposites

Coupling agents are well known to improve interfacial adhesion between two different materials in composites. PP is hydrophobic, whereas the nanoclay surface is hydrophilic. Although organic modification using onium ion or amine modifier in which the polar surfaces of the clay should be covered with nonpolar alkyl group can make the clay surface more nonpolar and more hydrophobic, the hybrid state in a PP matrix was rarely realized. Coupling agents, such as MAgPP, NH_2 - or NH_3^+ -terminated-PP, have polar or reactive groups, such as NH_3^+ , MA (or COOH group generated from the hydrolysis of the maleic anhydride group), which can combine with the negative sites and polar groups-OH on the clay surface to form ion bond or hydrogen bond. These strong bonds generate the driving force for the intercalation to result in coupling agent molecules to intercalate into the clay layers. On the other hand, the other end of molecular chains in coupling agent is alkyl chains which are well miscible with PP. Therefore, the ideal result is that the nanoclay layers are dispersed homogeneously in PP matrix (exfoliated nanocomposites). In this case, the coupling agent plays a crucial role.

Five types of coupling agent were examined in order to determine their effects on PP nanocomposites. The experiments were designed in four series: PP with coupling agent

alone, with coupling agent and 15A clay, with coupling agent and I31PS clay, and with coupling agent and I30E clay.

5.1 Effect of coupling agent (alone) on PP matrix

Table 5.1 shows the variables and conditions for this experimental set.

Table 5.1 Variables and experimental conditions of Experiment Set 5.1

Variables Sample	Types of clay	Types of coupling agent	Processing parameters		
			Temperature (°C)	Mixing time (min)	rpm
CA1	-	<i>CA1</i>	180	5	60
CA2	-	<i>CA2</i>	180	5	60
CA3	-	<i>CA3</i>	180	5	60
CA4	-	<i>CA4</i>	180	5	60

5.1.1 Rheological behavior

Figure 5.1 shows the torque curves of the PP and its blends with different coupling agents. Some obvious differences can be seen. The torque curve of the blend containing coupling agent CA4 is relatively stable, whose trend is similar with PP. However, the other coupling agents all resulted in a more pronounced downward trend. The general order of the effect of the coupling agent is thus CA2 \approx CA3 > CA1 > CA4 \approx None. The lowering of viscosity with time is most likely related to a reduction in molecular weight

caused by oxidation and/or degradation the matrix. The grafting process of MA into PP is based on a free radical reaction with an excess amount of reactants, and it is impossible to remove all the residuals and radicals from the material. Therefore, it is well known that MAgPP is in general not highly thermally stable. Of the four coupling agents, CA2 and CA3 had the greatest detrimental effect. In the case of CA2, solvent extraction showed that it contains approximately 0.2 wt% of soluble impurities, whereas for CA1 the amount was found to be negligible; this could explain the larger effect of the CA2. The higher content of MA groups in CA2 could also be a factor. The CA3 was prepared by reaction between CA1 and Jeffamine, so the low stability observed for CA3 could be related to residual amine groups. CA4 was obtained by soaking CA3 in an acid environment at high temperature, which might be expected to remove amine residues and other impurities and may explain the improved stability for CA4, even better than for the CA1 from which it originated.

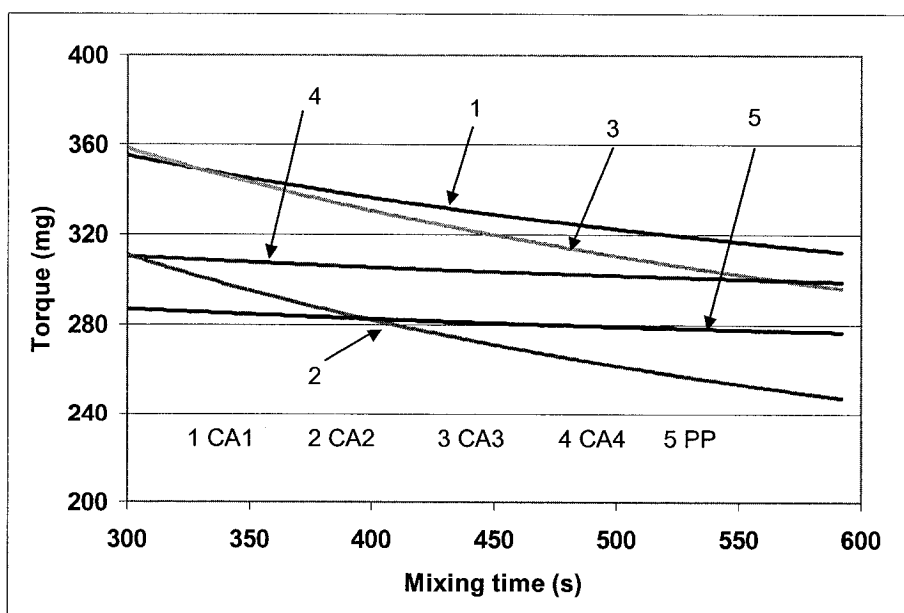


Figure 5.1 Torque-time curves of blends with different coupling agents

5.1.2 Thermal properties

5.1.2.1 Crystallization behavior

Figure 5.2 and Table 5.2 describe the crystallization behavior of PP and its blends containing different coupling agents. The presence of coupling agents in the PP matrix significantly increased the T_c of the blends. This verified the co-crystallization function of coupling agent. The increase varied with the types of coupling agent. CA2 blends had the lowest T_c and CA4 blends had the highest T_c among them. The order was CA4 > CA1 > CA3 > CA2 > PP. The X_c varied little.

5.1.2.2 T_m

Figure 5.3 and Table 5.2 show the melting behavior of PP and its blends. T_m of the blends is decreased or kept at the same level (CA4 blends) as compared to pure PP. This is because the coupling agent is lower molecular weight material and has lower T_m than PP.

Table 5.2 Crystallization and melting behavior of PP and its blends

Sample	T_c (°C)	T_m (°C)	X_c (%)
PP	107.6 ± 0.3	165.9 ± 0.2	43.9 ± 0.8
CA1	115.1 ± 0.1	163.7 ± 0.4	46 ± 0.4
CA2	112.2 ± 0.4	163.5 ± 0.3	42.6 ± 1.1
CA3	113.5 ± 0.3	163 ± 0.4	44.3 ± 0.3
CA4	117.9 ± 0.2	166.5 ± 0.5	44.9 ± 0.9

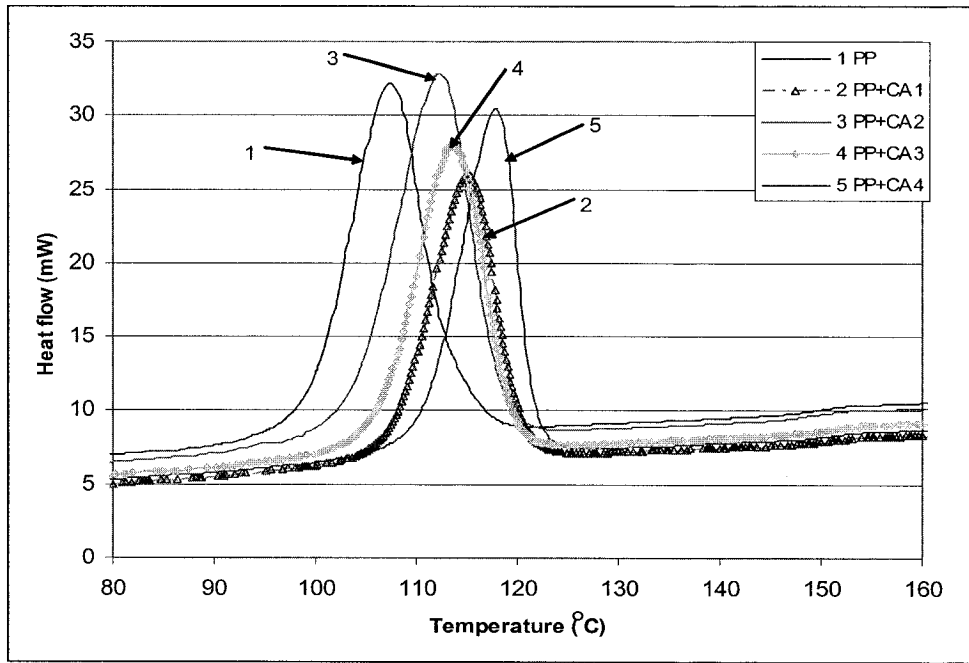


Figure 5.2 Crystallization curves of the blends (PP with different coupling agents)

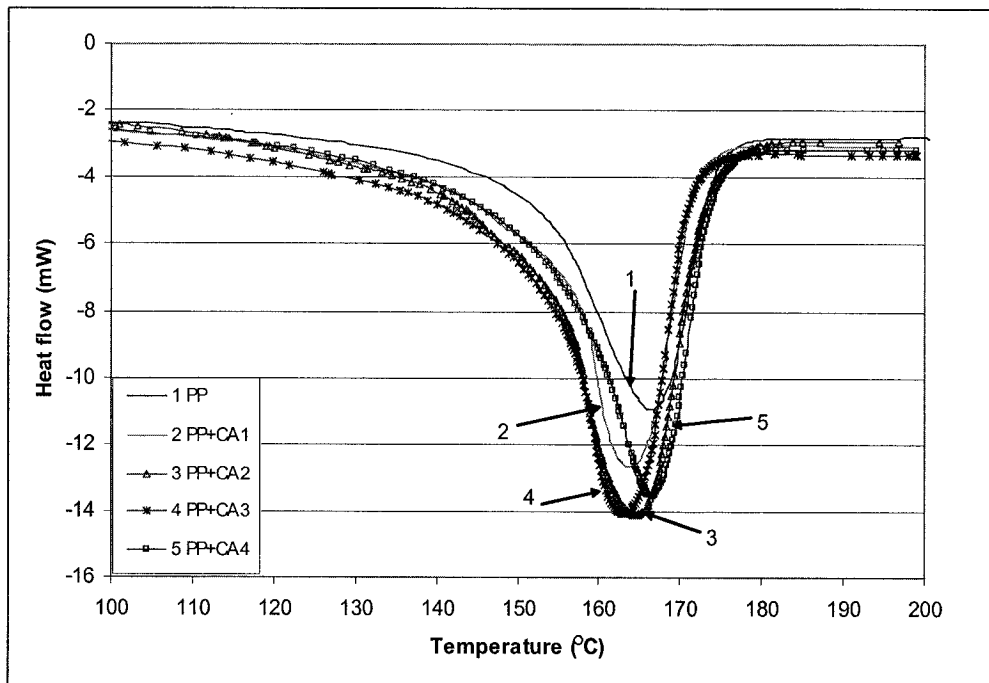


Figure 5.3 Melting behavior curves of the blends (PP with different coupling agents)

5.2 Effect of coupling agent in the presence of 15A clay

Table 5.3 shows the variables and experimental conditions of this experiment set.

Table 5.3 Variables and experimental conditions of Experiment Set 5.2

Variables Sample	Types of clay	Types of coupling agent	Processing parameters		
			Temperature (°C)	Mixing time (min)	rpm
CA1+15A	15A	<i>CA1</i>	180	5	60
CA2+15A	15A	<i>CA2</i>	180	5	60
CA3+15A	15A	<i>CA3</i>	180	5	60
CA4+15A	15A	<i>CA4</i>	180	5	60

5.2.1 Rheological behavior

Figure 5.4 shows the torque curves for the composites prepared with 15A clay in addition to the coupling agents. With the presence of 15A, the curves show some differences from Figure 5.1 in which only contains coupling agent. The order of the effect of the coupling agent on the degradation is now $CA2 > CA1 > CA3 > CA4 > \text{None}$. This is generally similar to the trend without nanoclay, except that CA3 has improved somewhat relative to the others.

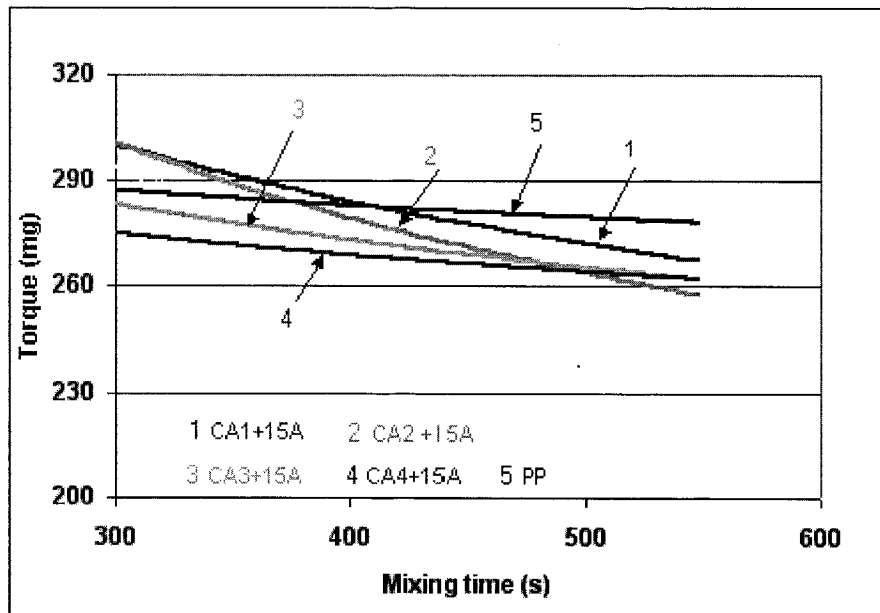


Figure 5.4 Torque – time curves of systems based on different coupling agents with clay 15A

5.2.2 Dispersion behavior

5.2.2.1 XRD

As mentioned in Section 4.2.2, the position (angle 2θ) of the peak in XRD curves is related to the clay gallery spacing and therefore the degree of intercalation, whereas the peak intensity is an indicator of the amount of intercalated clusters or the amount of non-intercalated (i.e. exfoliated) material. Figure 5.5 shows the XRD curves of the 15A clay alone and the composites containing coupling agent. 15A has three distinct peaks at 2.9° , 4.8° , and 7.3° , which can be related respectively to different extents of clay intercalation: high, poor, and none. Generally speaking, it appears that in the composite samples all three peaks shift to lower angles compared to those of the starting clay, and the intensity of the peaks also decreases to different extents. A shift of the peaks to lower angles

proves that intercalation has taken place during mixing. A reduction in the peak intensity indicates that the amount of intercalated clay has decreased, or in other words, the dispersion has been improved by breakdown of clusters or even exfoliation. From these two aspects, it may be concluded that some intercalation and exfoliation have simultaneously taken place in the composites obtained, although it is far from complete. The gallery distances of the composites are summarized in Table 5.4, which provides clearer evidence of the quality of the intercalation of the clays by the coupling agent. The gallery distance of 2.8 nm for the onium-treated 15A was slightly extended to 3.3-3.5 nm in the nanocomposites, depending on the type of coupling agent. Undoubtedly, the coupling agent plays an important role in forming an acceptable interface between the matrix and the clay surface. It is not unreasonable to conclude that the hydrophilic (polar) groups of the coupling agents have created some strong van der Waals and even hydrogen bonds with the hydroxyl groups on the clay surface. This kind of interface is like a bridge to help hydrophobic PP molecules to penetrate the hydrophilic galleries of the clay to form intercalated nanocomposites. Figure 5.6 is the schematic drawing of function of coupling agent in nanocomposites. The efficiency of each coupling agent is strongly dependent on its chemistry.

As seen in Figure 5.5, among the composites, the CA2 system had a first peak with a rather high intensity while the second peak shifted to a higher angle. This indicates that the clay was poorly dispersed in the matrix of this sample. Surprisingly, when the impurities in CA2 are removed the dispersion is greatly improved, since the intensity of all three peaks in the sample CA2P are noticeably weaker. It is also interesting to

observe in Figure 5.5 that in the CA4 composite the first peak shifted furthest to the left, with a corresponding gallery distance of 3.53 nm, showing that CA4 results in slightly better intercalation of the clay. In addition, the intensities of the second (poorly intercalated) and third (non-intercalated) peaks in this sample are almost negligible, suggesting that the amine cation in the CA4 may actively open up the non-intercalated clay galleries in the molten state. It can be understood that this could occur through reaction of the amine cations of the CA4 with anionic sites on the surface of the non-intercalated clay via an ion exchange reaction. CA1 and CA3 provided more or less the same level of dispersion, although CA1 led to slightly better intercalation as the peak shifted slightly to the left, while CA3 led to better exfoliation as the peak intensity decreased.

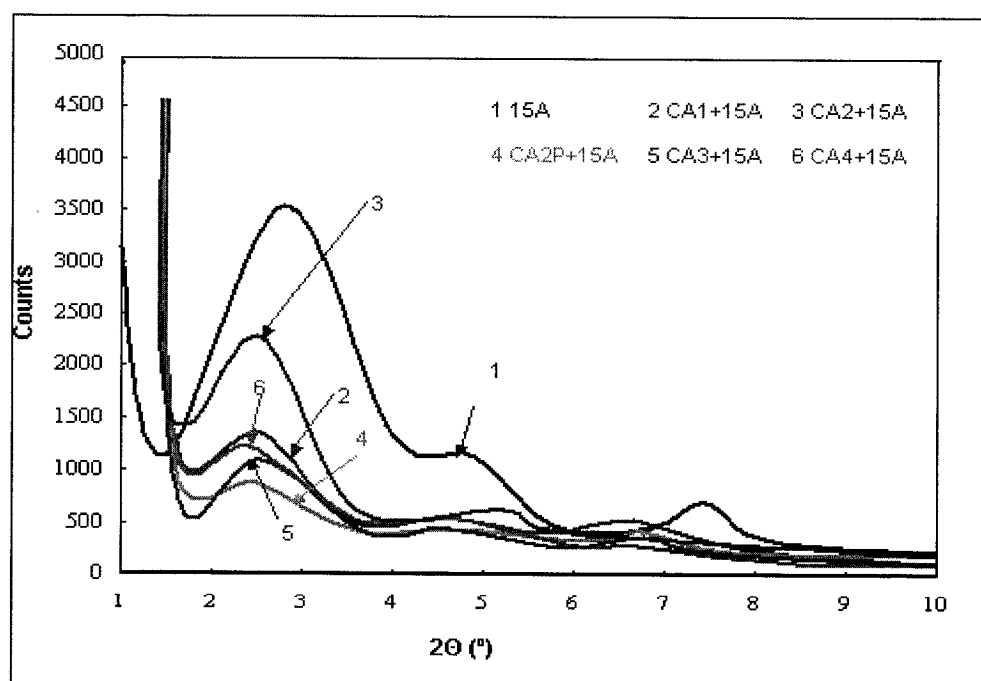


Figure 5.5 Effect of coupling agent on the X-ray diffraction results

Table 5.4 Gallery distances of the clays in the composites

Peak Samples	First peak		Second peak		Third peak	
	Angle (°)	Gallery distance (nm)	Angle (°)	Gallery distance (nm)	Angle (°)	Gallery distance (nm)
PP + 15A	2.91	2.83	4.86	1.81	7.30	1.20
PP + CA1 + 15A	2.61	3.37	4.6	1.92	6.75	1.31
PP + CA2 + 15A	2.60	3.40	5.2	1.79	6.77	1.30
PP + CA2P + 15A	2.58	3.42	4.74	1.82	6.81	1.30
PP + CA3 + 15A	2.71	3.26	4.78	1.81	6.82	1.30
PP + CA4 + 15A	2.50	3.53	4.70	1.88	—	—

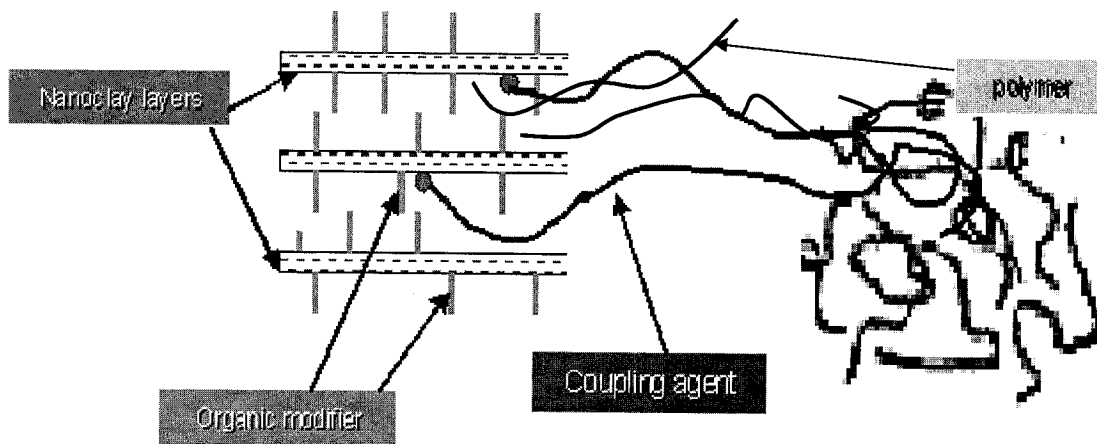


Figure 5.6 Schematic representation of the function of coupling agent in nanocomposites

All these results show that the coupling agent generally results in increased intercalation and exfoliation, although the extent of the effect varies from one agent to another because of the differences in their chemistry. According to references [33, 34, 49], the content of coupling agent and the ratio of coupling agent with clay can be changed to obtain complete exfoliation.

5.2.2.2 SEM

Figure 5.7 shows the SEM photo of nanocomposites based on 15A and CA2P (coupling agent with MA groups). Figure 5.8 is the SEM photo of nanocomposites based on 15A and CA4 (coupling agent with onium ions). In the presence of coupling agent, the size of the aggregates reduced significantly compared to the SEM photo (Figure 4.6) in the absence of coupling agent. A few large aggregates (diameter is over 1 μ m) were observed. Better interface between nanoclay and matrix can also be expected from the photos. Comparing Figure 5.7 with 5.8 (a), nanoclays had better dispersion (smaller aggregates) in the nanocomposites with coupling agent CA2P than that with CA4, which is commensurate with the XRD results. The fracture mode shown in Figure 5.8 is very interesting. Figure 5.8 (a) and (b) are the different areas in the same fracture surface, but one is brittle, another is very ductile, even more ductile than pure PP. This shows that the sample was not uniform and may indicate that the exfoliated nanocomposites were possibly obtained in some portion of the sample because Figure 5.8 (b) shows the fracture characteristics of the exfoliated nanocomposites.

The improvement of dispersion by coupling agent can be understood by the better interaction between coupling agents and nanoclays. The coupling agents have low molecular weight and high concentration of MA polar groups (for CA2P) or high molecular weight and low concentration of onium ion (for CA4). The low molecular weight increases the mobility of the polymer chain and hence facilitates the diffusion into the nanoclay galleries [80, 81]. The MA groups in CA2P can interact with hydroxyl

groups on the nanoclay surface to form hydrogen thus promote the diffusion process of the coupling agents into the galleries [57, 82]. However, CA4 besides the hydrobonding, it can also chemically react with the negative charge on the clay surface, which believes to create a strong interface. As a result of the physical and/or chemical interaction, the clay galleries must expand up to a certain level and the aggregates are broken into smaller pieces. At the same time, the interfaces between nanoclay and matrix are also improved significantly since the alkyl bone of the coupling agent has good compatibility with PP matrix. From the mechanical rupture of the sample, it seems that the CA4 provides a better interface which results in a partly fibrillar fracture surface. Therefore, a suitable coupling agent is critical to obtain nanocomposites.

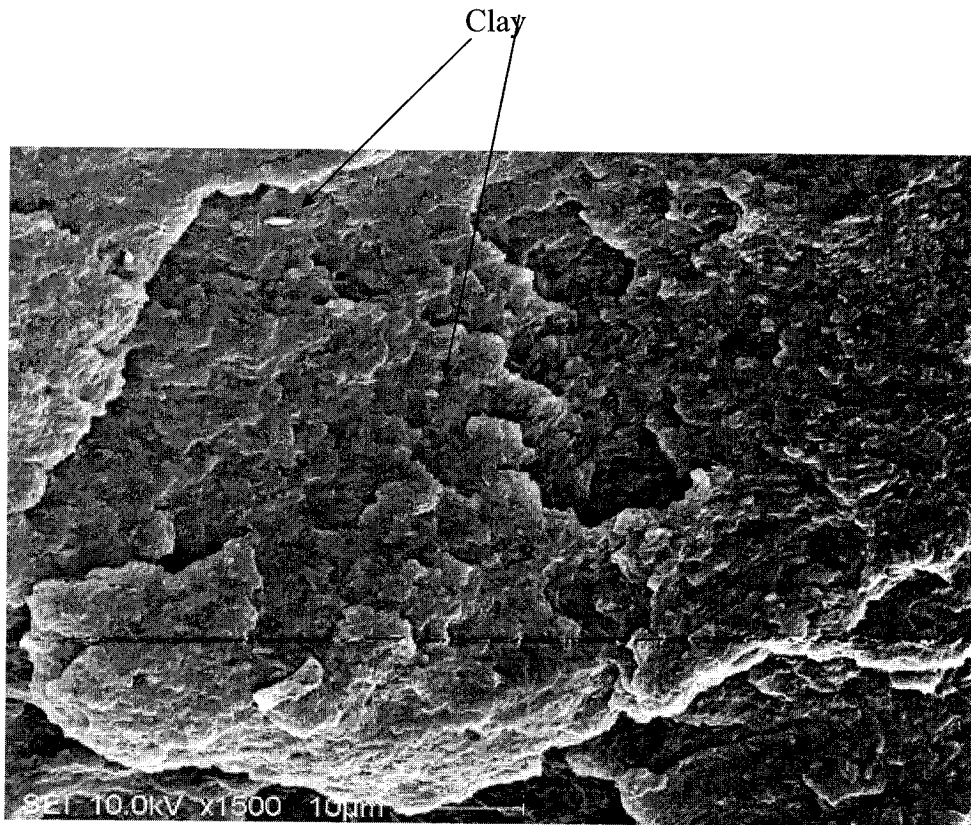


Figure 5.7 SEM photo of nanocomposites with 15A nanoclay and coupling agent CA2P

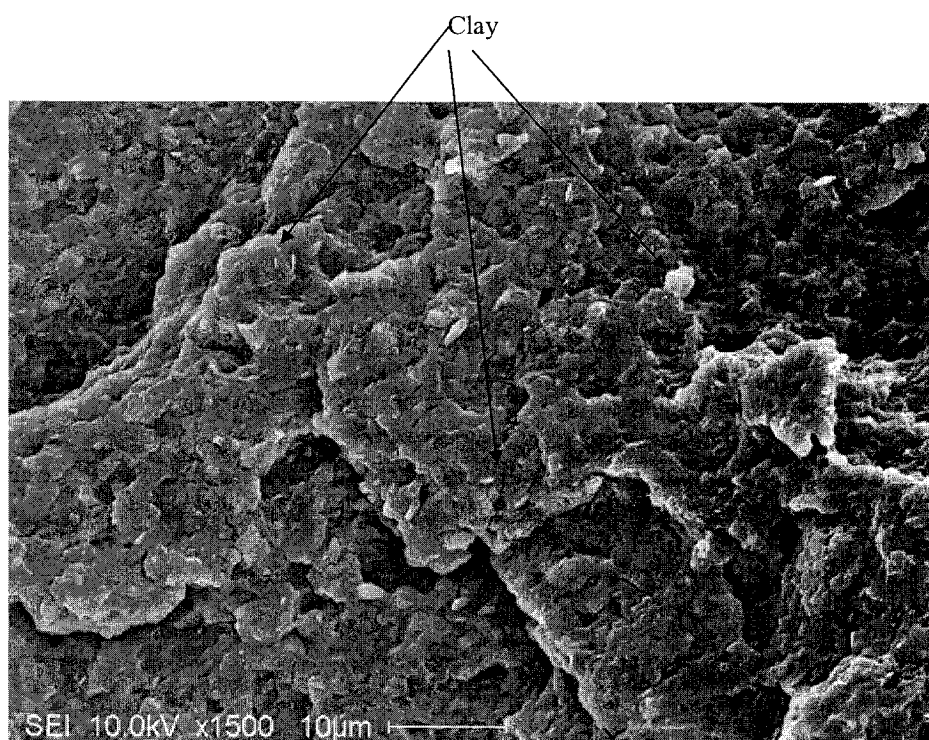


Figure 5.8 (a) SEM photo of nanocomposites with 15A and coupling agent CA4 (area 1)

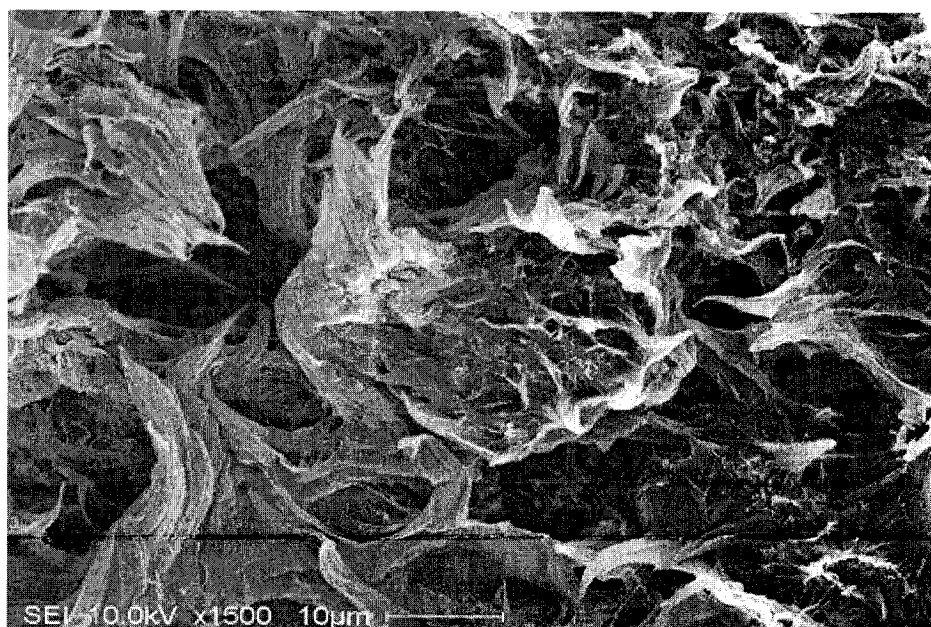


Figure 5.8 (b) SEM photo of nanocomposites with 15A and coupling agent CA4 (area 2)

5.2.3 Thermal properties

5.2.3.1 Crystallization behavior

Figure 5.9 shows the crystallization curves of the nanocomposites based on 15A clay and different coupling agents. Table 5.5 lists T_c and X_c of these composites. With the addition of coupling agent and nanoclay, the T_c of the nanocomposites is higher than that of PP. Moreover, significant differences of T_c appeared in the different types of coupling agents. CA4+15A nanocomposite had the highest T_c and 8°C higher than CA2. The order of the composites T_c is CA4>CA3>CA1>CA2>PP, which is similar to the blends without nanoclay except that CA3 nanocomposites had significantly higher T_c than its blends. It is interesting that CA1 and CA2 nanocomposites had similar T_c with their blends while CA3 and CA4 nanocomposites had higher T_c than their blends. Compared with the T_c of 15A mixtures without coupling agent (Table 4.2), CA1 and CA2 nanocomposites had lower T_c and CA3 and CA4 had higher T_c . Considering the same concentration (amount) of coupling agent and nanoclay and same processing parameter employed, these differences should be attributed to the chemistry of coupling agents and the interaction between coupling agent and nanoclay. Since CA3 was processed by co-extrusion with amine, excess amount of amine group or more impurities may cause the earlier crystallization. A similar situation can also happen to CA4. Another possibility is because CA3 and CA4 can form stronger bonds than CA1 and CA2 with the clay surfaces, the dispersion of nanoclay in these nanocomposites is better than CA1 and CA2 based ones. The better dispersion can produce more nucleating cores to make crystallization take place easily, which can result in better nucleating effect and higher T_c . The higher T_c

might show that a higher extent of segregation of the dispersed clay particles takes place around the boundary of the spherulites (interspherulite) [84].

From Table 5.5, the existence of coupling agents and nanoclays affects not only the crystallization temperature (T_c) but also the degree of crystallinity (X_c). With the addition of coupling agent and nanoclay, the X_c of nanocomposites increased somewhat (except CA1 based nanocomposite) compared with pure PP. Therefore, the nucleating effect should have a positive effect on the crystallinity. Further research is needed to explain the reason.

5.2.3.2 T_m

Figure 5.10 shows the melting behavior of the nanocomposites containing 15A and different coupling agents. T_m is listed in Table 5.5. The composites based on 15A and coupling agents have somewhat higher T_m than the mixtures without coupling agent, the blends without nanoclay and pure PP. CA4+15A had highest T_m . Because the low molecular weight material is detrimental to the T_m of the composites while the high level dispersion is helpful to improve the T_m , the balance between them determines the T_m of the composites. Apparently, the improvement of T_m of these nanocomposites is the result of better dispersion of nanoclay in matrix. The highest T_m of CA4 nanocomposites agreed with its best intercalation ability with 15A that was observed in Figure 5.5 and Table 5.4.

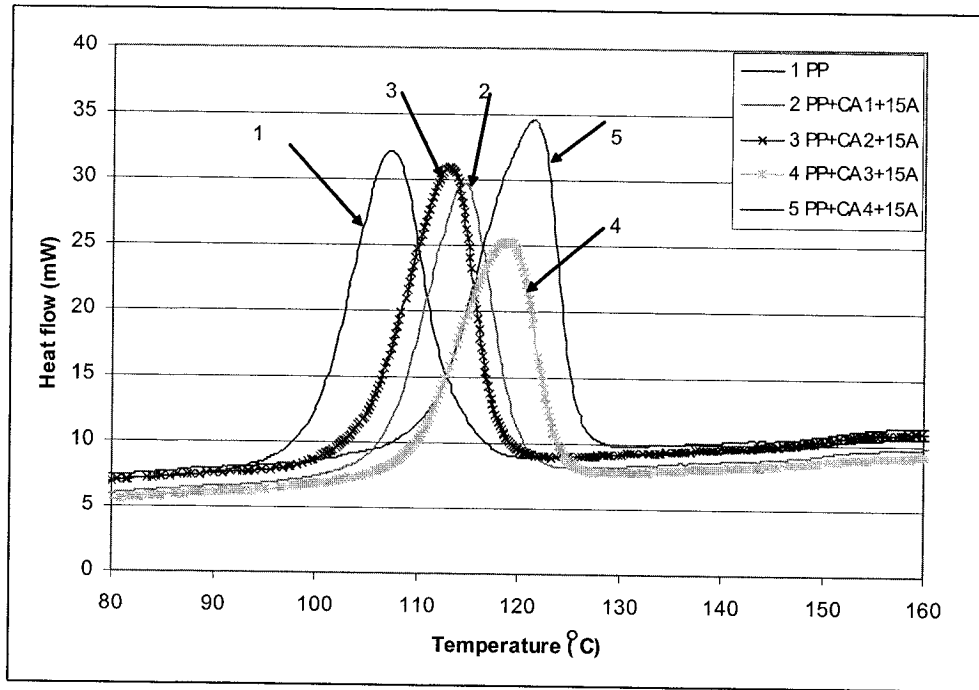


Figure 5.9 Crystallization curves of the nanocomposites with 15A clay and different coupling agents

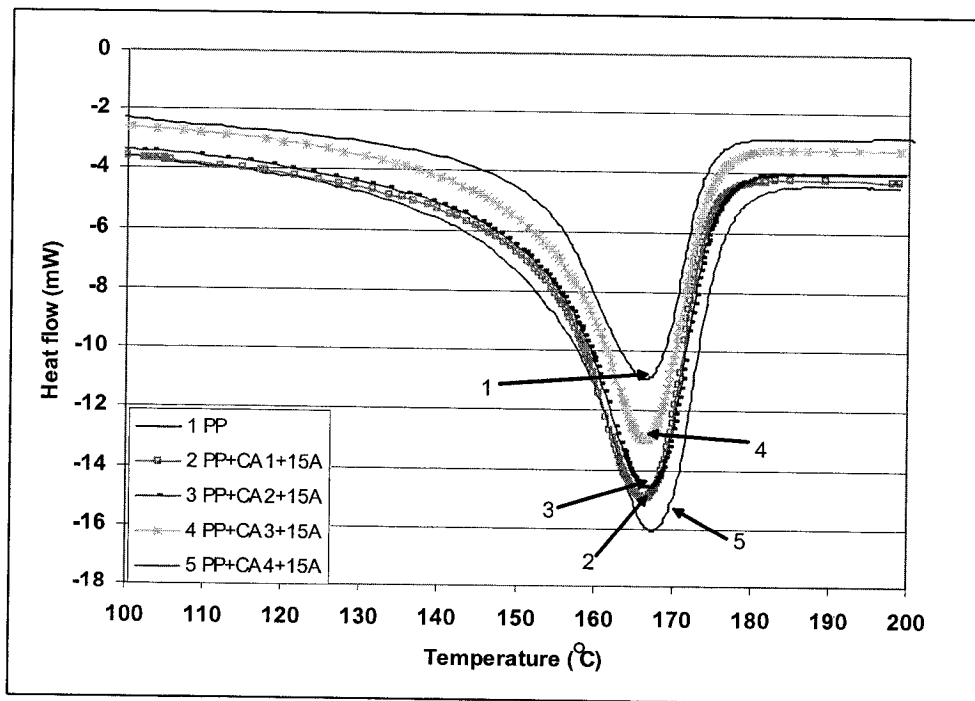


Figure 5.10 Melting behavior of the nanocomposites with 15A clay and different coupling agents

**Table 5.5 Crystallization and melting behavior of the nanocomposites
with 15A clay and different coupling agent**

Sample	T _c (°C)	T _m (°C)	X _c (%)
PP	107.6 ± 0.3	165.9 ± 0.2	43.9 ± 0.8
15A	116 ± 0.2	165.6 ± 0.2	46.1 ± 0.7
CA1+15A	114.5 ± 0.2	166.5 ± 0.5	43.8 ± 0.6
CA2+15A	113.1 ± 0.5	166.8 ± 0.3	45.1 ± 0.5
CA3+15A	118.8 ± 0.5	166.4 ± 0.3	48.9 ± 1.2
CA4+15A	121.4 ± 0.7	167.4 ± 0.4	45.5 ± 0.6

5.2.4 Dynamic mechanical properties

Figures 5.11 and 5.12 show the temperature dependence of the storage modulus E' and the loss modulus E'' of systems with different coupling agents. All the nanocomposite samples have a higher storage modulus E' than pure PP over the entire range of temperature. Among them, the CA4 sample have the highest E', almost 40% higher than pure PP at room temperature. The CA3 sample also showed good performance. The CA1 and CA2 samples (both maleic anhydride grafted PP) gave results intermediate between PP and CA4. The significant improvement of the modulus for CA3 and CA4 could be due to a better interface and dispersion in these samples as discussed earlier.

Two apparent changes also occur in these systems: a sharp drop in E' from -10°C to about 15°C (β transition) and a reduction in the rate of drop in E' with temperature over 80°C (α transition), which are similar with mixtures based on PP and nanoclays.

Corresponding with them, two obvious changes occur in Figure 5.12, namely a sharp (β transition) peak in E'' around 5°C and a broader weaker (α transition) peak above 80°C . The first peak is related to the glass transition of the amorphous phase in the PP matrix, while the second is attributed to softening of the matrix. From Figure 5.12, the glass transition (T_g) and the softening point (T_s) of the nanocomposites were determined as the peak temperatures of the E'' curves and are listed in Table 5.6. There was no significant difference in the T_g of the different samples, but the T_s showed some variation, being somewhat higher for CA3 and CA4. Again this is probably related to their better quality of dispersion and interface. However, further experiments must be conducted in order to have a better understanding of this effect.

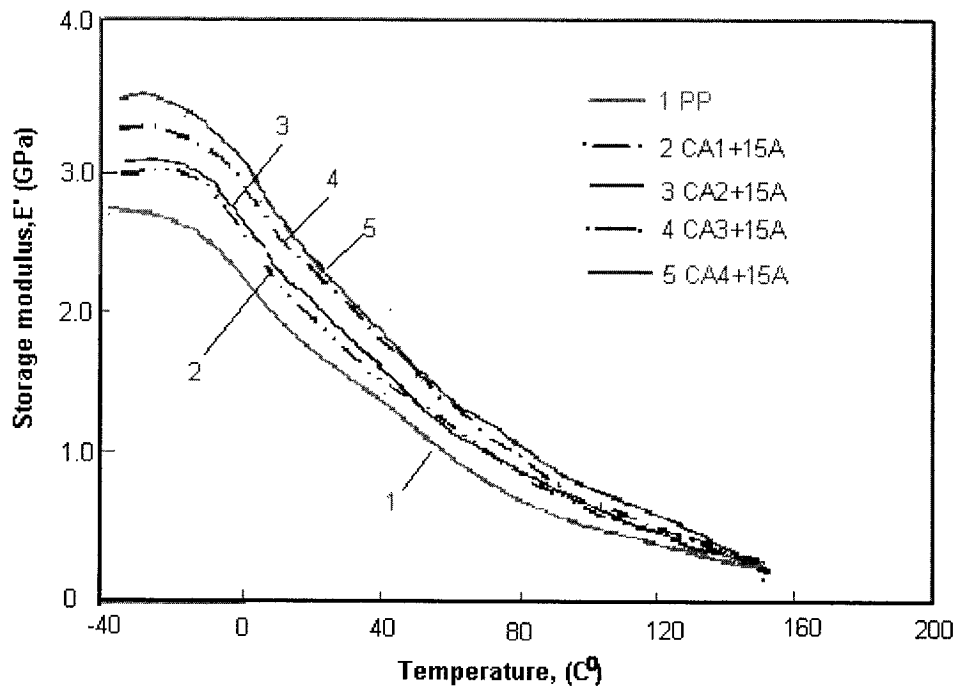


Figure 5.11 DMA curves (E') of the nanocomposites with 15A and different types of coupling agent

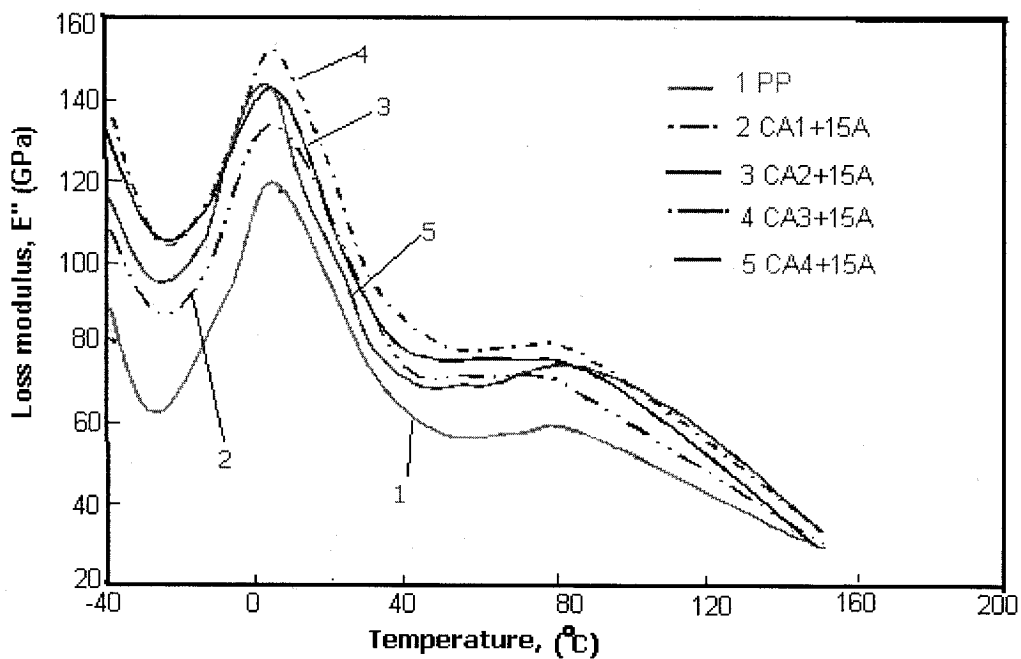


Figure 5.12 DMA curves (E'') of the nanocomposites with 15A and different types of coupling agent

Table 5.6 Effect of coupling agent on T_g and T_s

Samples	T_g ($^{\circ}\text{C}$)	T_s ($^{\circ}\text{C}$)
PP	6.2 ± 0.2	86.6 ± 0.6
15A	5.6 ± 0.2	85.3 ± 1.2
CA1+15A	5.1 ± 0.3	81.4 ± 1.0
CA2+15A	5.0 ± 0.2	84.5 ± 0.7
CA3+15A	5.1 ± 0.1	87.4 ± 0.5
CA4+15A	5.0 ± 0.5	89.0 ± 0.8

The position of the glass transition of a polymer can be influenced by adding low molecular weight materials which reduce intermolecular forces and essentially "lubricate" the macromolecular chains [92]. From Table 5.6 and Figure 5.12, all systems with coupling agent and 15A had lower T_g than pure PP. This indicates that low molecular weight coupling agents are just like intercalants which lubricate the macromolecular chains and play dominant role to influence the T_g . Although the interaction of coupling agents between clay and PP restricts the mobility of molecular chains, lubrication is the dominant factor when the temperature increased to T_g . However, when temperature increases to softening temperature (T_s), the situation changes. CA3 and CA4 based systems have higher T_s than pure PP and mixture with only 15A, which indicated that restriction from the interaction between coupling agent and PP and clay surface plays more important role than the lubrication.

From Table 5.6 and Figure 5.12, CA4 based systems has a relatively lower T_g than others but T_s (the peak of α transition) is higher than others. Its T_g is 3.7°C lower than pure PP and 3.05°C lower than system based on CA1, while T_s was 2.4°C higher than pure PP and 7.6°C higher than CA1 based system. This trend indicates that the amorphous molecules in CA4 based systems can be mobile easily at relatively lower temperature than others, but the mobility of the rigid amorphous molecules in crystals becomes more difficult than others at the same temperature.

Comparing these four types of coupling agent-based systems, the highest storage modulus of CA4 system and the highest softening temperature can be attributed to the

stronger intercalation and interface between PP and nanoclay surface. As discussed earlier, the ammonium ion group in CA4 can interact with negative sites on the clay surface to form strong ionic bond. These bonds are stronger than that ones which are from interaction between anhydride group in CA1 and CA2 and hydroxyl group on clay surface. These strong bonds may also make the crystallization better, restrict mobility of the rigid amorphous molecules, and result in the higher α transition temperature (softening temperature) in Figure 5.12. The highest T_c and high X_c in Table 5.6 can be related to this reason.

5.2.5 Tensile and flexural properties

Figures 5.13, 5.14 show the tensile and flexural properties of the composites based on 15A alone and 15A with coupling agents. As shown in the figures, the tensile strength and modulus, flexural strength and flexural modulus increased as a result of coupling agent incorporation for all the samples. For the PP/CA4/15A nanocomposites, the increases for tensile and flexural modulus are 52% and 31% as compared to pure PP, respectively. And the increase compared to the mixture PP/15A is about 35% for tensile modulus, about 15% in flexural modulus. At the same time, tensile strength and flexural strength also increased somewhat compared to pure PP. For other types of coupling agent, their mechanical performance is also improved, although the extent varied with the types of coupling agent and decided by their chemistry.

From above results, obviously, the coupling agent improves the dispersion of the nanoclays, as discussed earlier, while at the same time it also improves the interface between the PP matrix and the nanoclay surface so that the stress is much more effectively transferred from PP matrix to clay. The modulus is determined at a low stress level, so the quality of dispersion contributes more to the larger modulus.

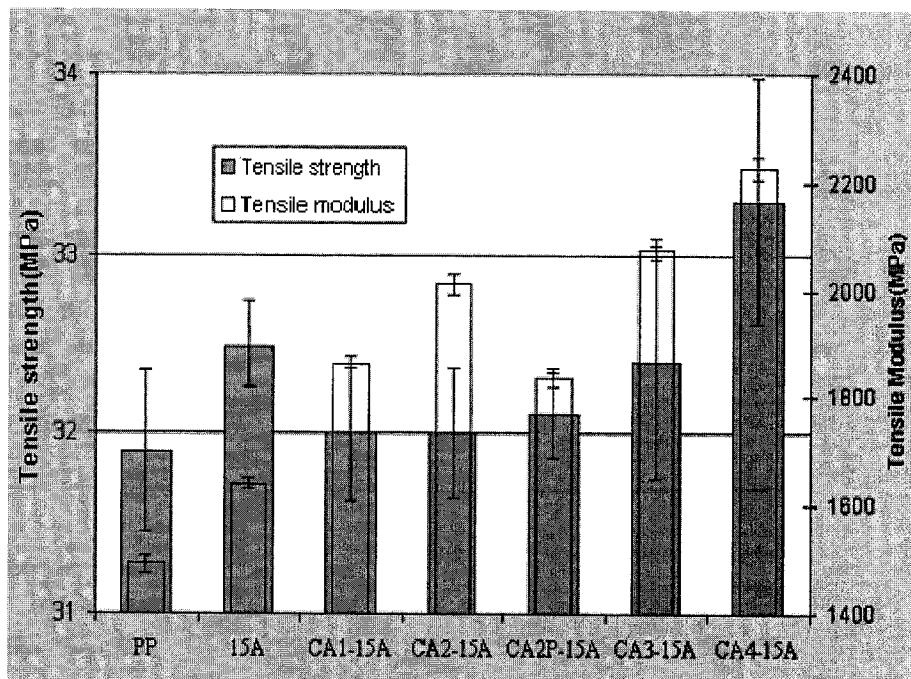


Figure 5.13 Effect of coupling agent on tensile properties of 15A based nanocomposites

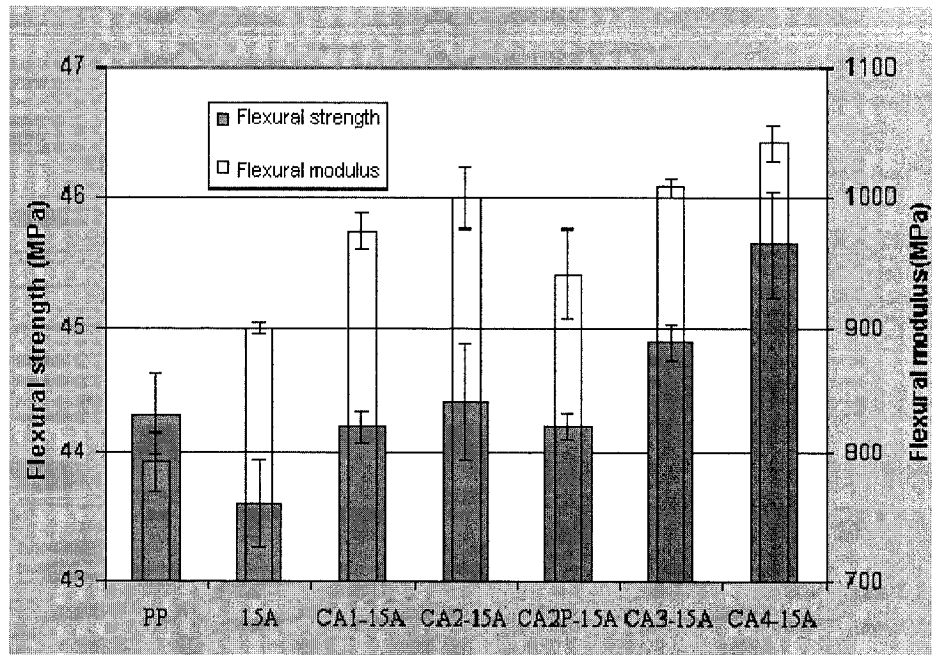


Figure 5.14 Effect of coupling agent on flexural properties of 15A based nanocomposites

5.3 Effect of coupling agent in the presence of I31PS clay

The variables and experimental conditions for this experiment set are listed in Table 5.7.

Table 5.7 Variables and experimental conditions of Experiment Set 5.7

Variables Sample	Types of clay	Types of coupling agent	Processing parameters		
			Temperature (°C)	Mixing time (min)	rpm
CA1+I31PS	I31PS	CA1	180	5	60
CA3+I31PS	I31PS	CA3	180	5	60
CA4+I31PS	I31PS	CA4	180	5	60

5.3.1 Rheological behavior

Effects of coupling agent on the torque – time curves of the composites with I30PS are shown in Figure 5.15. All the I31PS-composites curves show a pronounced downward trend compared to the pure PP curve and the blends curves in Figure 5.1. As the previous observation in Figures 5.1 and 5.2, the presence of coupling agents slightly promoted the drop of curves compared to the curve of the I31PS mixture; CA4 is the most stable one among the coupling agents. The order of the stability of the coupling agents is none > CA4 > CA1 > CA3, which is the same as Figure 5.1.

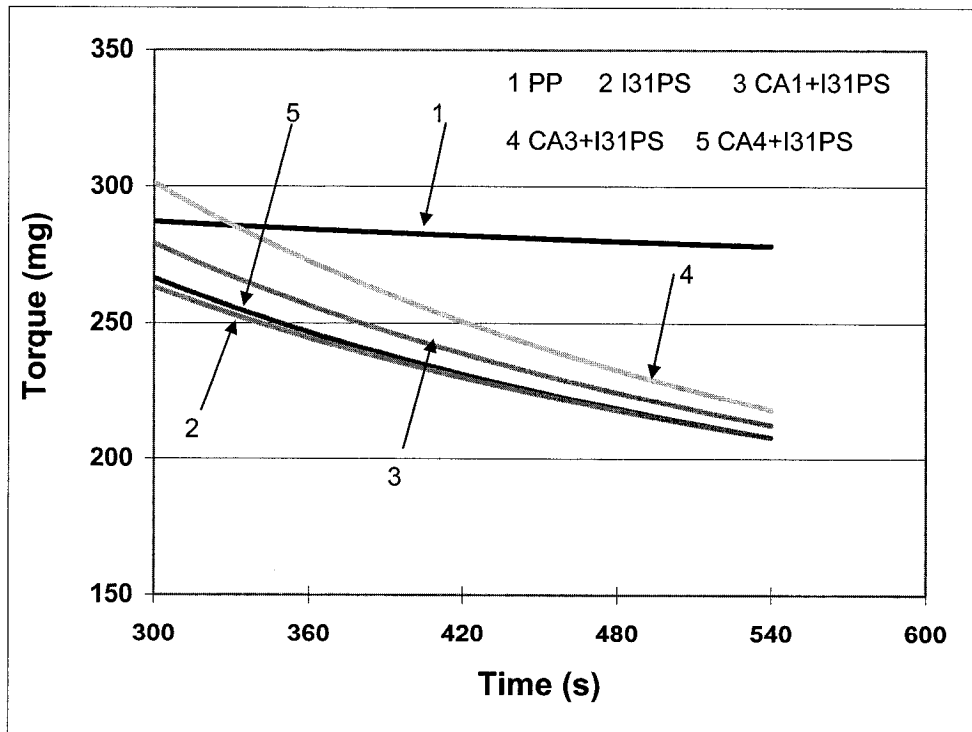


Figure 5.15 Torque – time curves of the composites with different coupling agents and I31PS clay

5.3.2 Tensile and flexural properties

Figures 5.16 and 5.17 show the tensile and flexural properties of I31PS-composites with different coupling agents. As seen from Figures 5.13 and 5.14, the tensile and flexural modulus of the composites containing coupling agent are also improved significantly. It is surprising that the PP/CA1/I31PS composites also have good properties. This indicates that the interaction and cooperation between different clays and different coupling agents can result in optimal composition for PP nanocomposites. The strengths tested in I31PS-composites have more variation probably because the degradation related to I31PS made the composites lack homogeneity and the strengths are very sensitive to all defects, such as voids, holes, cracks, etc. The modulus is determined at a low stress level, so it is affected less than the strength in this case.

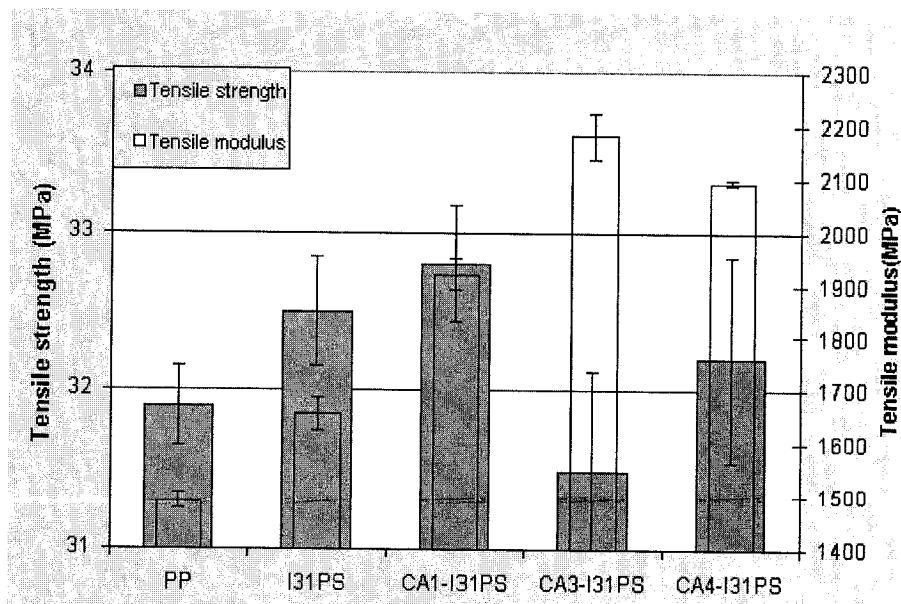


Figure 5.16 Effect of coupling agent on tensile properties of I31PS based nanocomposites

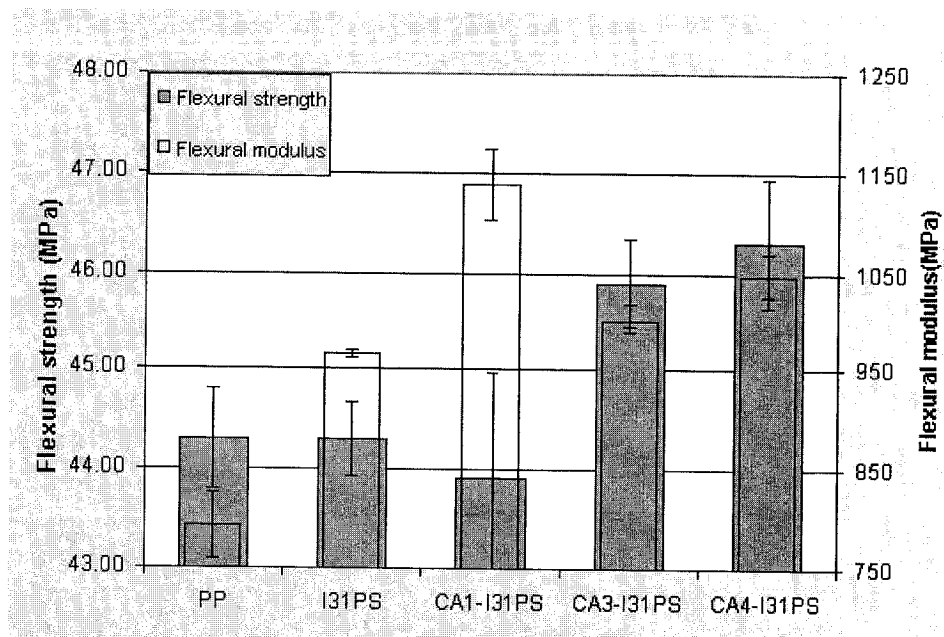


Figure 5.17 Effect of coupling agent on flexural properties of I31PS based nanocomposites

5.4 Effect of coupling agent in the presence of I30E clay

Table 5.8 describes the variables and experimental conditions of this experiment set.

Table 5.8 Variables and experimental conditions of Experiment Set 5.4

Variables Sample	Types of clay	Types of coupling agent	Processing parameters		
			Temperature (°C)	Mixing time (min)	rpm
CA1+ I30E	I30E	CA1	180	5	60
CA3+ I30E	I30E	CA3	180	5	60
CA4+ I30E	I30E	CA4	180	5	60

Figures 5.18 and 5.19 give the difference in mechanical performance of I30E-nanocomposites with different coupling agents. A significant increase can also be observed in the tensile and flexural modulus of the composites with coupling agent compared to pure PP and the mixture without coupling agent. In general, CA3 and CA4 based composites have better performance than CA1 based composites. The big variation in strength also appears in I30E-composites.

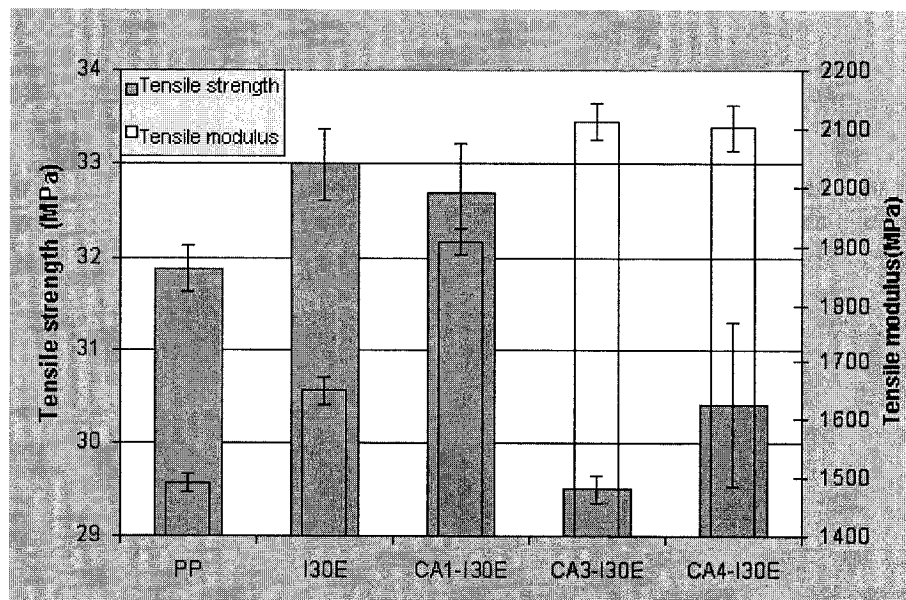


Figure 5.18 Effect of coupling agent on tensile properties of I30E based nanocomposites

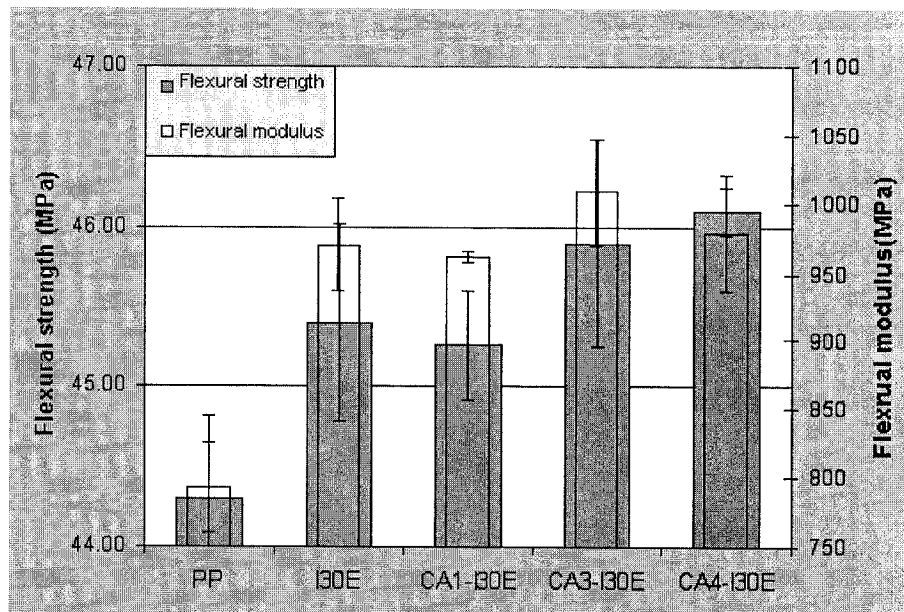


Figure 5.19 Effect of coupling agent on flexural properties of I30E based nanocomposites

5.5 Conclusion

The use of coupling agent is essential in the formation of PP nanocomposites. In contrast with conventional composites, the role of coupling agent in PP nanocomposites is not only to improve the interface but also to help clays disperse in the PP matrix. In general, the coupling agent resulted in increased intercalation and exfoliation so that the properties (modulus, strength, T_c , T_g , T_s , etc.) can be improved although the extent of the effect varies with the types of coupling agent because of the differences in their chemistry.

CA1, CA2 and CA2P are maleic anhydride grafted polypropylene (MAgPP). MAgPP has reactive maleic anhydride groups, which can interact with hydroxyl group on the clay surface to form hydrogen bonds. Furthermore, it is miscible with PP. Thus the

improvement of dispersion of clay in PP matrix and interface between clay and matrix can be expected. CA3 is amine (NH_2 -) terminated coupling agent. The amine group (NH_2 -) has special affinity with clay surfaces because it can strongly attract hydroxyl groups that exist on the clay surface with hydrogen bonds. CA4 is an onium ion (NH_3^+ -) terminated coupling agent, which not only can interact with $-\text{OH}$ groups but also reacts with negative sites that exist on the clay surface to form ionic bonds. Therefore, it can provide a stronger driving force to intercalate in the gallery of clay.

The types of functional group, the molecular weight, even the amount of functional groups, etc. of the coupling agent can significantly affect the performance of PP nanocomposites. In addition, different clays and different coupling agents can result in optimal composition for PP nanocomposites. Among five types of coupling agent used in this research, in general amine and onium ion terminated coupling agents had better performance than MAgPP. Especially, onium ion terminated coupling agent (CA4) with 15A based nanocomposites is the best one among them: best intercalation, best mechanical properties, highest T_s and highest T_c . With 6% coupling agent CA4 and 3% 15A clay, the improvement of the nanocomposites in tensile and flexural modulus can reach 52% and 31%, respectively, compared to pure PP.

6 Effect of processing parameters on the formulation and properties of PP nanocomposites

The formation of PP nanocomposites is affected not only by the chemistry of clay and coupling agent but also by the processing conditions (temperature, residence time and shear rate). The following experiments have been designed to study these effects. All samples have same composition, 6%wt coupling agent CA4 (ammonium ion terminated polypropylene), 3%wt Cloisite 15A.

6.1 Effect of processing temperature

Table 6.1 shows the variables and experimental conditions of this experiment set.

Table 6.1 Variables and experimental conditions of Experiment Set 6.1

Variables Sample	Types of clay	Types of coupling agent	Processing parameters		
			<i>Temperature (°C)</i>	Mixing time (min)	rpm
CA4+15A	15A	CA4	<i>170</i>	5	60
CA4+15A	15A	CA4	<i>180</i>	5	60
CA4+15A	15A	CA4	<i>200</i>	5	60

6.1.1 Rheological behavior

Since PP can be easily oxidized and degraded under high temperature and high shear rate, the temperature range from 170°C to 200°C was selected in this study. When an equal shear rate (or rotor speed) is applied, torque is proportional to the shear stress and the shear stress transmitted to silicate layers is proportional to the melt viscosity of the system [98]. On the other hand, the melt viscosity increases with decreasing the processing temperature, so the shear stress transmitted to the silicate layers increases with decreasing mixing temperature. Conversely, the shear stress decreases with increasing the temperature. Therefore, the curves can also display the shear stress that is applied to the system and the viscosity of system during mixing. In this set of experiments, the same materials and concentration were used, so the torque-time curves can be compared directly rather than their trend.

Figure 6.1 shows the torque-time curves of CA4+15A systems at different processing temperatures, 170°C, 180°C and 200°C. Among them, the curve at 180°C is most stable. At 170°C, the system torque is more than two times of one at 200°C, so the system bears much bigger stress at 170°C than at 200°C. Apparently, it is beneficial to get more disordered structure at the lower temperature. However, PP cannot melt homogeneously in a short time at 170 °C, which results in the lasting downward trend of the 170°C-system curve. While for 200°C-system longer time also leads to downward torque, which is probably due to degradation and/or oxidation of materials.

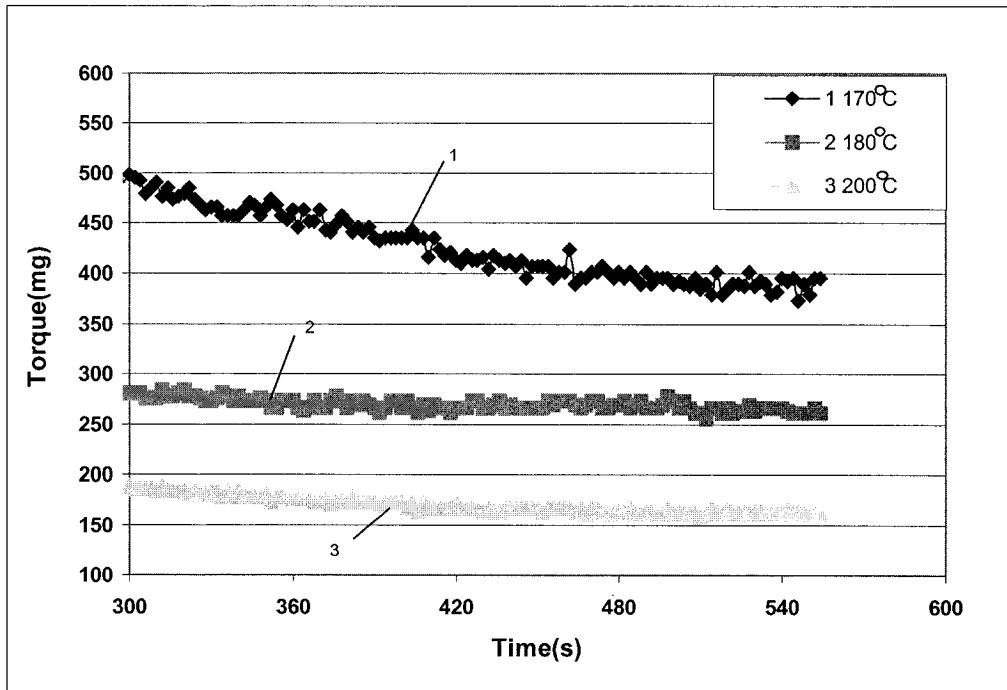


Figure 6.1 Effect of processing temperature on the torque curve

6.1.2 Dispersion behavior

Theoretically, PP molecules should be more active at high temperature and easily interact with the clay surface. Figure 6.2 shows the X-ray curves of the PP/CA4/15A nanocomposites under different mixing temperatures (170°C, 180°C and 200°C). They all have three peaks and do not have apparent differences, which suggested that they were not exfoliated nanocomposites and the dispersion behavior is similar. However, the first peaks of the nanocomposites for 170°C and 180°C are at relatively lower angles than the one for 200°C, which means that a better intercalation may be obtained at a relatively lower temperature. This can explain why the 200°C-nanocomposites have worse mechanical properties (see Section 6.1.3). The better dispersion is mainly attributed to the

relatively higher shear stress (melt viscosity) at relatively lower temperature. Since the shear stress transmitted to silicate layers is proportional to the melt viscosity when an equal shear rate (or rotor speed) is applied, the lower temperature is better for disordered structure to develop.

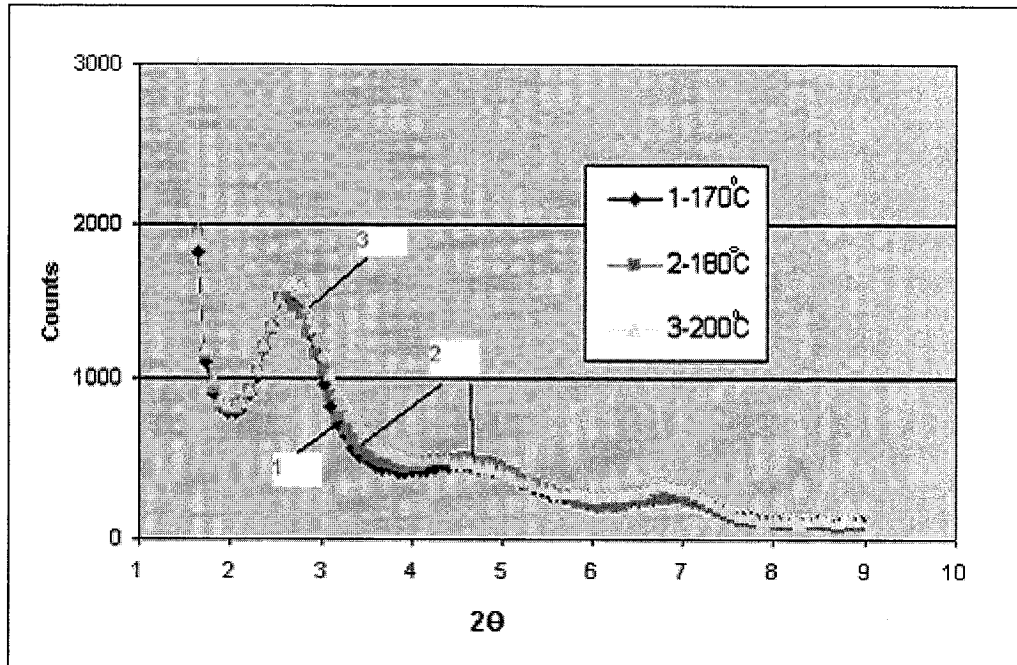


Figure 6.2 Effect of mixing temperature on XRD results (PP/CA4/15A)

6.1.3 Mechanical properties

Figures 6.3 and 6.4 show the effect of processing temperature on mechanical properties. 180°C-nanocomposites have higher tensile and flexural modulus and strengths than 170°C and 200°C-nanocomposites. This tendency should be related to the mobility of PP molecules and the dispersion of clay in matrix at different temperatures. At 170°C, PP

just melts and molecules are not active enough and cannot intercalate into the gallery of clay greatly although stronger stress was applied on the system. On the other hand, at 200°C, molecules are so active that they can be oxidized and tend to degrade (which can be observed from the torque –time curve) so that the mechanical properties decrease. As discussed earlier, more disordered structure could be developed at the lower temperature, but this temperature should guarantee the activity of PP molecules. Therefore, 180°C should be a balanced and best processing temperature for PP nanocomposites.

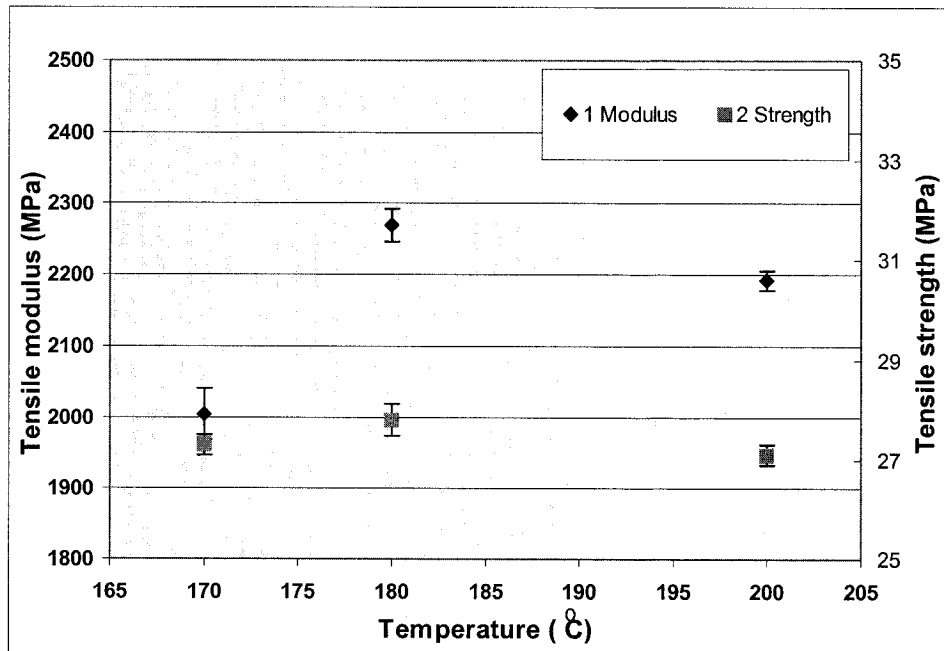


Figure 6.3 Effect of processing temperature on the tensile properties

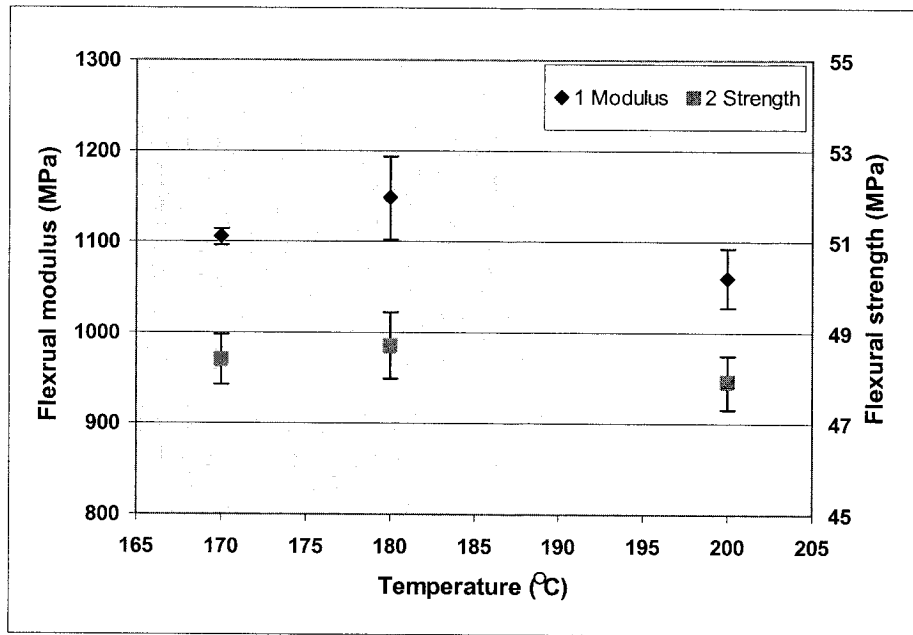


Figure 6.4 Effect of processing temperature on the flexural properties

6.2 Effect of residence time

The variables and experimental conditions of this experiment set are shown in Table 6.2.

Table 6.2 Variables and experimental conditions of Experiment Set 6.2

Variables Sample	Types of clay	Types of coupling agent	Processing parameters		
			Temperature (°C)	Mixing time (min)	rpm
CA4+15A	15A	CA4	180	2.5	60
CA4+15A	15A	CA4	180	5	60
CA4+15A	15A	CA4	180	10	60

6.2.1 Rheological behavior

Figure 6.5 shows the change of torque with residence time for CA4+15A systems. The curves do not show distinct differences. However, with the residence time increasing, the curve displayed a gradually downward trend, which means the viscosity of systems decreases or the degradation and/or oxidization have taken place.

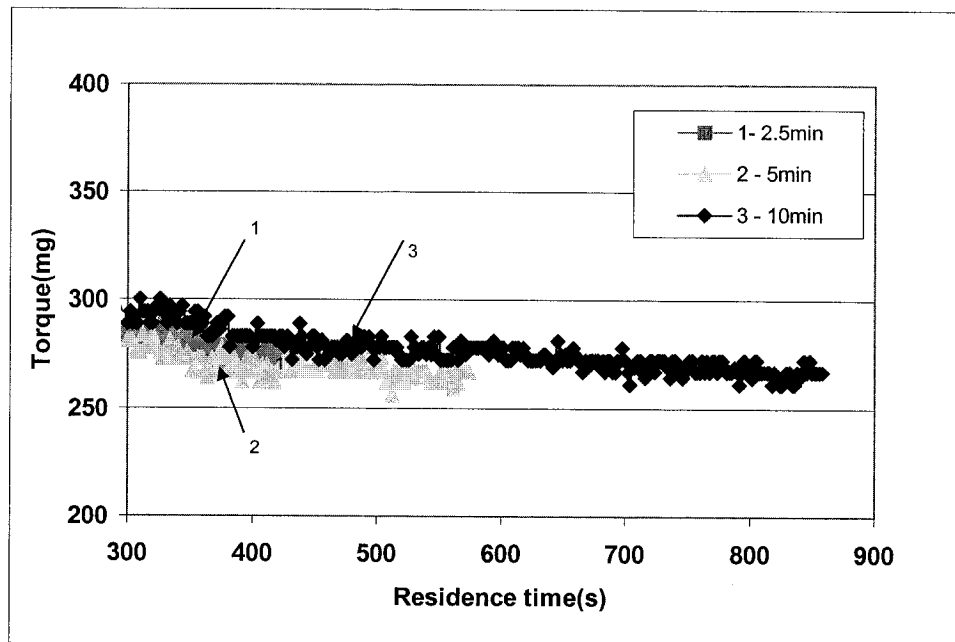


Figure 6.5 Effect of residence time on the torque curve (PP+CA4+15A)

6.2.2 Dispersion behavior

Logically, the procedure of PP molecules intercalating/exfoliating in the gallery of clay needs some time, so increasing residence time in the Brabender should improve the dispersion of clay in the PP matrix. However, increasing residence time risks the possibility of oxidation/degradation of PP. Figure 6.6 shows the X-ray curves of the nanocomposites with the same composition under different residence times without affecting other parameters. The similar peak location and intensity can be found at 2.5 min- and 5 min- nanocomposites, which suggests similar dispersion in these systems. However, the first peak and third peak of 10 min–nanocomposite appear at relatively higher angle than 2.5 min- and 5 min-nanocomposites. This indicates that the interlayer spacing decreases. The decrease of the spacing probably comes mainly from the thermal decomposition of Cloisite 15A during long time and higher temperature processing [99]. Thermal decomposition makes the surface of Cloisite 15A less organophilic, so the intercalation becomes more difficult. On the other hand, the intensity of peaks for 10 min–nanocomposites is lower than 2.5 min- and 5 min–nanocomposites, which means that better exfoliation was obtained than other two systems. Therefore, the long time mixing can be helpful to break the big clay clusters and improve exfoliation but harmful for the intercalation.

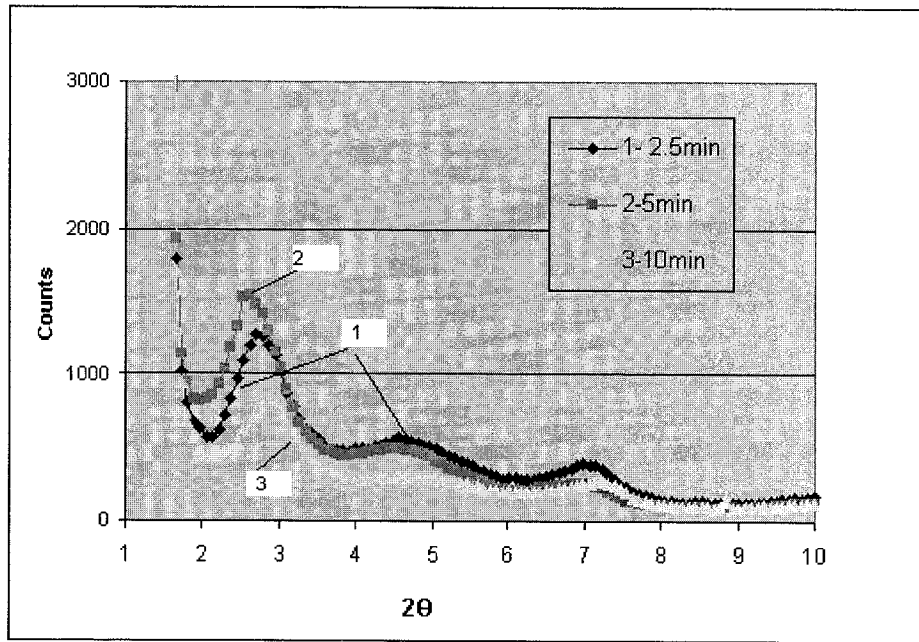


Figure 6.6 Effect of residence time on XRD results (PP+CA4+15A)

6.2.3 Mechanical behavior

Figures 6.7 and 6.8 show the effect of residence time on mechanical properties of CA4+15A nanocomposites. With the increase of residence time, the flexural modulus and strength both decrease, while the tensile modulus decreased sharply when residence time reaches 10 minutes. Apparently, longer residence time has a negative effect on the properties of PP-nanocomposites. This could be due to the materials oxidation and/or degradation.

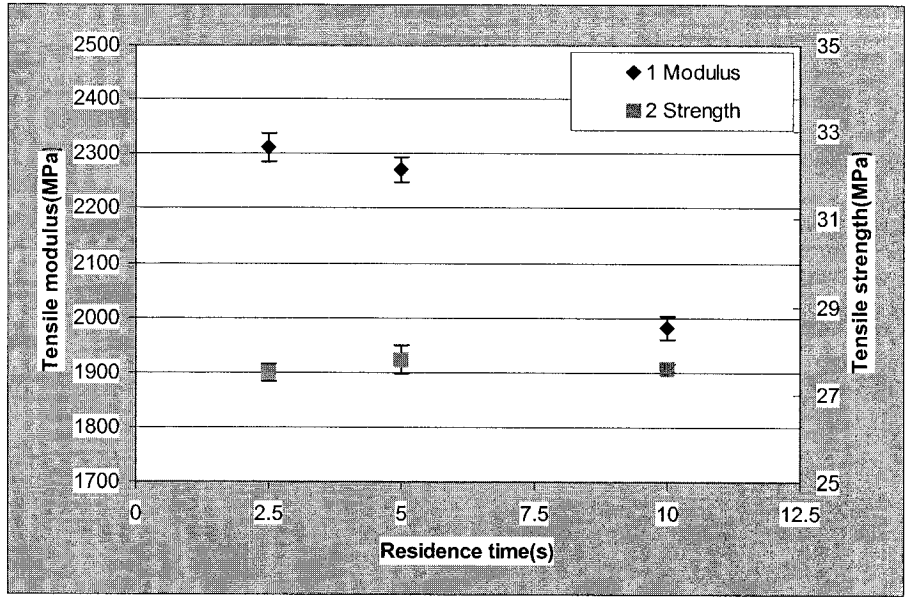


Figure 6.7 Effect of residence time on the tensile properties

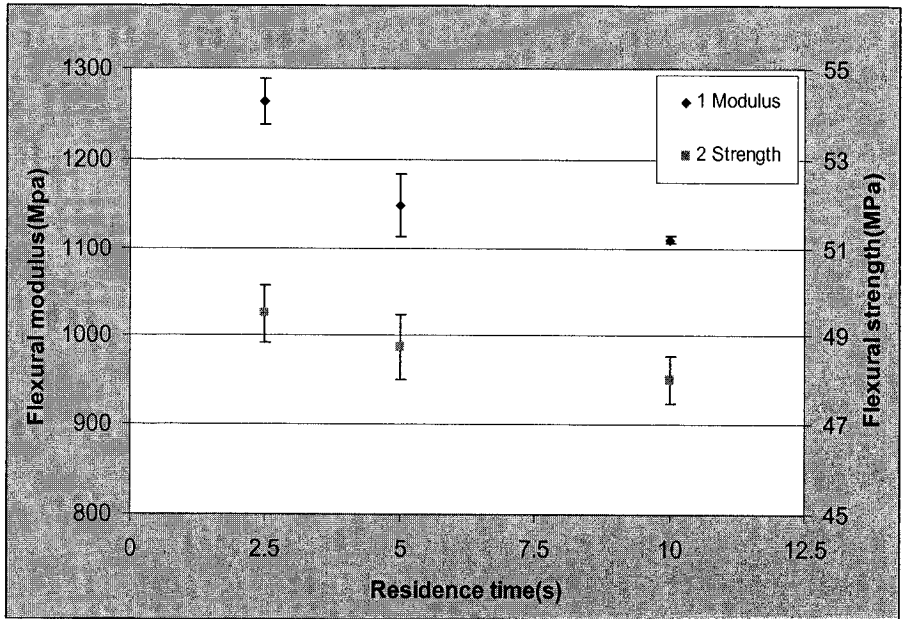


Figure 6.8 Effect of residence time on the flexural properties

6.3 Effect of processing rotor speed (shear rate)

Table 6.3 is the variables and experimental conditions applied in this experiment set.

Table 6.3 Variables and experimental conditions of Experiment Set 6.3

Variables Sample	Types of clay	Types of coupling agent	Processing parameters		
			Temperature (°C)	Mixing time (min)	<i>rpm</i>
CA4+15A	15A	CA4	180	5	40
CA4+15A	15A	CA4	180	5	60
CA4+15A	15A	CA4	180	5	80

6.3.1 Rheological behavior

Figure 6.9 shows torque –time curve for CA4+15A systems under different rotor speeds of 40rpm, 60rpm and 80rpm. From this figure, torque is proportional to rotor speed (shear rate) and nearly stays parallel during the same residence time. At the same time, since shear stress increases with shear rate (Generally thermoplastic melts are non-Newtonian fluid and the equation $\tau = k\gamma^n$ is applied. γ is shear rate; τ is shear stress; 'n' is the index that shows the non-Newtonian property), the magnitude of torque can illustrate the shear stress of the system. The higher torque at 80rpm means the system bears higher shear stress than other ones at 40rpm and 60rpm. Thus the shear rate during mixing may affect the intercalation and/or exfoliation of PP nanocomposites.

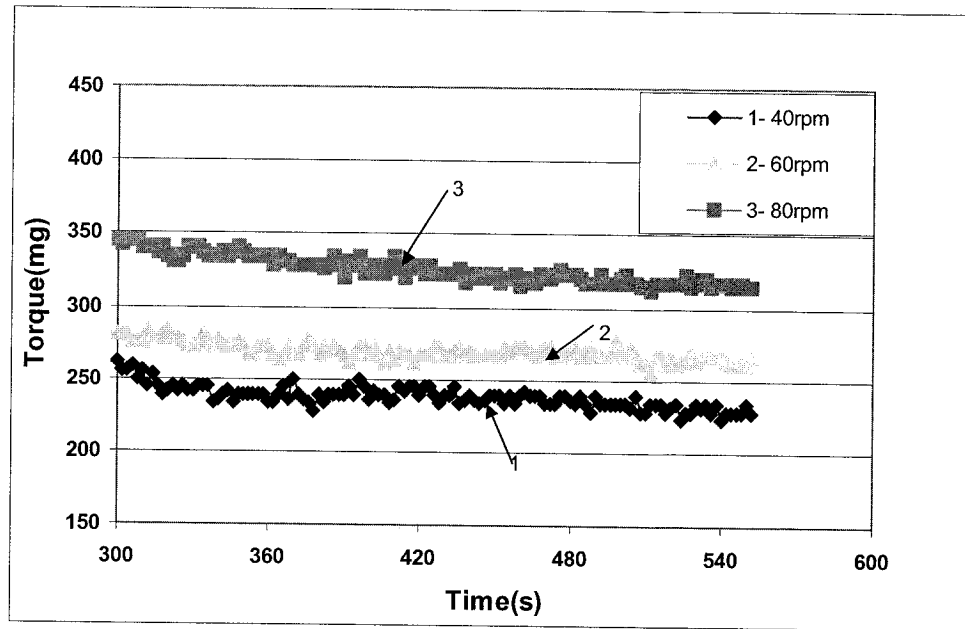


Figure 6.9 Effect of shear rate on torque of PP+CA4+15A systems

6.3.2 Dispersion behavior

Since the shear stress increases with the shear rate, it is expected that interaction/exfoliation would take place more easily as the shear rate increases during mixing and the mechanical properties would be improved greatly. Figure 6.10 shows the X-ray curves of the nanocomposites under different shear rates (rpm) without changing other parameters. At different rpms, the X-ray curves show almost same shape (the peaks are at the same location and the intensities are of the same level), which indicate that processing at high rate/ high rpm has a minimal effect on intercalation or exfoliation. These results are commensurate with ones made by P. Andersen [100].

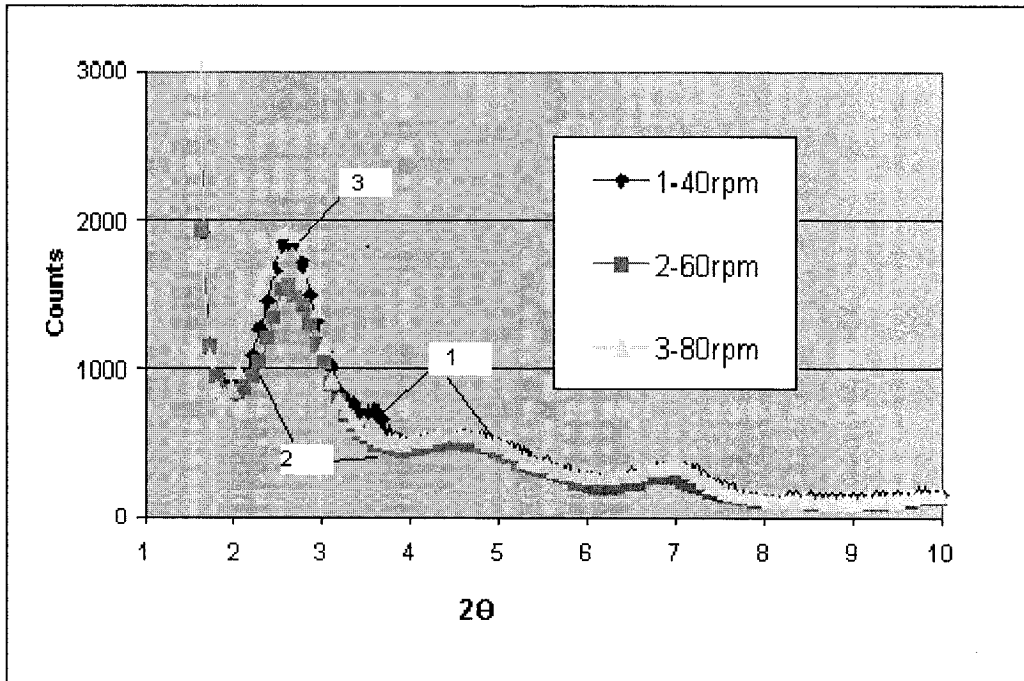


Figure 6.10 Effect of shear rate (rpm) on the XRD results (PP+CA4+15A)

6.3.3 Mechanical behavior

Figures 6.11 and 6.12 show the results of mechanical properties of CA4+15A nanocomposites under different shear rates of 40rpm, 60rpm and 80rpm. The results do not show big difference among them. The tensile and flexural moduli and strengths varied little when the shear rate changed from 40rpm to 80rpm. Considering the factor of experimental error, it seems that the mechanical properties of the nanocomposites do not depend on the magnitude of shear rate within the shear range used in this study. It is probably that some large clay aggregates (formed from nano-scale particles by electrostatic force) could be separated at low shear rate while small ones are so small and combined tightly that the shear rate applied in experimental range could not affect them a lot.

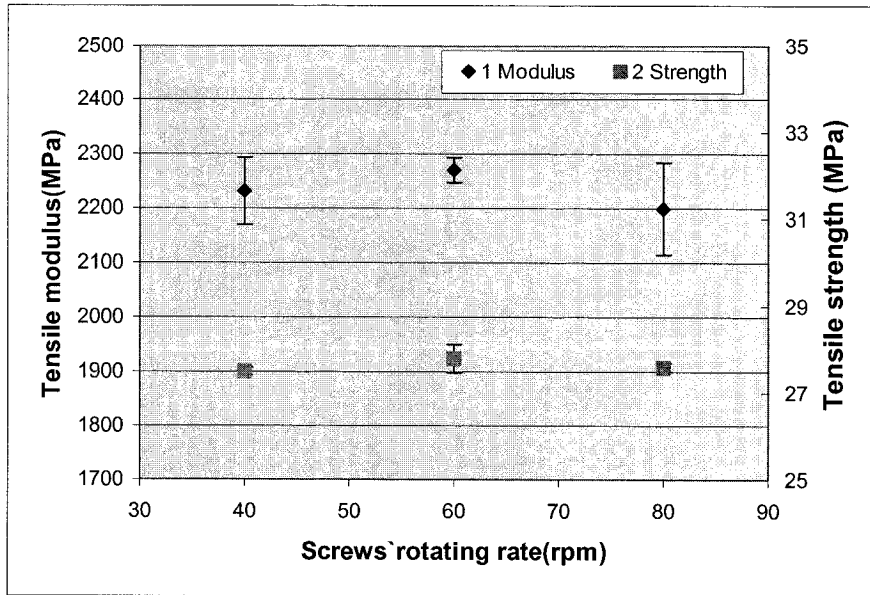


Figure 6.11 Effect of shear rate on the tensile properties (PP+CA4+15A)

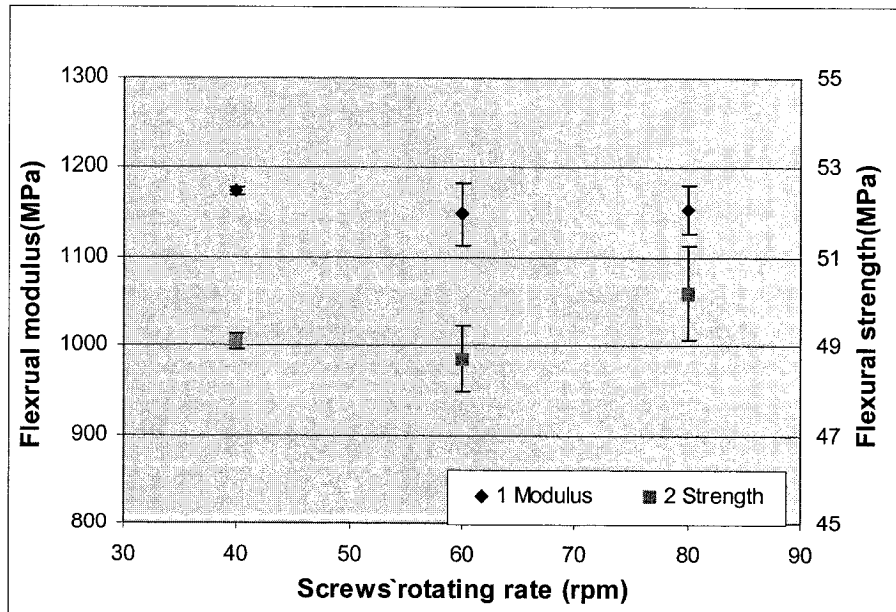


Figure 6.12 Effect of shear rate on the flexural properties (PP+CA4+15A)

6. 4 Conclusions

Processing parameters can have great effects on the fabrication of nanocomposites. With complete melting, a lower temperature is better to develop a disordered structure. 180⁰C is the best mixing temperature for PP nanocomposites. A longer residence time seems to be helpful to improve exfoliation but harmful for intercalation and mechanical properties due to the possible degradation. However, processing at high shear rate/high rpm has no significant effect on dispersion and properties.

7 Conclusions

The formulation and the properties of montmorillonite clay based polypropylene nanocomposites have been described in this thesis. Melt compounding method (Brabender) was used to fabricate the PP nanocomposites. The effects of clays, coupling agents and processing parameters on the fabrication and performance of PP nanocomposites were studied by various characterizations.

The effects of nanoclay on the formulation and properties on PP nanocomposites varied with the types of clays that are different in the types and concentration of intercalants. Among the five types of clays, 15A, 20A and 30B have better thermal stability than I30E and I31PS, while 15A, I30E and I31PS show better mechanical performance than the others. In addition, nanoclay has an apparent nucleating effect as it increases the crystallization temperature (T_c). The presence of 3% nanoclay without coupling agent cannot significantly improve tensile and flexural properties of PP matrix.

In contrast with conventional composites, the role of coupling agent in PP nanocomposites is not only to improve the interface but also to improve the clay dispersion in the PP matrix. Besides, coupling agent chemistry, such as the molecular weight, the type and amount of functional groups can significantly affect the performance of the nanocomposites. Among the five types of coupling agent used in this study, amine and onium ion terminated coupling agent lead to a better dispersion and better performance than MAgPP. It is very interesting to stress here that, the new type of

coupling agent CA4 was studied for the first time and has demonstrated a great potential for the development of polyolefin nanocomposites. With a modest organo-clay content of 3-wt%, the tensile and flexural moduli have significantly improved by 52% and 31% respectively, compared to pure PP. In addition, the combination of the clay chemistry and coupling agent chemistry has to be fully considered in order to obtain the optimum nanocomposites performance. The combination of Cloisite 15A and ammonium terminated PP CA4 is highly recommended.

Among processing conditions, shear rate (rpm) does not have apparent effect on the clay dispersion and the performance of the nanocomposites. However, lower temperature (above the melting point) and residence time are recommended in order to obtain a good dispersion and thus performance, while minimize degradation.

8 Contributions

In this study, many factors that affect the formulation and properties of PP nanocomposites have been investigated, including different clay types, different coupling agents and processing parameters. The study did not only focus on a single parameter but also a combination of these parameters. These effects have tremendous impact on the manufacture of PP nanocomposites, which have not been fully explored so far. This thesis was designed to contribute to the understanding on these effects in more complex feature as follows.

1. The new coupling agents that possess functional groups - amine (NH_2) and ammonium (NH_3^+) were studied for the first time. Their nanocomposites performances were compared with those of nanocomposites prepared by the most commonly used coupling agent - MAgPP. The results indicated that the systems based on 15A clay and NH_3^+ terminated coupling agent are superior compared to the conventional one.
2. Effects of different types of MAgPP on PP nanocomposites, which contain different molecular weight, acid number and purity, were also examined. The combined impact of these issues of MAgPP have never been reported before.

3. Different types of clay (Na-montmorillonite clay) mean that clay is modified by different intercalants and/or different concentrations so that they have different gallery distances and different chemistries. Effect of modified clays has been demonstrated but no systematical research on the clay chemistry, clay source in combination with different types of coupling agent has been published so far.
4. This research found that some interesting combinations of clay and coupling agent, which provide good performance, such as CA1 with I31PS, CA4 with 15A.
5. Extruders are mostly employed to fabricate nanocomposites for industrial application, due to the disadvantages of extruder to control the parameters, the study in this thesis has been performed on the Plasticorder Brabender to fabricate nanocomposites. The results obtained have provided a very good fundamental understanding on how to control the balance between dispersion (thus good performance) and degradation.
6. Publications:
 - 1) M.-T. Ton-That, S. G. Lei, K. C. Cole, S. V. Hoa, I. Pesneau, "Effect of functionalization on the fabrication of polypropylene nanocomposites". *Second International Symposium on Polymer Nanocomposites Science and Technology*, Boucherville, QC, Canada, October 6-8, 2003.
 - 2) S. G. Lei, M.-T. Ton-That, K. C. Cole, S. V. Hoa, I. Pesneau, "The role of coupling agent on the formation of polypropylene nanocomposites". Paper submitted to *Canadian Materials Quarterly*.

9 Suggestions for future work

In this thesis, many effects have been studied to obtain high performance PP nanocomposites. The following work is felt necessary to be done in the future:

- 1) Since the loading of coupling agent and clay was very low in this work, changing the sequence of adding materials during Brabender mixing may be helpful to get better results: mix the coupling agent and clay first, then mix with PP.
- 2) Due to limits of Brabender mixing and compression molding, such as dead corner, limited volume, small specimens (results were easily affected by defects), etc., some work should be done using twin-screw extruder and injection molding machine based on the obtained results.
- 3) The coupling agent plays a crucial role in the formulation of PP nanocomposites by melt compounding method. To find/develop more effective coupling agent and optimum composition will be an important topic in PP nanocomposites research.
- 4) In order to obtain a better understanding of the experiments results, further work on the mechanism of the interaction between the clays and CA3 and CA4 coupling agent should be done.

References

- [1] D. Hans, *Plastics for engineers: materials, properties, applications*, Munich; New York: Hanser Publishers, 1993.
- [2] R. Arie, *Fundamentals of polymer engineering*, New York: Plenum Press, 1997.
- [3] *Plastics engineering handbook of the Society of the Plastics Industry*, New York: Van Nostrand Reinhold, 1991.
- [4] G. Graff, “Nanocomposite suppliers see promise for custom solutions”. *Modern Plastics* 76(6):37, 1999.
- [5] R. Leaversuch, “Nanocomposites: Broaden roles in automotive, barrier packaging”. *Plastics Technology* 47(10):64, 2001.
- [6] G. Q. Qian, J. W. Cho, T. Lan, “Preparation and properties of polyolefin nanocomposites”. www.nanocor.com.
- [7] J. Z. Liang, “Toughening and reinforcing in rigid inorganic particulate filled polypropylene: A review”. *Journal of Applied Polymer Science* 83(7): 1547, 2002.
- [8] Y. Jia, S. Lei, Q. Wu, “The modification of HDPE by inorganic particles”. *Plastics Industry* 5:97, 1996.
- [9] E. P. Giannelis, “Polymer layered silicate nanocomposites”. *Advanced Materials* 8:29, 1996.
- [10] M. Z. Rong, M. Q. Zhang, Y. X. Zheng, H. M. Zeng, R. Walter, K. Friedrich, “Structure–property relationships of irradiation grafted nano-inorganic particle filled polypropylene composites”. *Polymer* 42(1):167, 2001.

- [11] S. Lu, M. M. Melo, J. Zhao, E. M. Pearce, T. K. Kwei, "Organic-inorganic polymeric hybrids involving novel poly(hydroxymethylsiloxane)". *Macromolecules* **28**(14):4908, 1995.
- [12] A. Usuki, M. Kawasumi, Y. Kojima, A. Okada, T. Kurauchi, O. Kamigaito, "Swelling behavior of montmorillonite action exchanged for α -amino acids by ϵ -caprolactam". *Journal of Materials Research* **8**:1174, 1993.
- [13] A. Usuki, Y. Kojima, M. Kawasumi, A. Okada, Y. Fukushima, T. Kurauchi, O. Kamigaito, "Synthesis of nylon 6-clay hybrid". *Journal of Material Research* **8**:1179, 1993.
- [14] K. Yano, A. Usuki, T. Kurauchi, O. Kamigaito, "Synthesis and properties of polyimide-clay hybrids". *Journal of Polymer Science, Part A: Polymer Chemistry* **31**:2493, 1993.
- [15] Y. Kojima, A. Usuki, M. Kawasumi, A. Okada, T. Kurauchi, O. Kamigaito. "Synthesis of Nylon 6-clay hybrid by montmorillonite intercalation with ϵ -caprolactam". *Journal of Polymer Science Part A: Polymer Chemistry* **31**:983, 1993.
- [16] T. Lan, J. Cho, Y. Liang, J. Qian, P. Maul, "Applications of nanomer in nanocomposites: From concept to reality". *Nanocomposites 2001*, Chicago, IL, USA, June 25-27, 2001.
- [17] A. V. Richard, K. D. Jandt, J. K. Edward, E. P. Giannelis, "Kinetics of polymer melt intercalation". *Macromolecules* **28**(24):8080, 1995.
- [18] P. H. Nam, P. Maiti, M. Okamoto, T. Kotaka, N. Hasegawa and A. Usuki, "A hierarchical structure and properties of intercalated polypropylene/clay nanocomposites". *Polymer* **42**(23):9633, 2001.

- [19] Y. Kojima, A. Usuki, M. Kawasumi, A. Okada, Y. Fukushima, T. Kurauchi, O. Kamigaito, "Mechanical properties of nylon 6-clay hybrid". *Journal of Material Research* **8**:1185, 1993.
- [20] K. E. Strawhecker, E. Manias, "AFM of poly (vinyl alcohol) crystals next to an inorganic surface". *Macromolecules* **34**:8475, 2002.
- [21] P. Kelly, A. Akelah, S. Qutubuddin, A. Moet, "Reduction of residual stress in montmorillonite/epoxy compounds". *Journal of Material Science* **29**:2274, 1994.
- [22] A. S. Moet, A. Akelah, "Polymer-clay nanocomposites: polystyrene grafted onto montmorillonite interlayers". *Materials Letters* **18**:97, 1993.
- [23] P. B. Messersmith, E. P. Giannelis, "Synthesis and barrier properties of poly(ϵ -caprolactone)-layered silicate nanocomposites". *Journal of Polymer Science Part A: Polymer Chemistry* **33**:1047, 1995.
- [24] L. Biasci, M. Aglietto, G. Ruggeri, F. Ciardelli, "Functionalization of montmorillonite by methyl methacrylate polymers containing side-chain ammonium cations". *Polymer* **35**(15):3296, 1994.
- [25] M. Alexandre, P. Dubois, "Polymer-layered silicate nanocomposites: preparation, properties and uses of a new class of materials". *Materials Science and Engineering* **28**:1,2000.
- [26] Nanocor Inc. Web site: www.nanocor.com
- [27] A. Jr. Lawrence, J. Charles, E. G. Raymond, "Melt compounded thermoplastic nanocomposites". *Polymer Nanocomposites 2001*, Montreal, Canada, November 14-16, 2001.

- [28] B. Velde, *Introduction to clay minerals: chemistry, origins, uses, and environmental significance*; London; New York: Chapman & Hall, 1992.
- [29] E. P. Giannelis, R. Krishnamoorti and E. Manias, "Polymer-silica nanocomposites: model systems for confined polymers and polymer brushes". *Advances in Polymer Science* **118**:108, 1999.
- [30] H. R. Dennis, D. L. Hunter, J. W. Cho, D. R. Paul, D. Cheng, S. Kim, J. L. White, "Guidelines for the production of polypropylene nanocomposites". *ANTEC*, Orlando, Florida, U.S.A., Society of Plastic Engineers, May, 2000.
- [31] M. Kawasumi, N. Hasegawa, M. Kato, A. Usuki, and A. Okada, "Preparation and mechanical properties of polypropylene-clay hybrids". *Macromolecules* **30**:6333,1997.
- [32] N. Hasegawa, M. Kawasumi, M. Kato, A. Usuki, A. Okada, "Preparation and mechanical properties of polypropylene-clay hybrids using a maleic anhydride-modified polypropylene oligomer". *Journal of Applied Polymer Science* **67**:87, 1998.
- [33] E. Hackett, E. Manias, E. P. Giannelis, "Molecular dynamics simulations of organically modified layered silicates". *Journal of Chemical Physics* **108**(17):7410, 1998.
- [34] Z. Wang, J. Massam and T. J. Pinnavaia, *Polymer-clay Nanocomposites*. John Wiley & Sons Ltd., Chichester, England, 2000.
- [35] N. Hasegawa, H. Okamoto, M. Kato, A. Usuki, "Preparation and mechanical properties of polypropylene-clay hybrids based on modified polypropylene and organophilic clay". *Journal of Applied Polymer Science* **78**(11):1918, 2000.
- [36] R. N. Krishna, N. Bulakh, "Effect of clay treatment on mechanical properties of Polypropylene based composites". *Polymer Nanocomposites 2001*, Montreal, Canada, November 14-16, 2001.

- [37] J. G. Doh, J. Cho, "Synthesis and properties of polystyrene-organoammonium montmorillonite hybrid". *Polymer Bulletin* **41**:511, 1998.
- [38] M. W. Weimer, H. Chen, E. P. Giannelis, D.Y. Sogah, "Direct synthesis of dispersed nanocomposites by in situ living free radical polymerization using a silicate-anchored initiator". *Journal of American Chemical Society* **121**(7):1615, 1999.
- [39] K. E. Strawhecker and E. Manias, "AFM of poly(vinyl alcohol) crystals next to an inorganic surface". *Macromolecules* **34**:8475, 2001.
- [40] A. S. Zerda and A. J. Lesser, "Intercalated nanocomposites: morphology, mechanics and fracture behavior", Polymer Poster Symposium, University of Massachusetts Amherst, U.S.A., 2002.
- [41] J. S. Ma, Z. N. Qi, Y. L. Hu, "Synthesis and characterization of polypropylene/clay nanocomposites". *Journal of Applied Polymer Science* **82**(14):3611, 2001.
- [42] T.J. Pinnavaia, G.W. Beall. *Polymer – clay Nanocomposites*. John Wiley & Sons, Ltd., Chichester, England, 2000.
- [43] R.A. Vaia and E. P. Giannelis., "Lattice model of polymer melt intercalation in organically-modified layered silicates". *Macromolecules* **30**(25):7990, 1997.
- [44] R.A. Vaia and E. P. Giannelis., "Polymer melt intercalation in organically-modified layered silicates: model predictions and experiment". *Macromolecules* **30**(25):8000, 1997.
- [45] A.C. Balazs, C. Singh, and E. Zhulina, "Modeling the interactions between polymers and clay surfaces through self-consistent field theory". *Macromolecules* **31**(23):8370,1998.

- [46] E. P. Giannelis, R. K. Krishnamoorti, and E. Manias, "Polymer-silicate nanocomposites: model systems for confined polymers and polymer brushes". *Advances in polymer science* **138**:107, 1998.
- [47] E. Manias, A. Touny, L. Wu, K. Strawhecker, B. Lu, and T. C. Chung, "Polypropylene/montmorillonite nanocomposites. Review of the synthetic routes and materials properties". *Chemical Materials* **13**:3516, 2001.
- [48] E. Manias, H. Chen, R. Krishnamoorti, J. Genzer, E. J. Kramer, and E. P. Giannelis, "Intercalation kinetics of long polymer in 2 nm confinements". *Macromolecules* **33**:7955, 2000.
- [49] M. Kato, A. Usuki, and A. Okada, "Synthesis of polypropylene oligomer-clay intercalation compounds". *Journal of Applied Polymer Science* **66**:1781,1997.
- [50] A. Oya, Y. Kurokawa, and H. Yasuda, "Factors controlling mechanical properties of clay mineral/polypropylene nanocomposites". *Journal Material Science*, **35**:1045, 2000.
- [51] R. Peter, N. Hansjorg, K. Stefan, B. Rainer, T. Ralf, M. Rolf, "Poly(propylene)/organoclay nanocomposite formation: Influence of compatibilizer functionality and organoclay modification". *Macromolecular Materials and Engineering* **275**:8, 2000.
- [52] N. Hasegawa, H. Okamoto, M. Kawasumi, M. Kato, A. Tsukigase, A. Usuki, "Polyolefin-clay hybrids based on modified polyolefins and organophilic clay". *Macromolecular Material Engineering* **280/281**:76, 2000.
- [53] M. Ladika, R. Fibiger, C. Chou, A. Balazs, "Functionalized polymer nanocomposites". *World Intellectual Property Organization*, 15 November 2001, WO 01 85831 A2.

- [54] M. Mehrabzadeh, M. R. Kamal, "Polymer-clay nanocomposites based on blends of polyamide-6 and polyethylene". *Polymer Nanocomposites 2001*, Montreal, Canada, November 14-16, 2001.
- [55] P. Kodgire, R. Kalgaonkar, S. Hambir, N. Bulak, J. P. Jog, "PP/clay nanocomposites: Effect of clay treatment on morphology and dynamic mechanical properties". *Journal of Applied Polymer Science* **81**:1786, 2001.
- [56] D. Garcia-Lopez, O. Picazo, J.C. Merino, J. M. Pastor, "Polypropylene-clay nanocomposites: effect of compatibilizing agents on clay dispersion". *European Polymer Journal* **39** (5):945, 2003.
- [57] M. T. Ton-That, F. Perrin, P. Lacand, K. C. Cole, J. Denault, and G. Enright, "Preparation and performance of nanocomposites based on polypropylene and layered nanoclays". *Polymer Nanocomposites 2001*, Montreal, Canada, November 14-16, 2001.
- [58] J. Heinemann, P. Reichert, R. Thomann, R. Mulhaupt, "Polyolefin nanocomposites formed by melt compounding and transition metal catalyzed ethene homo- and copolymerization in the presence of layered silicates". *Macromolecular Rapid Communications* **20**(8):423.1999.
- [59] S. Hambir, N. Bulakh, P. Kodgire, R. Kalgaonkar, J. P. Jog, "PP/Clay nanocomposites: A study of crystallization and dynamic mechanical behavior". *Journal of Polymer Science: Part B: Polymer Physics* **39**:446, 2001.
- [60] A. Usuki, M. Kato, A. Okada, T. Kurauchi, "Synthesis of polypropylene-clay hybrid". *Journal of Applied Polymer Science* **63**(1):137, 1997.

- [61] N. Hasegawa, H. Okamoto, M. Kato, A. Usuki, "Preparation and mechanical properties of polypropylene-clay hybrids based on modified propylene and organophilic clay". *Journal of Applied Polymer Science* **78**:1918, 2000.
- [62] S. Yin, T. G. Rials, M. P. Wolcott, "Crystallization behavior of polypropylene and its effect on woodfiber composite properties". The Fifth International Conference on Woodfiber-Plastics Composites, pp.139. Madison, WI.; Forest Products Society. May 26-27,1999.
- [63] D. J. Suh, O. Park, "Nanocomposite structure depending on the degree of surface treatment of layered silicate". *Journal of Applied Polymer Science* **83**:2143, 2001.
- [64] I. Pesneau, "Reactive extrusion: materials customization", *Polymer Technology Symposia*, Boucherville, Quebec, Industrial Materials Institute- NRC and Quebec Materials Network, April 9, 2003.
- [65] J.W. Who, J. Logsdon, S. Omachinski, G.Q. Qian, T. Lan, T. W. Womer, and W. S. Smith. "Nanocomposites: A single screw mixing study of nanoclay-filled polypropylene". ANTEC 2000, Orlando, Florida, USA, Society of Plastic Engineers, May 2000.
- [66] www.cromptoncorp.com - "product document" – website of Uniroyal Chemical.
- [67] www.eastman.com - "customer center" – website of Eastman Chemical Company.
- [68] www.nanoclay.com – website of Southern Clay Product.
- [69] S. Hambir, N. Bulakh, and J. P. Jog, "Polypropylene/clay nanocomposites: effect of compatibilizer on the thermal, crystallization and dynamic mechanical behavior". *Polymer Engineering and Science* **42** (9):1800, 2002.
- [70] M. L. Berins, *SPI Plastics Engineering Handbook of the Society of the Plastics Industry, Inc.*, Van Nostrand Reinhold, New York, U. S. A., 1991.

- [71] M. D. Milton, *X-ray diffraction and the identification and analysis of clay minerals*. Oxford, New York; Oxford University press, 1997.
- [72] B. Velde, *Introduction to clay minerals: chemistry, origins, uses, and environmental significance*; London; New York: Chapman & Hall, 1992.
- [73] B. Wunderlich, *Macromolecular Physics. Vol. 3, Crystal Melting*, New York: Academic, 1980.
- [74] W. J. Sichina, "Thermal analysis for the characterization of polymer impact resistance". *Thermal analysis-application note*, PerkinElmer instruments, 2001.
- [75] 2003 Seminar Series, Thermal analysis & rheology. TA Instruments. Montreal, QC, 2003.
- [76] J. Wu, *Mech 343*, Department of Mechanical Engineering, Hong Kong University of Science and Technology, 2003.
- [77] P. J. Haines, D. M. Price, *Principles of thermal analysis and calorimetry*, Chapter 4, Cambridge : Royal Society of Chemistry, 2002.
- [78] *ASTM-D790-99*. An American National Standard, ASTM, West Conshohochen, PA, United States.
- [79] *ASTM-D638-99*. An American National Standard, ASTM, West Conshohochen, PA, United States.
- [80] A. C. Balazs, C. Singh, E. Zhulia, "Modeling the Interactions between Polymers and Clay Surfaces through Self-Consistent Field Theory". *Macromolecules* **31**:8370, 1998.
- [81] V. V. Ginzburg, A. C. Balazs, "Calculating Phase Diagrams of Polymer-Platelet Mixtures Using Density Functional Theory: Implications for Polymer/Clay Composites". *Macromolecules* **32**:5681, 1999.

- [82] V. V. Ginzburg, C. Singh, A. C. Balas; "Theoretical Phase Diagrams of Polymer/Clay Composites: The Role of Grafted Organic Modifiers". *Macromolecules* **33**:1089, 2000.
- [83] P. Kodgire, R. Kalgaonkar, S. Hambir, N. Bulakh, J. P. Jog, "PP/clay nanocomposites: Effect of clay treatment on morphology and dynamic mechanical properties". *Journal Applied Polymer Science* **81**(7):1786, 2001.
- [84] P. Maiti, P. H. Nam, M. Okamoto, N. Hasegawa, A. Usuki, "Influence of crystallization on intercalation, morphology, and mechanical properties of polypropylene/clay nanocomposites". *Macromolecules* **35**:2042, 2002.
- [85] J. Ma, S. Zhang, Z. Qi, G. Li, Y. Hu, "Crystallization behaviors of polypropylene/montmorillonite nanocomposites". *Journal of Applied Polymer Science* **83**:1978, 2002.
- [86] L. Liu, Z. Qi, X. J. Zhu, "Studies on nylon 6/clay nanocomposites by melt-intercalation process". *Journal of Applied Polymer Science* **71** (7):1133, 1999.
- [87] A. R. Sanadi, D. Feng, D. F. Caufield, "Highly filled lignocellulosic reinforced thermoplastics: effect of interphase modification". *Proceedings of the 18th Riso International Symposium on Material Science: Polymeric Composites*, Riso National Laboratory, Roskilde, Denmark, 1997.
- [88] G. McCrum, B. E. Read, G. Willanms, *Anelastic and Dielectric Effects in Polymer Solids*, John Wiley& Sons Ltd., London, 1967.
- [89] P. Jarvela, L. Shucaï, and P. Jarvela, "Dynamic mechanical properties and morphology of PP/maleated polypropylene blends". *Journal Applied Polymer Science* **62**:813,1996.

- [90] A.R. Sanadi, D. F. Caulfield, N.M. Stark, C. C. Clemons, "Thermal and mechanical analysis of lignocellulosic polypropylene composites". *The fifth International Conference on Woodfiber-Plastic Composites*, Forest Product Society, 1999.
- [91] J. Duvall, C. Sellitti, C. Myers, A. Hiltner, E. Baer, *Tomorrow's Materials Today: Alloys, Blends, and Modified Polymers*. In: SPE Conf. Proc., 1993.
- [92] <http://www.anasys.co.uk/library>
- [93] K.N. Kim, H. Kim, J.W. Lee, "Effect of interlayer structure, matrix viscosity and composition of a functionalized polymer on the phase structure of polypropylene-montmorillonite nanocomposites". *Polymer Engineering and Science* **41**(11):1963, 2001.
- [94] P. C. Lebaron, Z. Wang, T. J. Pinnavaia, "Polymer-layered silicate nanocomposites: an overview". *Applied Clay Science* **15**:11, 1999.
- [95] D. Schmidt, D. Shah, E. P. Giannelis, "New advances in polymer/layered silicate nanocomposites". *Current Opinion in Solid State and Materials Science* **6**:205, 2002.
- [96] G. Schmidt, M. M. Malwitz, "Properties of polymer-nanoparticle composites". *Current Opinion in Colloid and Interface Science*, in press, 2002.
- [97] J. X. Li, J. Wu, C. M. Chan, "Thermoplastic nanocomposites". *Polymer* **41**:6935, 2000.
- [98] S. W. Kim, W. H. Jo, M. S. Lee, M. B. Ko, J. Y. Jho, "Preparation of clay-dispersed poly(styrene-co-acrylonitrile) nanocomposites using poly(ϵ -caprolactone) as a compatibilizer". *Polymer* **42**(24):9837, 2001.
- [99] J. W. Lee, Y. T. Lim, O. O. Park, "Thermal characteristics of organoclay and their effects upon the formation of polypropylene/organoclay nanocomposites". *Polymer Bulletin* **45**:191, 2000.

[100] P. Andersen, *SPE Extrusion Minitec*, National Research Council Canada and Quebec Materials Network, 2003.

[101] A. Yamahita, A. Takahara, T. Kajiyama, "Aggregation structure and fatigue characteristics of (nylon 6/clay) hybrid". *Composites Interfaces* 6:247, 1999.